JOURNAL OF RESEARCH of the National Bureau of Standards — A. Physics and Chemistry
Vol. 74A, No. 4, July-August 1970

Relevance of Knight Shift Measurements to the Electronic Density of States*

L. H. Bennett

Institute for Materials Research, National Bureau of Standards, Washington, D.C. 20234

R. E. Watson[1]

Brookhaven National Laboratory[2]**, Upton, New York 11973**

G. C. Carter

Institute for Materials Research, National Bureau of Standards, Washington, D.C. 20234

The Knight shift, $\mathcal{K}$, measures the magnetic hyperfine field at the nucleus produced by the conduction electrons which are polarized in a magnetic field. Knight shifts are often dominated by the Pauli term and, in its most simple form, can be written as $\mathcal{K} = \langle a \rangle \chi_p$. Here χ_p is the conduction electron Pauli spin susceptibility which depends on the density of states at the Fermi level, $N(E_F)$, and $\langle a \rangle$ is an average magnetic hyperfine coupling constant associated with the wave function character at the nucleus, $|\psi_F(0)|^2$, for conduction electrons at the Fermi surface.

The Knight shift therefore provides, through $\langle a \rangle$, insight into the wave-function character associated with $N(E_F)$. Calculations of $\langle a \rangle$ involving an averaging over k-space have been attempted for a few simple metals up to the present time. For alloys and intermetallic compounds, rather different $\langle a \rangle$'s are experimentally observed for different local environments, indicating that $\mathcal{K}$ samples the variation in *local* wave-function character, or a variation in *local* density of states. There is no unique way of separating the local variation of $N(E_F)$ from $|\psi_F|(0)|^2$.

In this article the methods developed for relating $\mathcal{K}$ to the electronic properties for most of the types of cases encountered in the literature are reviewed. We discuss "simple" metals including problems of orbital magnetism and changes in $\mathcal{K}$ caused by electronic transitions such as melting. Knight shifts and their temperature dependence in metals and intermetallic compounds involving unfilled d shells, are discussed. We give estimates of atomic hyperfine fields due to single electrons, appropriate to those cases where problems due to electronic configurations do not make deductions from experiment too ambiguous. A density of states curve calculated for Cu is given, showing the relative importance of s-p, and d character for that metal. In a qualitative sense this Cu curve implies such information for other transition metals. We discuss alloy solid solutions for the cases where a "rigid" band model might be used to explain the results, and for cases where local effects have to be taken into account. The charge oscillation and RKKY approaches and their limitations are reviewed for cases of dilute nonmagnetic and d- or f-type impurities.

Key words: Electronic density of states; hyperfine fields; Knight shift; nuclear magnetic resonance; susceptibility; wave functions.

1. Introduction

Twenty years ago W. D. Knight [1][3] discovered that the nuclear magnetic resonance (NMR) of ^{63}Cu occurs at about a quarter percent higher frequency in metallic copper than in a salt, CuCl. Since then, there have been over 500 papers reported on the theory and observation of this effect, the "Knight shift," in a wide

*An invited paper presented at the 3d Materials Research Symposium, *Electronic Density of States*, November 3-6, 1969, Gaithersburg, Md.

[1] Also Consultant, National Bureau of Standards.

[2] Work supported by the U.S. Atomic Energy Commission.

[3] Figures in brackets indicate the literature references at the end of this paper.

variety of metals and alloys. The first observation of the Knight shift is shown in figure 1. This paramagnetic shift of the resonance between the diamagnetic salt, CuCl, and the diamagnetic metal, Cu, was attributed

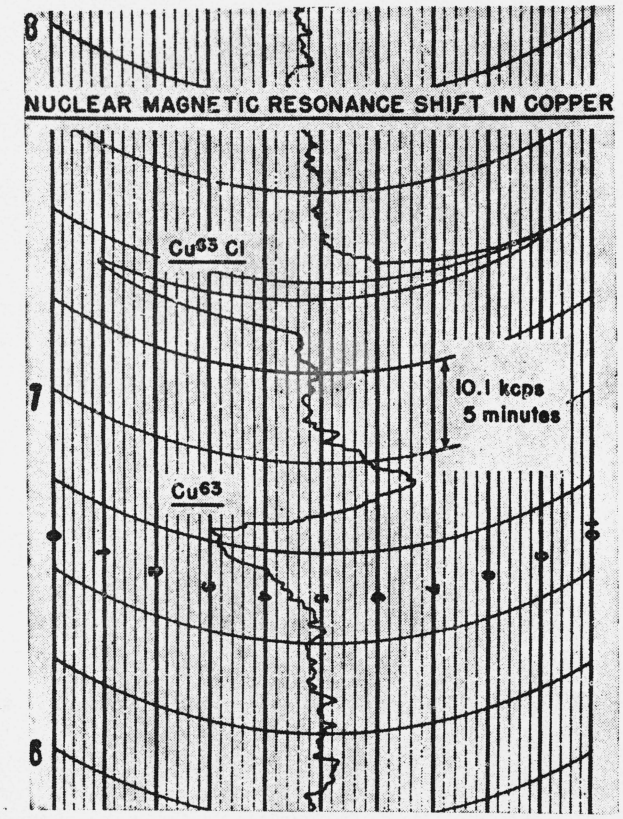

FIGURE 1. *The ^{63}Cu resonance in CuCl (upper resonance) and metallic copper (lower resonance), illustrating the Knight shift* [1].

[2] to the Pauli paramagnetism of the conduction electrons. The shift is much larger than could be explained by the average susceptibility of the conduction electrons. It was proposed [2] that the nuclei sampled a concentrated local susceptibility, arising from the fact that the conduction electrons in a metal have a very large probability density at the nucleus. In its simplest form, the Knight shift ($\mathcal{K}$) may be written

$$\mathcal{K} = \langle a \rangle \chi_p, \tag{1}$$

where $\langle a \rangle$ is an appropriate sampling of the hyperfine interaction of the conduction electrons at the Fermi surface.

For noninteracting electrons, χ_p is proportional to $N(E_F)$, the electronic density of states at the Fermi level,

$$\chi_p = \mu_B{}^2 N(E_F) \tag{2}$$

where μ_B is the Bohr magneton. Thus in this simple approximation, the Knight shift samples, via $\langle a \rangle$, local behavior of the density of states (at the Fermi level) at a particular atomic site.

In this article we will inspect in detail this relationship of $\mathcal{K}$ with the density of states, thereby omitting several important topics on other aspects of NMR in metals. Good review articles have appeared earlier on this broader topic [3-5].

Unfortunately, as with most of the methods for studying the electronic density of states discussed at this symposium, untangling the factors folded in with the density of states is not an easy task. Very often, the experimental Knight shift is used to measure the factor $\langle a \rangle$, χ_p having been obtained from other experiments such as electronic specific heat or bulk magnetic susceptibility. The Knight shift provides a particularly complicated weighted sampling of electronic character but with these complications comes the possibility of obtaining unique information which is otherwise experimentally inaccessible.

A more complete expression for the Knight shift would include other terms,

$$\mathcal{K} = \mathcal{K}_{\text{Pauli}} + \mathcal{K}_{\text{dia}} + \mathcal{K}_{\text{orb}} + \text{higher order terms.} \tag{3}$$

$\mathcal{K}_{\text{Pauli}}$, given by eq (1), includes isotropic and anisotropic effects, directly by contact and spin dipolar interactions, and indirectly via core polarization and polarization of conduction band electrons below the Fermi level. The orbital paramagnetic and diamagnetic terms, $\mathcal{K}_{\text{orb}}$ and $\mathcal{K}_{\text{dia}}$, are important at times. We will review in this paper the various contributions to $\mathcal{K}$, as summarized in eq (3), in the light of experimental observations, together with theoretical methods for relating these results to the electronic structure of metals.

2. General Observations

In NMR one looks at transitions of a nucleus (with spin states $m = I, I-1, I-2, \ldots 1-I, -I$) from spin state m to $m \pm 1$, by measuring the frequency, ν, of the photons involved in these transitions. The energy difference between the two states, $\Delta E_{m \to m-1} = h\nu$, is directly proportional to the applied magnetic field, H_{appl}. However, even for a given isotope, the proportionality constant is different for different solids because the electrons in the solid respond differently to H_{appl} (paramagnetically or diamagnetically) causing an additional (positive or negative) field at the resonating nucleus. This magnetization field, as seen by the nucleus, is often referred to as the "internal field," H_{int}.

The Knight shift, $\mathcal{K}$, measures the internal field at the nucleus produced by those electrons in metals which respond linearly (with one exception, noted in sec. 6) to an applied field. Thus $\mathcal{K} \equiv H_{\text{int}}/H_{\text{appl}}$. Specifically, this definition excludes materials with spontaneous magnetization.

For simple metals, the conduction electrons cover a broad band of energy states. Those electrons at the Fermi surface are aligned paramagnetically by an external applied magnetic field. The resulting polarization of these electrons causes large internal fields, via the Fermi contact interaction hamiltonian, $\mathcal{H}_F$,

$$\mathcal{H}_F = \frac{16\pi}{3}\mu_B\gamma\hbar\mathbf{I}\cdot\mathbf{S}(\mathbf{r})\delta(\mathbf{r}), \tag{4}$$

where γ is the nuclear gyromagnetic ratio, and $\mathbf{S}(\mathbf{r})$ is the electron spin as a function of its position vector $\mathbf{r}$ from the nucleus. The contact (or δ-function) interaction samples the probability density $|\psi_A(0)|^2 \equiv P_A$ at the nucleus, for an electron in the atom. It is related to the atomic hyperfine coupling constant, $a(s)$, by

$$a(s) = \frac{16\pi}{3}\gamma\hbar\mu_B P_A. \tag{5}$$

The $\delta(\mathbf{r})$ thus restricts this effect to s-electrons and to the minor components of relativistic p-electrons. The s-effects are large, while the p-terms are almost invariably small and will henceforth be neglected. This large hyperfine term is generally absent in nonmetallic materials, because for each s-electron of spin-up, there is an s-electron of spin-down, and these are not decoupled by the usual applied magnetic fields.

For monovalent metals, $a(s)$ is obtained with high accuracy from atomic beam experiments. Values of $a(s)$ for the alkali metals are shown in table 1. The quantity more important to Knight shift considerations, P_A, is also shown. Note that P_A increases monotonically with atomic number for a given group, whereas $a(s)$ is dominated by the nuclear moment and appears random. Except for a possible small hyperfine structure anomaly, P_A is the same for all isotopes of a given element, whereas $a(s)$ depends on the given isotope.

TABLE 1. *Comparison of different ways of expressing the hyperfine coupling of a single s-electron, for the alkali metals.*

	$a(s)$ (cm^{-1})	P_A(cm^{-3})	$H_{\text{eff}}^{\text{atom}}$ (kOe)
^{7}Li.....	0.0134	15.7×10^{23}	122
^{23}Na.....	.0296	50.2×10^{23}	390
^{39}K.....	.00770	74.6×10^{23}	580
^{87}Rb.....	.114	154×10^{23}	1200
^{133}Cs.....	.0766	257×10^{23}	2000

The data for $a(s)$ were derived from data given by P. Kusch and H. Taub. Phys. Rev. **75**, 1477 (1949); the other columns were calculated from these using eqs (5) and (12).

In a metal the appropriate probability density P_F is obtained by taking a suitable average over the Fermi surface, $P_F = \langle\psi(0)^2\rangle_{E_F}$. The Knight shift, eq (1), has shown [2] to be

$$\mathcal{K} = \frac{8\pi}{3}\chi_p P_F, \tag{6}$$

where χ_p is the Pauli spin susceptibility per atom. Sometimes an explicit volume or mass factor appears in the expression for $\mathcal{K}$, but this depends on the appropriate normalization of $\langle\psi^2(0)\rangle_{E_F}$ and on whether a mass, volume, atomic or molar susceptibility is used.

If we define

$$\langle a\rangle \equiv \frac{8\pi}{3}\langle\psi(0)^2\rangle_{E_F} = \frac{8\pi}{3}P_F, \tag{7}$$

then we obtain eq (1).

Alternately it is convenient to introduce the effective hyperfine field H_{eff}, which is the field measured directly in ferromagnetic materials by, for example, ferromagnetic NMR or by Mössbauer spectroscopy. Then

$$H_{\text{eff}} \equiv \mu_B\langle a\rangle = \frac{8\pi}{3}\mu_B P_F. \tag{8}$$

Hence

$$\mathcal{K} = \frac{1}{\mu_B}\chi_p H_{\text{eff}}. \tag{9}$$

It has been found useful to define a factor ξ, sometimes called Knight's ξ factor [3], as

$$\xi \equiv \frac{P_F}{P_A} \equiv \frac{H_{\text{eff}}^{\text{metal}}}{H_{\text{eff}}^{\text{atom}}}. \tag{10}$$

In the simplest cases, ξ has been said to express the fraction of s-character at the nucleus in the metal at E_F, but as we shall see, ξ is more complex in its meaning for less simple cases. The Knight shift then becomes

$$\mathcal{K} = \frac{1}{\mu_B}\chi_p\xi H_{\text{eff}}^{\text{atom}}, \tag{11}$$

where

$$H_{\text{eff}}^{\text{atom}} = 19650\ a(s)\frac{I}{\mu_I}. \tag{12}$$

Here $a(s)$ is in cm^{-1}, $H_{\text{eff}}^{\text{atom}}$ in kOe, and μ_I is in nuclear magnetons. Values of $H_{\text{eff}}^{\text{atom}}$ are listed in table 1 for the alkali metals and in table 2 for some B-subgroup metals. The values for the monovalent metals are derived from atomic beam measurements. For polyvalent metals, Knight [3] has used measurements

on *excited ionic* states and then corrected for the degree of ionization. Knight estimated his resulting values of $a(s)$ to be accurate to perhaps 50 percent. Rowland and Borsa [6] avoided the problem of corrections by using measurements on *excited neutral* atom states. The values for the polyvalent metals in table 2 do not depend on *excited* state measurements, but instead were determined by scaling, based on atomic calculations, from the known monovalent values [7].

TABLE 2. H_{eff}^{atom} *values obtained by scaling from monovalent values* [7].

Group	*Atom*	H_{eff}^{atom} (kOe)
I	Cu	2,600
	Ag	5,000
	Au	20,600
II	Cd	7,000
	Hg	25,800
III	B	1,000
	Al	1,900
	Ga	6,200
	In	10,100
	Tl	34,000
IV	Sn	12,800
	Pb	41,400
V	N	3,300
	P	4,700
	As	8,900
	Sb	14,500
	Bi	49,000
VI	Te	17,200
X	Pt	20,000

The ξ factor accounts for any deviation in hyperfine coupling from free atom behavior. It may deviate from a value of one for a variety of reasons. For example, the average conduction electron density in a metal is greater than that in the free atom (*i.e.*, P_ψ is normalized to a Wigner-Seitz cell in the metal whereas the free atom P_ψ extends over a significantly larger volume). If no other factors were present, ξ would then be greater than unity. A Fermi surface orbital, ψ_F, has only partial s-character and this causes a reduction in ξ. In a "free electron metal," ψ_F is a plane wave ϕ_F (suitably orthogonalized to atomic core states) or a linear combination of plane waves. With increasing number of electrons in the bands the s-character of ψ_F decreases [8]. In a metal such as Tl, Pb, or liquid Bi, this reduction is quite substantial. In metals with one "free" conduction electron (*e.g.*, the alkali and noble metals), $\mathbf{k}_F$ is relatively small, and the reduction could be expected to be slight. Here, other orthogonalized plane waves, $\phi_{\mathbf{k}_F+\mathbf{Q}}$ (where $\mathbf{Q}$ is a reciprocal lattice vector) are mixed into ϕ_F and the normal *sign* of the mixing is such that interference causes $|\psi_F(0)|^2$ to be less than that predicted by $|\phi_F(0)|^2$ alone. This, as well as d-band hybridization and core-polarization factors which will be considered shortly, tend to predominate over the normalization effect reducing ξ to values typically between 0.1 and 0.8 in "simple" metals.

Experimental values for $\mathcal{K}$ are given in figures 2a and 2b. Using these measured values of $\mathcal{K}$, and obtaining χ_p as explained in the next section, the systematic trends for ξ seen in figure 3 are obtained.[4] In each period the largest ξ values are found for the monovalent metals, with ξ falling smoothly to lower values as the group valence increases, as would be expected from the wave function behavior just discussed. It is interesting that these results are obtained despite the changing crystal structures. About one-half the observed drop in ξ is expected from simple estimates [8] of the reduction in s-character with increasing $\mathbf{k}_F$; the increasing atomic volumes of the polyvalent over the monovalent metals further enhances the trend.

The induced conduction electron Pauli spin density may also contribute to the hyperfine coupling constant, $\langle a \rangle$, via the spin dipolar interaction

$$\mathcal{H}_{SD} = -2\mu_B \gamma N\hbar \mathbf{I} \cdot \left(\frac{\mathbf{S}}{r^3} - \frac{3\mathbf{r}(\mathbf{S}\cdot\mathbf{r})}{r^5} \right), \qquad (13)$$

where $\mathbf{r}$ is the vector from the nucleus to the electron. This interaction is anisotropic and contributes an orientation dependent Knight shift term, $\mathcal{K}_{\text{anis}}$, for nuclei at noncubic sites, and occasionally at cubic sites if spin-orbit coupling is present. In powders, this term results in structure and broadening of the NMR line.

The induced Pauli spin density interacts *directly* with the nucleus only via the contact and spin dipolar interactions but it may act *indirectly* as well. The spin density has a spin dependent exchange interaction associated with it, which arises from the Pauli exclusion principle. This may polarize the closed shells of an ion core and the paired electrons in the conduction bands *below* E_F, producing spin densities which will then interact with the nucleus via the contact (and for noncu-

[4] From figure 3, a ξ value for Zn between that of Cd and Hg can be extrapolated. From this $\mathcal{K}$ for Zn is predicted to be 0.20 percent. This is not far from the value 0.26 percent predicted [9] from quite different considerations.

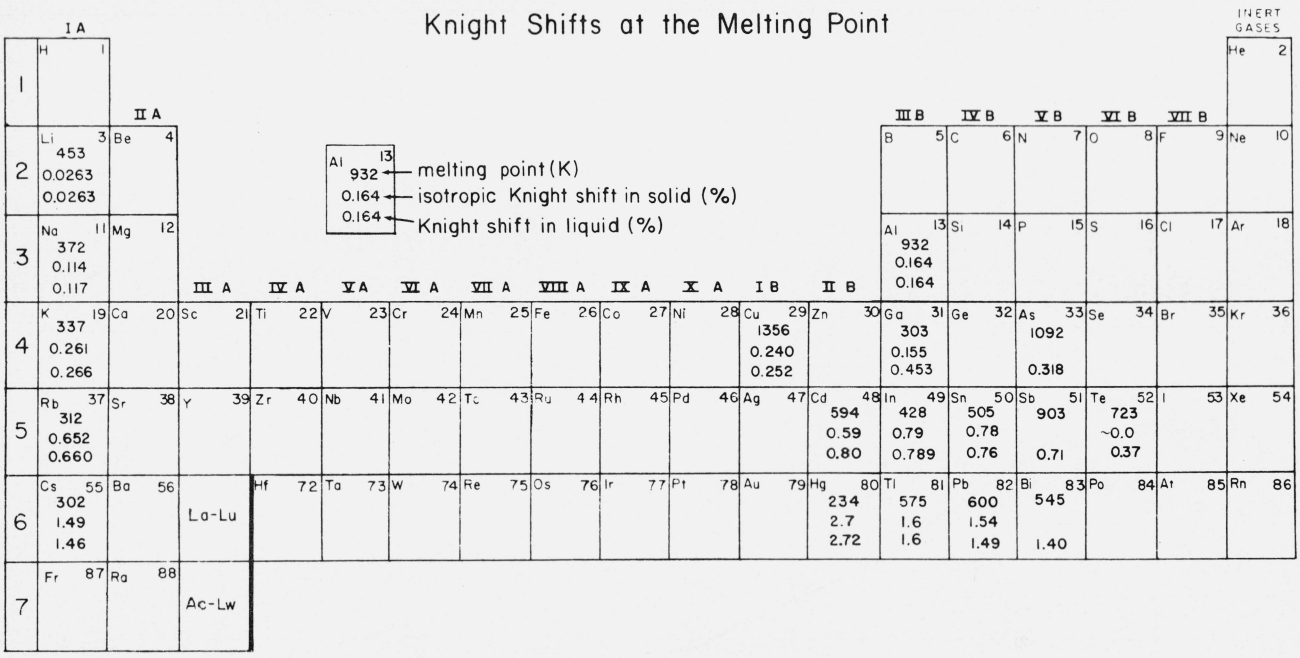

FIGURE 2a. *Knight shifts in metals as compiled at the Alloy Data Center (NBS). Note: Literature references available on request. (a) Knight shifts in the solid and liquid state at the melting point.*

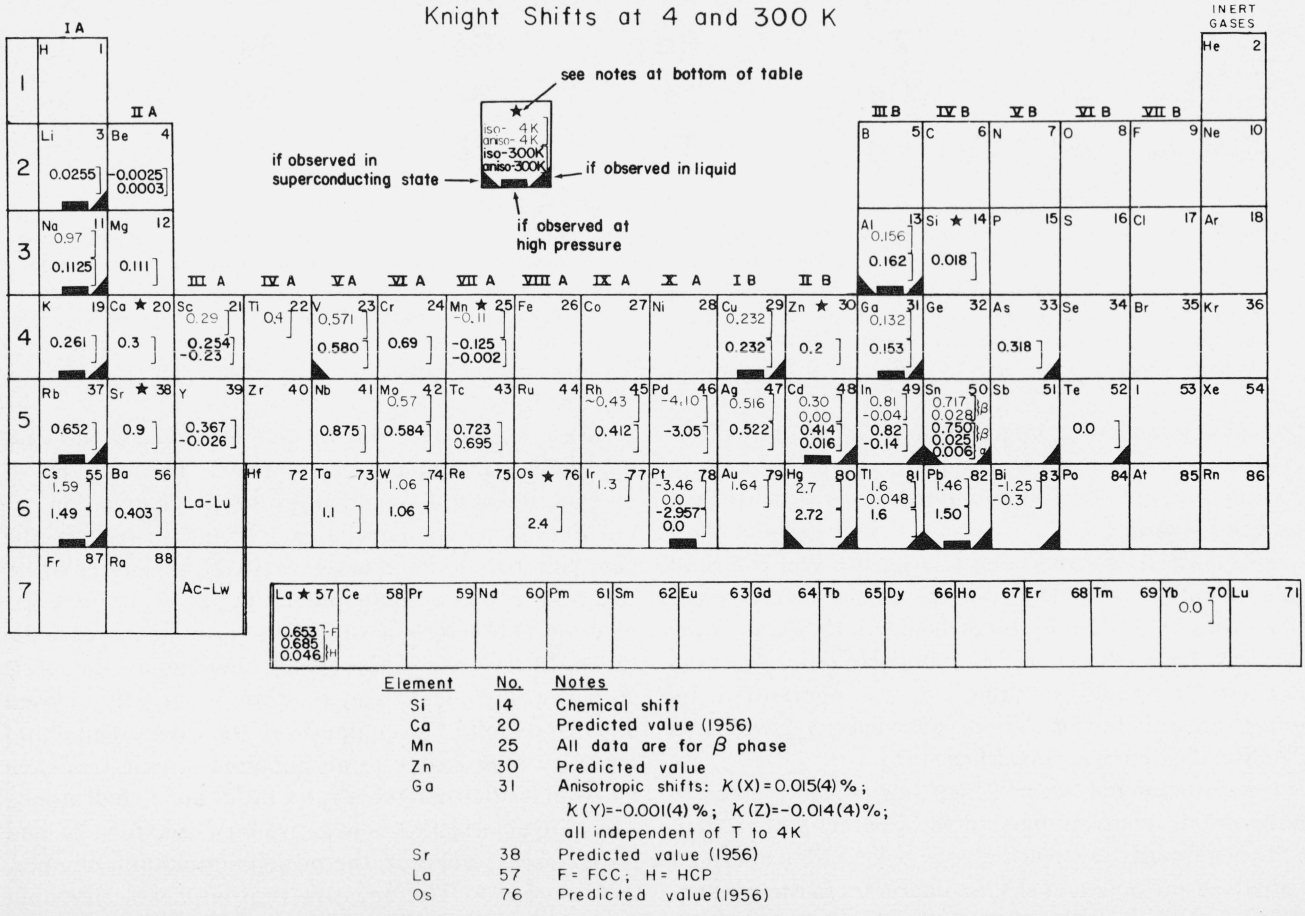

Element	No.	Notes
Si	14	Chemical shift
Ca	20	Predicted value (1956)
Mn	25	All data are for β phase
Zn	30	Predicted value
Ga	31	Anisotropic shifts: $K(X) = 0.015(4)\%$; $K(Y) = -0.001(4)\%$; $K(Z) = -0.014(4)\%$; all independent of T to 4K
Sr	38	Predicted value (1956)
La	57	F = FCC; H = HCP
Os	76	Predicted value (1956)

FIGURE 2b. *Knight shifts in metals as compiled at the Alloy Data Center (NBS). Note: Literature references available on request. (b) Isotropic and anisotropic Knight shifts at room and liquid helium temperatures.*

383-876 O - 70 - 8

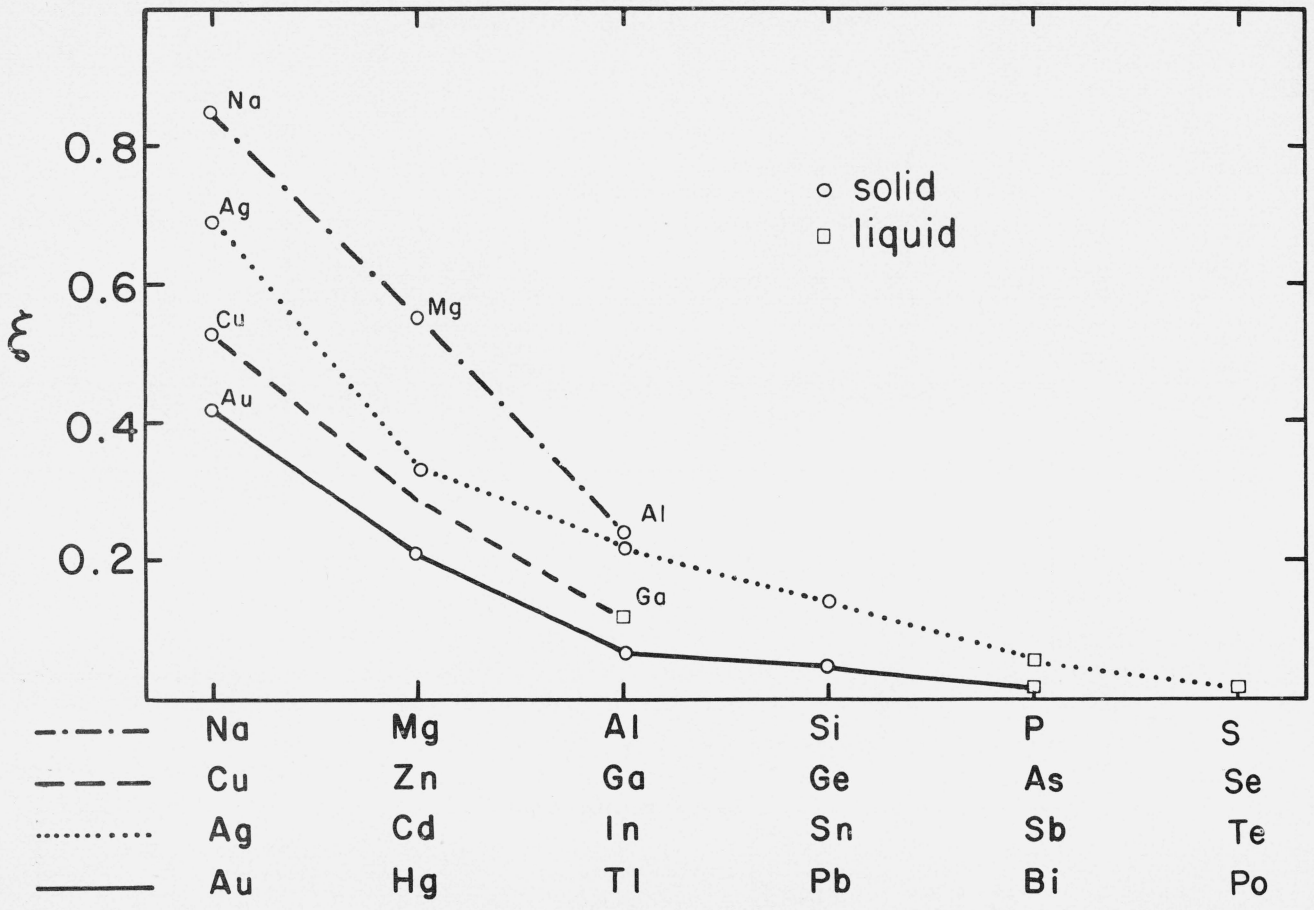

FIGURE 3. *Behavior of Knight's ξ values for metallic elements as a function of their position in the periodic table. The points for each row in the table are connected using the sumbols for lines as shown outside the left lower corner of the plot. Those points shown as circles are for the metals in the solid state and those shown as squares were calculated for the metals in the liquid phase. For the former points χ_p was calculated using γ_{el} values [37]; for the liquid metals χ_p was taken to be $3/2(\chi_{expt}-\chi_{dia}^{core})$ using χ_{expt} from the Landolt-Börnstein Tables and χ_{dia}^{core} from Hurd and Coodin [33]. The absolute values of ξ are affected by uncertainties in the estimates of χ_p and H_{eff} but the relative behavior (from element to element) along each row is probably realistic. Points for solid Ga and liquid As are omitted for lack of accurate values for $\mathcal{K}_{iso}$ and $\chi_p(liq)$, respectively. The plot provides an estimate for the Knight shift of Zn which has yet to be observed.*

bic sites, spin dipolar) interaction(s). These interactions arise from *differences* induced in the spatial behavior of spin up and spin down pairs of electrons with *zero net spin* induced in the electron pairs. Their existence has been established experimentally by the fact that half filled shell (p^3, d^5, and f^7) S-state atoms have nonzero hyperfine fields. While the exchange interaction is believed to be the origin of this spin polarization, correlation effects should, in principle, be important to its quantitative behavior. These interactions have been discussed extensively elsewhere [10].

For the moment we will limit our considerations to intra-atomic contributions to the contact interaction. This necessarily involves the spin polarization of closed s-shells of the core and of the s-character in the conduction bands below E_F, since only these will interact directly with the nucleus. Estimates of these core polarization effects from valence electrons in the various shells are summarized in table 3. These are based on experimental data and on exchange polarization calculations (*i.e.*, no correlation effects). Listed are the sign and magnitude characteristic of the core polarization response to a single unpaired s-, p-, d-, or f-valence electron characteristic of various rows of the periodic table. (In the case of the open p-shell atoms, the listed response includes that associated with the closed valence s-shell.) For comparison, the direct contact interaction appropriate to an unpaired atomic s-valence electron is shown in table 4, for the d- and f-shell atoms. The core polarization is negative for d- and f-shells, and for np-shells, where n, the principal quantum number, is 4 or greater. The negative sign implies a core spin density at the nucleus, whose orientation is *antiparallel* to the unpaired spin responsible for the

TABLE 3. *Rounded value for hyperfine fields due to the core polarization response to a* single *unpaired open valence shell electron.*

Open valence shell	Core polarization hyperfine field, H_{eff}, per unpaired valence electron, *kOe*	Comments on source(s) of core polarization values. (For further comments and details of most of the data see Ref. 10).
$2p$.....	+30	Experiment, appropriate to neutral N alone.
$3p$.....	+15	Experiment, appropriate to neutral P alone.
$4p$.....	−50	Experiment, (neutral As $4s^24p^3\ ^4S$).
$5p$.....	−150	Experiment (neutral Sb $5s^25p^3\ ^4S$).
$6p$.....	−300	Experiment (neutral Bi $6s^26p^3\ ^4S$).
$3d$.....	−125	Calculation and experiment for $3d^n4s^0$ ions.
$4d$.....	−350	Calculation and limited experiment for $4d^n\ 5s^0$ ions.
$5d$.....	−750	Calculation (J. V. Mallow, A. J. Freeman and P.S. Bagus, J. Appl. Phys., to be published).
	−600	Inferred from hyperfine anomaly, [G. J. Perlow, W. Henning, D. Olson and G. L. Goodman, Phys. Rev. Letters **23**, 680 (1969)].
$4f$.....	0 to −50	Calculation and limited experimental data.
ns.....	>0	Estimated by calculation to make a 10–50% enhancement of a ns shell's direct contact interaction.

TABLE 4. *Direct plus associated core polarization contact hyperfine fields due to a single unpaired valence* s*-electron for various rows in the periodic table.*

s shell	Atoms	*s*-contact hyperfine field, H_{eff}, kOe
$2s$.....	$2p^1$–$2p^3$ elements	1,000– 4,000
$3s$.....	$3p^1$–$3p^3$ elements	2,000– 5,000
$4s$.....	$3d$ transition metals	2,000– 3,000
$4s$.....	$4p^1$–$4p^3$ elements	4,000–10,000
$5s$.....	$4d$ transition metals	4,000– 5,000
$5s$.....	$5p^1$–$5p^3$ elements	7,000–15,000
$6s$.....	rare earths	9,000–15,000
$6s$.....	$5d$ transition metals	15,000–20,000
$6s$.....	$6p^1$–$6p^3$ elements	25,000–50,000

polarization. The core polarization response to an unpaired s-valence electron is positive and simply serves to enhance the contact interaction associated with the valence electron. [When using experimental atomic hyperfine data to evaluate P_A, this effect is already included.] The $3d$, and $4d$ (little is known yet for the $5d$) core polarization values appear to be quite stable for their respective rows in the periodic table. The quoted values hold to within twenty percent for any member of a row and it is believed that these values are appropriate to the core polarization response to a d-moment in a metal.

The situation is less certain and more complicated for the p-shell elements. Experimental data for which there are no competing orbital and spin dipolar terms exist only for the p^3 S-state atoms. It should be noted that these experimental values include the contribution coming from the polarization of the closed *valence* s-shells. In a metal this term is associated with the conduction band and not the core states. There is some uncertainity as to the sign and magnitude of this core plus valence s polarization term as one goes across the $2p$ and $3p$ rows. Recent spin polarized Hartree-Fock calculations of Bagus *et al.* [11] for these rows suggest that both the core and valence contributions are significant with the total becoming less positive (or more negative) as one goes to the lighter elements in the row. As with earlier efforts [10], these calculations do not satisfactorily reproduce the experimental data and must be used with caution, (*e.g.*, the wrong sign is predicted for atomic P). Bagus *et al.* also obtained results for the $4p$ row. Again the total becomes more negative by a factor of, say, two for the lighter elements but now the valence term dominates. This latter fact suggests that such atomic hyperfine constants will be of little quantitative utility when inspecting p-electron metals until one understands the polarization response of s-electron character deep in a conduction band. An example in the literature of the use of a p-core polarization term larger than that shown in table 3, is Ga in $AuGa_2$ [12], where a p-term of an order of magnitude larger than that of As (table 3) was used to explain the observed negative Knight shift.

One complication associated with extracting wave function and density of states information from Knight shift measurements is suggested by the numbers in table 3. Consider the $3d$- and $4d$-transition metals. As discussed in section 7, the Pauli Knight shift term almost invariably has the opposite sign of temperature dependence as the Pauli susceptibility [13]. This is consistent with having d-bands at E_F, with negative hyperfine constants of the sort seen in the table. Now, the s-contact densities are an order of magnitude larger than the corresponding d-core polarization hyperfine constants. Thus a few percent admixture of s-character into the Fermi surface d-states can violently affect $\langle a \rangle$.

While complicating matters, such interband hybridization is of considerable interest in itself and one can attempt to use Knight shift data to ascertain its nature and extent [14,15].

Relatively little is known of the intra-atomic hyperfine contribution arising from the exchange polarization of conduction band states below E_F, except that it probably makes a positive contribution to $\langle a \rangle$ for transition metals. Some measure of the effect can be obtained for the $3d$ metals by inspection of the spin polarization of the $4s^2$ shell in the neutral $3d^n4s^2$ atoms. Experiment and exchange polarized calculations indicate [10,16] a $4s^2$ hyperfine field of $\sim +100$ kOe per unpaired d-electron, a contribution which almost cancels the $1s^2 + 2s^2 + 3s^2$ core polarization. One expects a smaller effect in a metal since there are typically one, not two, electrons worth of "s" character below E_F. One might expect a further reduction, in view of the fact that ξ values defined for Fermi level states always lie below 1. Paired Block states near the bottom and throughout an occupied "conduction" band contribute to the exchange polarization. These states have stronger hyperfine coupling than those at E_F which contribute to the Knight shift, as is evidenced by internal conversion experiments [17]. It is probable that there is little or no reduction in this polarization term due to band effects.

There may be *inter*-atomic as well as *intra*-atomic contributions to $\langle a \rangle$, since an applied magnetic field induces spin moments on the neighboring atoms as well as the atom in question. The two contributions are indistinguishable for the pure monatomic metals, but there is indirect evidence, from alloying, that the interatomic term is quantitatively important in some transition metals. *Inter*-atomic contributions will be seen to be important in transition metal alloys and intermetallics. As with the concept of a *local* density of states, there will frequently be ambiguity when attempting to divide $\mathcal{K}$ into inter- and intra-atomic terms.

In addition to these contributions to the Knight shift coming from the Pauli paramagnetism of the conduction electrons, there is an important contribution, especially in transition metals, from the orbital magnetic moment of the conduction electrons induced by the applied magnetic field. We can write, in analogy with eq (1)

$$\mathcal{K}_{\text{orb}} = \langle b \rangle \chi_{\text{orb}} \tag{14}$$

where $\langle b \rangle$ is an appropriate orbital hyperfine coupling constant. In contrast to the Pauli contribution to the Knight shift, the orbital Knight shift is not proportional to $N(E_F)$.

The orbital Knight shift [18-20] involves the orbital moment induced in occupied conduction electron states by an applied magnetic field, **H**. It is a second order term of the form

$$\mathcal{K}_{\text{orb}} = \frac{2\mu_B^2}{IH} \sum_{E_i < E_F} \sum_{E_f > E_F} \frac{\langle i | \mathbf{H} \cdot \vec{\ell} | f \rangle \left\langle f \left| \frac{2\vec{\ell} \cdot \mathbf{I}}{r^3} \right| i \right\rangle \delta(\mathbf{k}_f - \mathbf{k}_i)}{E_i - E_f}$$

$$\equiv \langle b \rangle \chi_{\text{orb}} \equiv 2\chi_{\text{orb}} \langle r^{-3} \rangle . \tag{15}$$

Here the matrix elements are evaluated over a Wigner-Seitz cell. The occupied and unoccupied Bloch states, i and f, are admixed by the application of the field. The resulting admixture produces a moment which interacts with the nucleus. Except for pathological cases, where there are a substantial number of strongly admixed states within kT or E_F, there is little or no temperature dependence in this term, as is the case in the analogous Van Vleck temperature-independent paramagnetism in ionic salts. A rough estimate of the strength of the orbital Knight shift is given by [17].

$$\mathcal{K}_{\text{orb}} \approx \frac{n_i n_f \left\langle \frac{1}{r^3} \right\rangle}{\Delta} , \tag{16}$$

where n_i and n_f are the numbers of occupied and unoccupied Bloch states respectively and Δ is the conduction electron bandwidth. This equation suggests that particularly strong orbital effects are expected in roughly half-filled d-band transition metals. In half-filled bands the product $n_i n_f$ is a maximum, and in transition metals, Δ is small. Strong effects have indeed been found in W [21], Nb [20], V [19,20,22], Cr [23] and CrV alloys [24].

Although we have treated the Pauli and orbital hyperfine parameters, a and b, as multiplicative factors of the appropriate susceptibilities, it should be emphasized that $\langle a \rangle$ and $\langle b \rangle$ are not the simple averages customarily employed, but are more correctly the weighted averages

$$\langle a \rangle \equiv \frac{\langle a \chi_p \rangle}{\chi_p} \tag{17}$$

and, as is clear from eqs (14) and (15),

$$\langle b \rangle \equiv \frac{\langle b \chi_{\text{orb}} \rangle}{\chi_{\text{orb}}} . \tag{18}$$

The $\langle\,\rangle$ denote an average over all bands. For the Pauli term, the average is over segments of Fermi surface where the contribution of a segment to χ_p is multiplied

by the hyperfine constant, a, appropriate to that segment (*i.e.*, to its electron character). Equation 15 defines the average for the orbital term, where the induced orbital moments associated with initial and final states, i and f, are weighted by their hyperfine coupling constants. With this, the general expression for the Knight shift, eq (3), becomes

$$\mathcal{K} = \langle a\chi_p \rangle + \mathcal{K}_{\text{dia}} + \langle b\chi_{\text{orb}} \rangle + \text{higher order terms.} \quad (19)$$

The Knight shift provides samplings of wave function and, in some senses, density of states character different from that obtainable in other experiments. The Pauli term can in principle, and does occasionally in practice, yield considerable insight into the Fermi surface states contribution to $N(E_F)$. A particular case is that of alloys and intermetallic compounds with different $\langle a \rangle$'s at different atomic sites. This involves the variation in wave function character from site to site and, if you will, the variation in a *local* density of states. There is some arbitrariness as to whether one wishes to describe this in terms of $\langle a \rangle$ or a local χ_p.

A particularly clear example of this local nature is that of α-Mn. For this structure there are four crystallographically inequivalent sites. Above the Néel temperature of 95 K, four distinct resonances were observed [25,26]. Two of these had large negative shifts of -5.2 and -2.6 percent at room temperature [26], and were temperature dependent [25], with the former value increasing to -5.85 percent at 120 K, where χ shows a maximum. The nuclei at the other two crystallographically inequivalent sites showed much smaller, and temperature independent, Knight shifts (-0.45 and -0.15%).

A number of complications have been indicated in this section. There is more than one term in the Knight shift; also the hyperfine constants $\langle a \rangle$ and $\langle b \rangle$ are significantly affected by band character and hybridization. There will in general be *inter-* and *intra-*site contributions to $\langle a \rangle$. As will be seen, two important "tools" are available to aid in the identification of the different contributions to $\mathcal{K}$: the Korringa relation [27] relating Knight shifts to nuclear spin-lattice relaxation times, and the temperature dependence of both $\mathcal{K}$ and χ [13]. Finally one can sample Knight shift behavior at sites involving different atoms in an alloy or intermetallic compound. Matters such as these, while complicating Knight shift interpretations in terms of density of states, can supply insight into the electronic structure and local wave function character which cannot generally be obtained from other experiments.

3. Pauli Spin Susceptibility

The Knight shift samples the density of states via the Pauli spin susceptibility, χ_p. However, in pure metals, the density of states has usually been obtained in other ways and the Knight shift then used to explore the associated wave-function character. In this section, we will review some of these methods of obtaining χ_p, and their implications to our understanding of Knight shift behavior.

First let us note that the expression relating the Pauli susceptibility to the density of states given in eq (2) neglects correlation and exchange effects between conduction electrons. Electron gas estimates are frequently applied to "free" electron metals [28,29], and exchange enhancement theories to transition metals [30-32]. With a conduction-electron conduction-electron exchange interaction parameter $\mathcal{J}_{\text{eff}}$ defined in reciprocal space and taken to be constant, the random phase approximation yields [30-32] an exchange enhanced susceptibility

$$\chi_p = \frac{\chi_p^0}{1 - \mathcal{J}_{\text{eff}}\chi_p^0}, \quad (20)$$

where χ_p^0 is the unenhanced susceptibility of eq (2). The induced spin sets up an exchange field encouraging further polarization hence an enhanced χ_p. Similar looking expressions, with $N(E_F)$ appearing in numerator and denominator are obtained from correlated electron gas theory. These as well as interband effects obviously complicate the averages taken in eq (17). In general one is forced to neglect them in $\langle a \rangle$ and assume their presence in χ_p alone. Even with this simplification, there is no simple linear relation between an observed Knight shift and the density of states at the Fermi surface. As remarked earlier, this shortcoming is shared with the experimental data obtained by many of the other techniques reviewed in this symposium.

It might appear that an adequate value of χ_p could be obtained from direct measurements of magnetic susceptibilities, χ_{exp}, especially since these would already have the exchange enhancement included. We will return to the case of transition metals later, but in simple metals it turns out that bulk susceptibility results usually do not give reliable values of χ_p. Consider, for instance, the noble metals. The bulk susceptibilities (χ_{exp}) are each negative, *i.e.*, the metals are diamagnetic. The ion core diamagnetism ($\chi_{\text{dia}}^{\text{core}}$) plus conduction electron diamagnetism ($\chi_{\text{dia}}^{\text{cond}}$) is larger than χ_p. Hartree-Fock [7] and Hartree-Fock-Slater [33] calculations for $\chi_{\text{dia}}^{\text{core}}$ agree to within two percent. However these calculations are for singly ionized valence states

which is not a totally satisfactory description in the metal. This, and interband mixing effects, raise the probable error in χ_{dia}^{core} considerably. By the same token, χ_{dia}^{cond} is poorly known due to electron-electron interactions. The net result is that χ_p obtained from χ_{exp} is probably good to no better than twenty percent for the noble metals. Various ξ values for the noble metals obtained by use of various schemes are shown in table 5. It can be seen that ξ values employing the traditionally quoted values for χ_{dia}^{core} are not consistent with those using more modern Hartree-Fock or Hartree-Fock-Slater estimates. The situation in the case of the alkali metals is not as bad for two reasons. First the theoretical evaluation of both the core- and conduction-electron diamagnetism is on firmer ground, especially for the free electron-like metal, Na. Secondly, χ_p has been obtained directly (*i.e.*, without the need for the troublesome diamagnetic corrections) using conduction electron spin resonance (CESR) for the alkali metals and for Be. Combined CESR-NMR has also been used in Na and Li [34-36] to obtain χ_p.

For many metals it has been customary to use electronic specific heat, γ, measurements for information about χ_p^0 using the one-electron relationship

$$\chi_p^0 = 3\left(\frac{\mu_B}{\pi k}\right)^2 \gamma, \qquad (21)$$

where k is the Boltzmann constant. There are two difficulties here. One is that there may be many-body contributions to γ (such as electron-phonon or paramagnon enhancement). The other is that the exchange enhancement part of χ_p is missing here [see eq (20)]. The ξ values derived from γ, given in table 5, were obtained from eq (21) and experimental γ values [37], and therefore neglect these corrections for enhancement effects. It may be that in some cases these two factors approximately cancel one another. The ξ values plotted for the elements in figure 3 were obtained by use of uncorrected γ values [37]. The final set of ξ values in table 5 utilizes a set [38] of band theory predictions for χ_p^0. Cancellations of various enhancement factors do not occur. The resultant ξ values are therefore larger.

TABLE 5. *ξ values for Cu, Ag and Au using various available data for χ_p* (see text for details).

	Cu	Ag	Au
From $3/2(\chi_{exp} - \chi_{dia}^{core})$ Hartree-Fock core.....	.37	.50	.32
From $\chi_{exp} - \chi_{dia}^{core} - \chi_{dia}^{cond}$ Hartree-Fock core.....	.45	.45	.36
From $3/2(\chi_{exp} - \chi_{dia}^{core})$ Hartree-Fock-Slater core.....	.38	.52	.36
From $3/2\ (\chi_{exp} - \chi_{dia}^{core})$ traditional core.....	.45	.16	.08
From uncorrected electronic specific heat, γ...	.53	.69	.42
From band calculations presented at this Symposium, χ_p^{bare} [38].....	.57	.68	.56

It is instructive [39] to compare the value of χ_p^0 (obtained from γ) to the value of $\xi\chi_p$ obtained by dividing $\mathcal{K}$ by atomic H_{eff} values (tables 1 and 2). This is done in figure 4. The trend in our plot differs from that of Ziman [39] primarily due to our choice of atomic, rather than mass, units. The lightest alkali, Li, displays significantly less *s*-character than the other alkali metals [40-47]. The ξ values for the *B*-subgroup metals are all considerably lower, especially for the polyvalent elements; this might be expected, since the Fermi level lies higher in conduction bands, implying less *s*-character at E_F and hence a smaller contact term. The associated increase in *p*- and *d*-character will generally make a negative (core-polarization) contribution to $\mathcal{K}$, also lowering ξ.

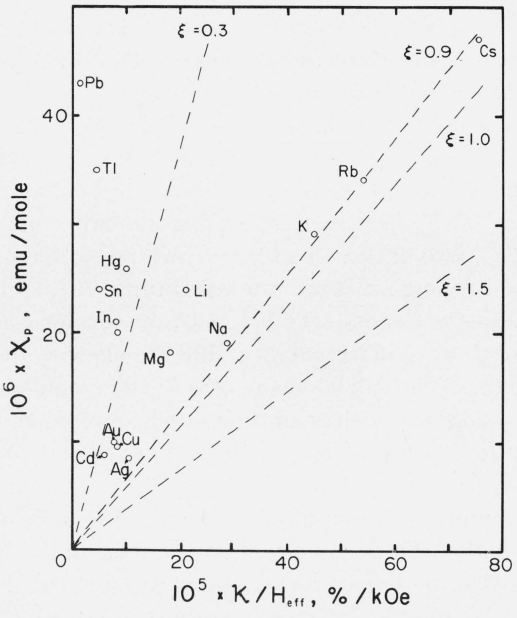

FIGURE 4. *χ_p versus $\mathcal{K}/H_{eff}$ for pure metals in customary units. Lines of constant ξ (dashed) are shown. Due to the small ξ values for the heavier metals most of the data points are bunched at the left hand side of the plot. The χ_p values were obtained from electronic specific heat data [37]. In the case of potassium a large uncertainty in the specific heat gives rise to an error of nearly half the size of the vertical dimension. The point shown for potassium represents the listed [37] γ value.*

We note an interesting correlation in figure 4 in that the alkali metals, except for Li, fall on a straight line near $\xi = 0.9$. That is to say, the *s*-density of states apparently increases proportionately to the total density of states at the Fermi level for Na, K, Rb and Cs. The

increase in χ_p from Na to Cs is attributable primarily to the large volume increase in this series. The constancy of ξ might seem to be surprising, since simple volume renormalization should effect ξ as well as χ_p. It is to be recalled, that volume renormalization of ξ depends on the atomic volume in the metal *relative* to that of the free ion. It would thus appear that the alkali metal lattice constants faithfully reflect the sizes of the free ions, and hence ξ is roughly constant implying that the amount of *s*-character is essentially constant for the alkali metals Na to Cs. This constancy was already noted by Pauling [47]. His calculations of *s-p* hybridization of bond orbitals indicated fractional *s*-characters of 0.72 to 0.74 for Na to Cs and a lower value (0.59) for Li, similar to the trend of figure 4.

Knight shift experiments on the pressure dependence, as well as alloying, show that the contact density in metals is not simply an inverse function of volume [7]. This is also illustrated by recent pressure dependence calculations [48] on monovalent metals. The wave function effects which depress ξ values below 1, suppress the dependence of ξ on volume.

In this section, we have seen the difficulty in obtaining a reliable value of χ_p for use in obtaining ξ values for simple metals. Nonetheless, even in these cases, the Knight shift provides a rather unique measure of the *s*-contribution to the density of states in "simple" metals.

4. "Simple" Metals

It is an interesting challenge to obtain the absolute value of the Knight shift, or its change with temperature or pressure, from band-theoretical calculations. A number of near *a priori* calculations have been made with varying degrees of semiquantitative success. For example, Das and coworkers, using the orthogonalized plane wave (OPW) method, have calculated wave functions and densities-of-state at various points on the Fermi surface for Al [49], Be [50-53] and In [54]. A few of these papers are of particular interest in that they represent efforts to use the weighted average form of $\langle a \rangle$ as given in eq (17). In the case of the divalent metals Be, Mg and Cd, the spin susceptibility has been extracted from Knight shift measurements by use of such estimates of $\langle a \rangle$ [55]. Comparison with theoretical values of their bare χ_p [*i.e.*, eq (2)] permitted estimates of the exchange enhancement to be made. This process resulted in a reduction in χ_p for Be; the authors concluded that this arose from inadequacies in the energy band estimate of χ_p^0 and $\langle a \rangle$.

The alkali metals, particularly Li and Na, have traditionally attracted theoretical attention, often giving relatively close agreement with experiment [40-42]. Even in these simplest "free electron" metals, corrections to the hyperfine coupling constant due to non-free electron-like band structure effects, can amount to 25 percent or more [45,56,57].

It should be stressed that for the heavier simple metals (*i.e.*, potassium and above) *d*-hybridization associated with *d*-bands above or below the conduction band affects the Knight shift and other properties at (and off) the Fermi level (see, for example, Kmetko [46]). In the case of Cu and Au these *d*-hybridization effects are large. Such effects do not arise in the Li row, but there may be abnormal "2*p*" effects due to the near degeneracy of atomic 2*s*- and 2*p*-levels [58-61]. In these "simple" metals, the change in Knight shift at the melting point [62] (fig. 2a) is usually not large, and its temperature dependence in the solid, slight (fig. 2b). As an example, consider Al. At the melting point, $\mathcal{K}$ has the same value for both liquid and solid. The temperature dependence in the solid is illustrated by the data of Feldman [63] (fig. 5). The change in Knight shift of Al is less than 2 percent of $\mathcal{K}$ over a temperature range from 4 to 300 K. The solid line in figure 5 represents a simple volume renormalization theory based on the thermal lattice expansion, which fits quite well at temperatures above the Debye temperature. No satisfactory explanation has been given for the deviation from this theory at low temperatures. Similar effects were observed in Na and Pb [63].

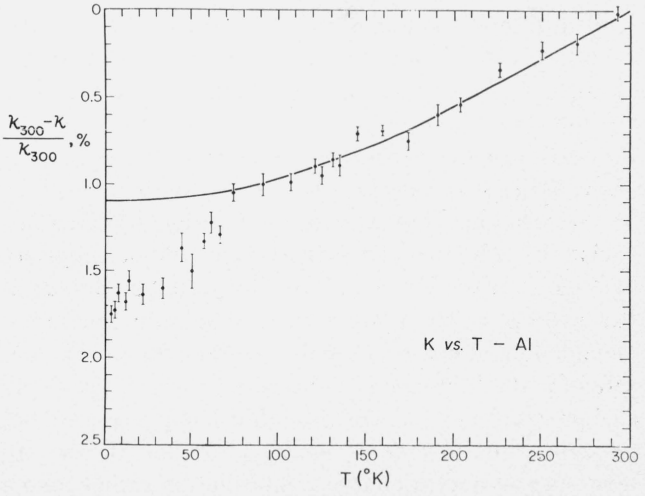

FIGURE 5. *Change in the aluminum Knight shift with temperature, as taken from Feldman [63]. The solid line is theoretical.*

A more unusual case is that of cadmium [64-70]. In the solid the Knight shift varies considerably. $\mathcal{K}$ increases ten times more rapidly in Cd than in Al, over the same temperature range (4-300 K). At 600 K, $\mathcal{K}$ in

Cd is about 70 percent larger than its value at 4 K. This change is seen in figure 6. An additional increase in $\mathcal{K}$ ($\sim 33\%$ of $\mathcal{K}$) is observed upon melting (see sec. 5). The anisotropic Knight shift, $\mathcal{K}_{\text{anis}}$, [see eq (13)] also increases with temperature. Cd exhibits a large change

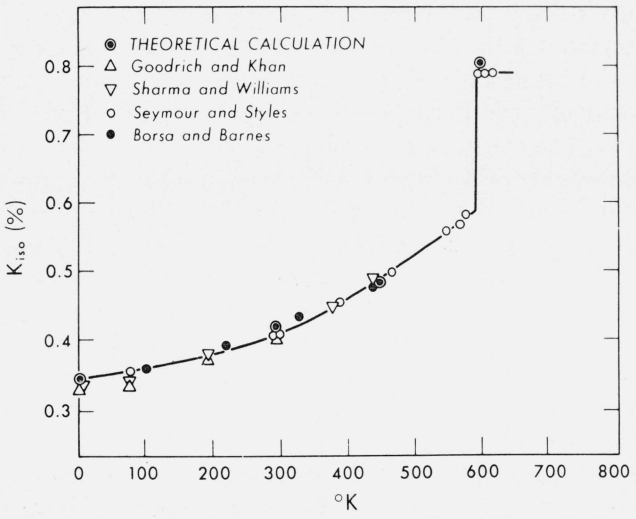

FIGURE 6. *Change in the cadmium Knight shift with temperature, as taken from Kasowski and Falicov [68].*

in the shape (c/a ratio) and volume of the unit cell with temperature and it had been suspected that the changes with temperature of $\mathcal{K}_{\text{iso}}$ and $\mathcal{K}_{\text{anis}}$ could somehow be correlated with these cell dimensions. Kasowski and Falicov [68] have explained the behavior with a different scheme: in the solid the lattice vibrations cause an increase in both χ_p and in the s-character as the temperature is raised, thereby increasing $\mathcal{K}_{\text{iso}}$. On the other hand, $\mathcal{K}_{\text{anis}}$ arises from the non-s part of the wave-function, which of course is decreasing as the s-part is increasing. However, again invoking eq (17), we require not the average hyperfine coupling associated with the non-s part, but the appropriate average over the Fermi surface. Cancellation occurs in this average at low temperatures. The reduction in the cancellation at higher temperatures more than compensates for the increase in s-character, thereby providing an increase in $\mathcal{K}_{\text{anis}}$. On the other hand, pressure dependence measurements of $\mathcal{K}_{\text{anis}}$ for Sn [71] was interpreted as due to charge redistribution rather than a change in the s-p character of the wave-function.

Other data further indicate the complexity of the behavior of the Knight shift in solid Cd. Borsa and Barnes [65] note that alloying Mg (in quantities of $\sim 1\%$) with Cd will cause substantial changes in cell size and shape without affecting the Knight shift. Kushida and Rimai [72] have separated the implicit and explicit contributions to the temperature dependence of $\mathcal{K}$ by their measurements of the pressure dependence in Cd. Volume renormalization was found inadequate to explain the observed pressure dependence [72].[5]

5. Sudden Changes in $\mathcal{K}$

The abrupt change in $\mathcal{K}$ of Cd upon melting was presumed by Ziman [39] to indicate an abrupt change in $N(E_F)$ associated with solid and liquid Cd. This conclusion was examined in two different calculations, each employing nonlocal pseudopotentials [68,70], resulting in opposite conclusions. Shaw's calculated [70] values for $N(E)$ per unit volume for solid and liquid Cd are shown in figure 7. $N(E_F)$ is found to be 0.7 percent *lower* in the liquid than in the solid. Shaw concludes that "Ziman's assertion that the strong change in the Knight shift of cadmium is a density-of-states effect is not borne out by our detailed calculations." In contrast Kasowski and Falicov [68] assume that Cd is free-electron-like in the liquid and finds that most of the change in $\mathcal{K}$(Cd) upon melting is due to an increase in $N(E_F)$. They note that "this agrees with Ziman's hypothesis and confirms it quantitatively." Although these two calculations [68,70] resulted in opposite conclusions, in part due to choice of different model-potentials, there is an abrupt increase in $N(E_F)$ in Shaw's calculations if solid Cd is compared with the free electron value, as indicated in figure 7.

An interesting example of an even more abrupt increase in $\mathcal{K}$ upon melting is found in the behavior of the III-V compound InSb [73]. In the semiconducting solid the Knight shift of either the In or Sb in InSb is zero, but in the metallic liquid state, the Knight shifts have normal metallic magnitudes. Another example is Bi [62], in which $\mathcal{K}$ has the opposite sign in the liquid from the solid.

There are various cases besides melting where a sudden change in $\mathcal{K}$ occurs. In an alloy system, $\mathcal{K}$ usually changes smoothly with composition within a particular phase, but shows a jump across a phase boundary. An example of this is shown for the AgCd system in figure 8, taken from Drain [74]. By correlating $\mathcal{K}$ and γ across a phase boundary, Drain showed that in this case the abrupt change is associated in part with changes in densities of states.

[5] There are other examples of an observation concerning the volume dependence of $\mathcal{K}$. As noted earlier, in our discussion of figure 4, simple volume renormalization is not often useful in explaining Knight shift results. See also [7] for a discussion of this point.

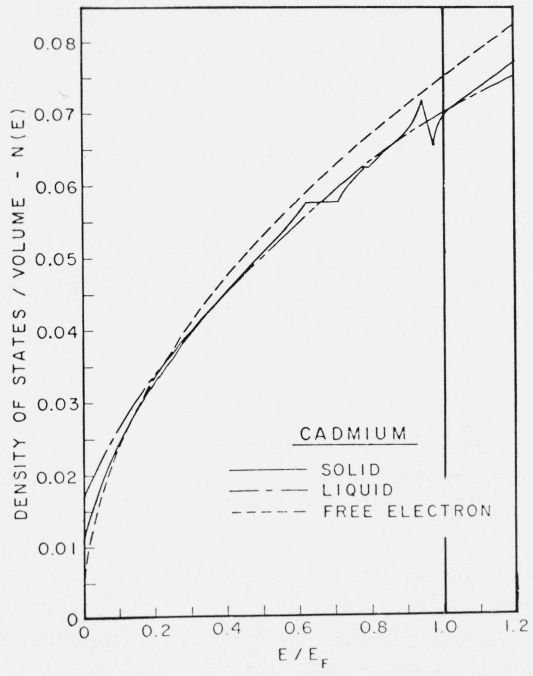

FIGURE 7. *Calculated values of* N(E) *for Cd, as taken from Shaw and Smith* [70].

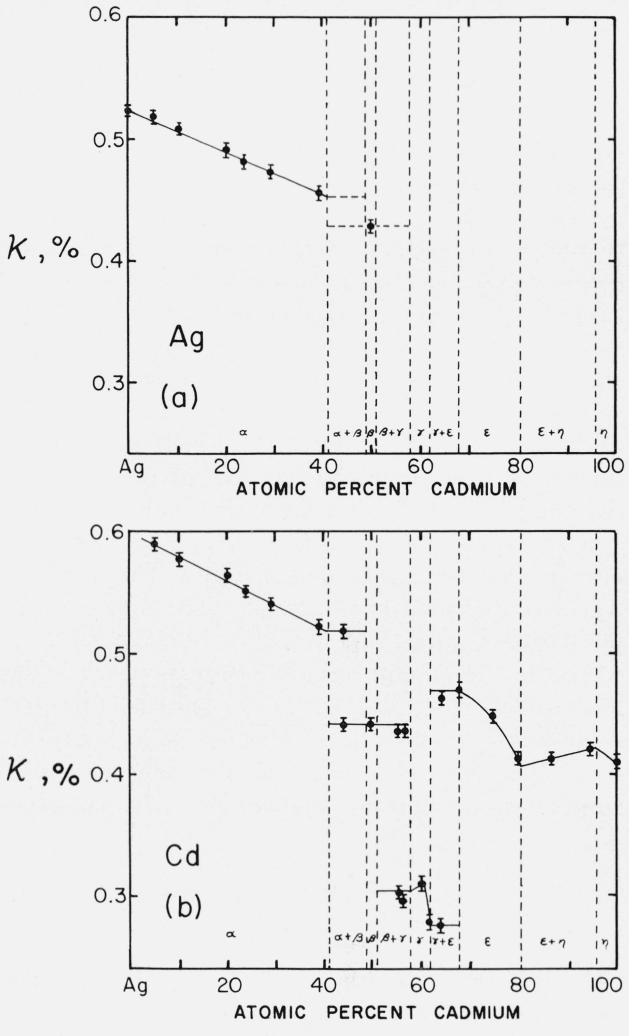

FIGURE 8. *Knight shifts in AgCd for (a) the Ag resonance and (b) the Cd resonance, as taken from Drain* [74]. *In the two phase regions, Cd resonances for both phases are simultaneously seen, due to the rather different* $\mathcal{K}$*'s for the different phases. For ranges of solid solubility* $\mathcal{K}$ *changes smoothly.*

The semiconductor-(or insulator-) to-metal transition, whether or not a Mott transition, offers a number of examples in which the Knight shift changes more or less suddenly. For example, when tin changes from its metallic to its semiconducting phase, $\mathcal{K}$ changes from 0.75 percent to near zero (see fig. 2b). Also consider VO_2 which is metallic above and semiconducting below a crystal structure change occurring at $T_c = 68$ °C [75,76]. The Knight shift is ~ -0.4 percent at 100 °C and $\sim +0.2$ percent below. The negative shift above T_c is attributed to a metallic *d*-band.

A case where there is an electronic transition without further structural changes is that of phosphorous-doped silicon [77-79]. At donor concentrations (n_d) greater than 2×10^{19} cm^{-3}, the material appears to be a metal, the Knight shift is proportional to $n_d^{1/3}$, and the Korringa relation holds. Below this critical concentration, $\mathcal{K}$ drops sharply. In the transition range, $3 \times 10^{18} < n_d < 2 \times 10^{19}$, there is a measurable $\mathcal{K}$, but the Korringa relation no longer holds. The electrons are "delocalized" in some type of impurity "band."

Other systems exhibiting nonmetal-to-metal transitions are the alkali-ammonia solutions. As the metal to ammonia ratio is increased, the liquid becomes gradually metallic, and the conductivity as well as the Knight shift increases substantially [80-83].

6. Orbital Magnetism in Simple Metals

The Bardeen, Cooper and Schrieffer theory of superconductivity [84] predicts that, as a result of spin pairing, χ_p vanishes at $T = 0$. Hence it was expected [85] that $\mathcal{K} \to 0$ as $T \to 0$ for superconductors. This expectation often is not borne out. It seems certain that the residual Knight shift is predominantly of orbital origin for transition metals such as V and Nb [22]. Ferrell [86] and Anderson [87] proposed that spin-reversal scattering due to spin-orbit coupling is another possible mechanism for obtaining a residual Knight shift. This mechanism requires that $\mathcal{K}$ be a function of mean free path, *i.e.*, particle size and impurity scattering. This

spin-orbit term has been shown by Wright [88] to be important in Sn. Wright also reviews earlier experiments on other metals. He concludes that although spin-orbit coupling is dominant in some cases, two types of orbital magnetism cannot be ruled out in simple metals. These are the Van Vleck orbital paramagnetism [18-22] and a higher order mechanism introduced by Appel [89]. Similar higher order mechanisms were discussed earlier by Clogston *et al.* [20]. We have already discussed the Van Vleck term and will note its importance in the transition metals and alloys to be discussed later. The Appel mechanism involves spin-orbit and $\vec{\ell}\cdot\vec{\mathbf{H}}$ coupling to an intermediate excited conduction electron state, which contributes to the Knight shift through the contact interaction. It is of the order of $\lambda/\Delta E$ times the contact Knight shift, where λ is the spin-orbit interaction energy, and ΔE is the energy between states connected by λ. The sign of the Appel contribution to the Knight shift may be either positive or negative.

Another important orbital effect is the Landau-Peierls diamagnetism [90]. The magnitude of this term is not easy to predict. In the simplest (and greatly oversimplified) free electron approximation the Knight shift, $\mathcal{K}_{dia}$ arising from Landau-Peierls diamagnetism, is

$$\mathcal{K}_{\text{dia}} = -\frac{8\pi}{3}\left(\frac{1}{3}\chi_p\right)\left\langle\frac{m}{m^*}\right\rangle^2, \qquad (22)$$

where m^* is an appropriate electron effective mass. This term has been proposed to explain a number of negative, or near zero, Knight shifts in nontransition metals. In transition metals, *d*-core polarization (see table 3) gives an important negative contribution to $\mathcal{K}$, through the Pauli paramagnetism of the *d*-band. In nontransition elements *p*-core polarization has often been proposed as an alternate to $\mathcal{K}_{\text{dia}}$ as a negative contribution to $\mathcal{K}$ (see table 3). For example Das and Sondheimer [90] first suggested the importance of the Landau term to the negative Knight shift in Be. In later papers, Das and coworkers [50-52] performed detailed calculations for the contact and the *p*-core polarization terms in this metal. A reluctance to believe that the diamagnetic shift is as large as was originally suggested [90] is evident from these papers [50-52]. Although they do not give further quantitative estimates for $\mathcal{K}_{\text{dia}}$ in this later work, in each case they are forced [52] to the same conclusion that the remaining negative shift is of diamagnetic origin. Using eq (22), available m^* values can, in fact, give a $\mathcal{K}_{\text{dia}}$ of -0.003% [52,53].

Yafet [91] considered the importance of $\mathcal{K}_{\text{dia}}$ for Bi, but Williams and Hewitt [92] proposed *p*-core polarization as the origin of the quite substantial negative Knight shift in Bi of -1.25%. It is interesting to note that if χ_p is estimated from the electronic specific heat [37], using eq (21), and if there is no *s* contact contribution to $\mathcal{K}$, the *p*-core polarization necessary to explain a shift of -1.25% is 800 times larger than the experimental value [93] for atomic Bi (table 3). The presence of an *s* term will increase this estimate of 800. Note that the experimental atomic "core" polarization term includes the polarization of the 6*s-valence* electrons which are part of the conduction bands in the metal. This atomic value therefore provides an estimate of the *s* polarization in the core *and* throughout the occupied conduction band: the applicability of this value to the metal depends on the distribution of *s*-character in the occupied bands (as compared with the free atom). Granted the uncertainty in χ_p and the question of relevance of the atomic hyperfine constant to this metal it would still appear that *p*-core polarization is at least one hundred times too small to account for the experimental Knight shift. On the other hand, Bi has m/m^* ratios which, using eq (22), are large enough to suggest a Landau diamagnetic shift that can approach magnitudes of the order of the observed $\mathcal{K}$ value.

Other examples of negative shifts in diamagnetic, non-*d* materials are Tl in NaTl [9,94-96] and In in BiIn at 77 K [97]. For these cases the situation is much less clear due to the lack of data for χ_p, m^*, and γ. In addition we do not have free atom experimental values for *p*-core polarization for Tl and In. Using some upper estimates for the unknown quantities, it is evident that either *p*-core polarization or Landau diamagnetism is hard pressed to reproduce the observed shifts. A discussion of diamagnetic Knight shifts and *p*-core polarization effects in these materials will be given elsewhere [98].

Das and Sondheimer [90] also indicated that oscillations would be present in the diamagnetic term. These would be periodic in $1/H$, similar to de Haas-van Alphen oscillations. However, when this effect was first observed by Reynolds *et al.* [99,100], the amplitude of the oscillations was considerably larger than that expected from the diamagnetic term [101-106]. Glasser [107] explained this by proposing that the Fermi surface wave functions also change with $1/H$, and that this introduces oscillations into the Pauli term which dominate over the diamagnetic oscillations. Goodrich *et al.* also observed Knight shift oscillations in Cd [108]. Their data are shown in figure 9.

The importance of observing oscillations in $\mathcal{K}$ is that it is possible to obtain the Knight shift over a segment of the Fermi surface. Thus the Knight shift has become

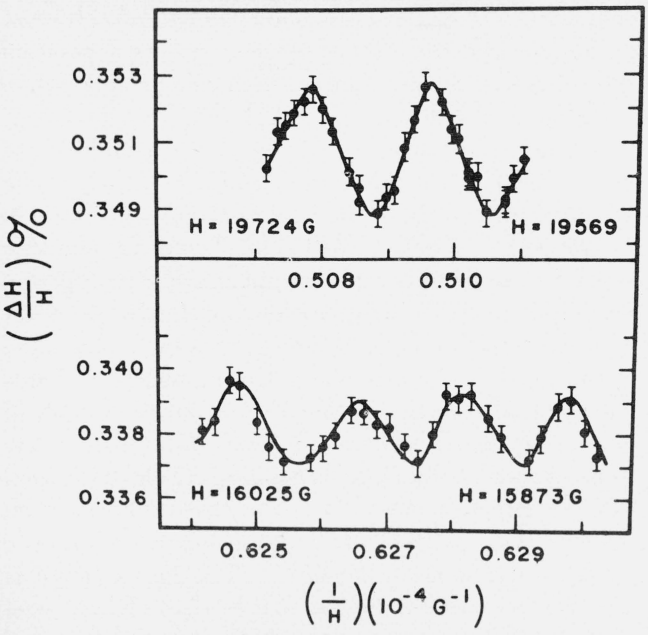

FIGURE 9. *Knight shift in Cd, illustrating oscillations in $\mathcal{K}$ with 1/H, as taken from Goodrich, Khan and Reynolds [108].*

a potentially important tool for examining the wavefunction character associated with $N(E_F)$ not only in the average sense of eq (19), but also in finer detail over Fermi surface segments.

7. Transition Metals

The simple metals considered in the preceding sections display, in the main, only weak orbital Knight shifts and temperature independent, usually positive, Pauli terms. Transition and noble metals with their *d*-bands tend to have a negative Pauli term arising from *d*-core polarization (see table 3). Narrow *d*-bands, with many states close in energy to E_F, often have substantial orbital effects [see eq (15)]. Structure and curvature in $N(E_F)$ contribute a temperature dependence to the Pauli term. Given the presence of *d*- and non-*d*, or "conduction" band character, it has been normal to describe the paramagnetic transition metals in terms of a "two band" model involving discrete "*s*" and "*d*" bands. We follow common nomenclature in designating the conduction band as an *s*-band. (The *d*-bands, of course, also contribute to conduction.) The orbital Knight shift is associated with the *d*-band; the average taken in the Pauli term is rewritten

$$\langle a\rangle\chi_p = \langle a_s\rangle\chi_p^s + \langle a_d\rangle\chi_p^d(T), \qquad (23)$$

where the "*s*" or conduction band is assumed to contribute a positive, temperature independent term, and the *d*-bands, a negative temperature dependent term. The latter dominates since $N(E_F)^d$, hence χ_p^d, is much larger than its *s*-band counterpart. It is assumed in eq (23) that the temperature dependence of $\mathcal{K}$ is entirely associated with the susceptibility and not with any variation in the hyperfine coupling constants [13]. The fact that the slope, $d\mathcal{K}/d\chi$, is a constant for these metals offers some experimental justification for this assumption. An example of this is seen [109] in figure 10, where $\mathcal{K}$ is plotted versus χ_{tot}, with temperature the implicit variable, for Pd. In this case $\chi(T)$ goes through an extremum with increasing T, but is faithfully tracked by $\mathcal{K}(T)$. Pd displays the largest temperature variation in χ among the paramagnetic metallic elements. As is discussed in Mott and Jones [110], such a temperature dependence arises from sampling by the Fermi function of structure and curvature in the density of states in the vicinity of E_F.

While the two band model has proven most useful when discussing Knight shifts and other experimental data, there is, in fact, strong hybridization of *s*- and *d*-band character and a transition metal is not constituted of discrete *d* and "*s*" bands. Some measure of this is given in figure 11, which displays the density of states obtained[6] for fcc Cu.

The results can be taken as characteristic of all transition metals. The density of states behavior is similar to that reported by Mueller for Fe [115], and to that obtained by Goodings and Harris [116], and by Cuthill *et al.* [117] in their estimates of soft x-ray spectra for Cu. The density of states has been plotted separately for the first, second and sixth bands while that for the third, fourth and fifth has been added together for the sake of legibility. In figure 11, the Cu Fermi energy is designated by E_F and that appropriate to Ni by E(Ni). The high density of states peak, intersected by E(Ni), is due to the fifth band. Details of this band and of its Fermi surface are essential to the differ-

[6] These results [111] involve a sampling of $\sim 1.5 \times 10^6$ points in 1/48th of the Brillouin zone. The sampling employed a quadratic fit to a set of pseudopotential bands by Ehrenreich *et al.* [112, 113] involving a mesh of 28 intervals from Γ-X in the zone. The pseudopotential bands were obtained from an adjusted analytic fit of some new APW calculations for Cu [114]. Spin-orbit coupling effects, though slight, have been included. The Fermi surface is in better agreement with experiment than is usual for calculations. Details of the density of states and grosser features of the wavefunction analysis are, of course, dependent on the use of a pseudopotential band description (which assumes tight binding *d*-bands and a set of four orthogonalized plane waves for the non-*d* part). These results can be considered analogous to the OPW results, obtained by Das and coworkers [49-52, 55] for the Knight shift in various "simple" metals.

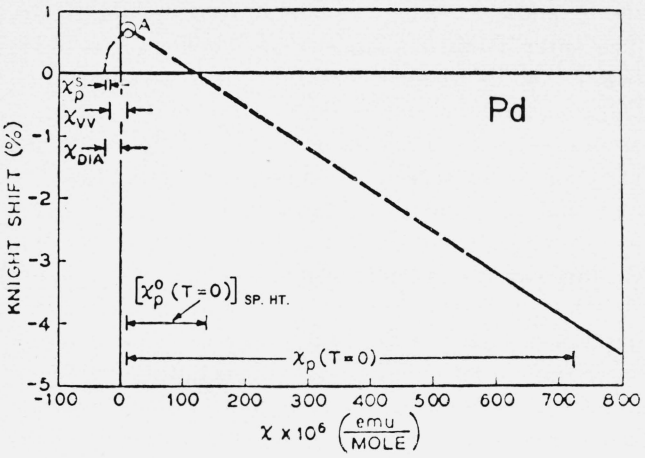

FIGURE 10. *$\mathcal{K}$(T) versus χ(T) plot for Pd, as taken from Seitchik, Gossard and Jaccarino [109].*

ing magnetic behavior of Ni, Pd, and Pt. The Cu Fermi level intersects the sixth band, often named the "free electron" band, which lies above the five "*d*" bands.

The density of states associated with non-*d* electron character; $N(E)_{\text{non-}d}$, is also shown in figure 11. It must be emphasized that details of these results depend on the scheme used to describe the bands (in this case a pseudopotential description [111] with tight binding *d*-functions). Hybridization effects cause a build up of non-*d* character at the bottom and a depletion in the middle and just above the bulk of the *d*-bands (*i.e.*, in the range $-0.35 \leq E \leq -0.15$ Ry). The peak seen at ~ -0.4 Ry can be important to optical and soft x-ray properties. The sixth band is predominantly of *d*-character at the bottom and remains almost thirty percent *d* at the Fermi level. This particular set of results [111] yields 9.8 electrons worth of *d*-character out of a total of eleven electrons, in the bands below E_F. [A free electron parabola, holding the remaining 1.2 electrons, and with an effective mass chosen so that its Fermi level matches E_F, has been drawn for comparison with the actual non-*d* density of states.] The lowest band is strongly free-electron like up to $E \sim -0.45$ Ry and 0.61 of the two electrons residing in the band are of non-*d* character. Roughly 0.35 of the remaining 0.6 non-*d*-

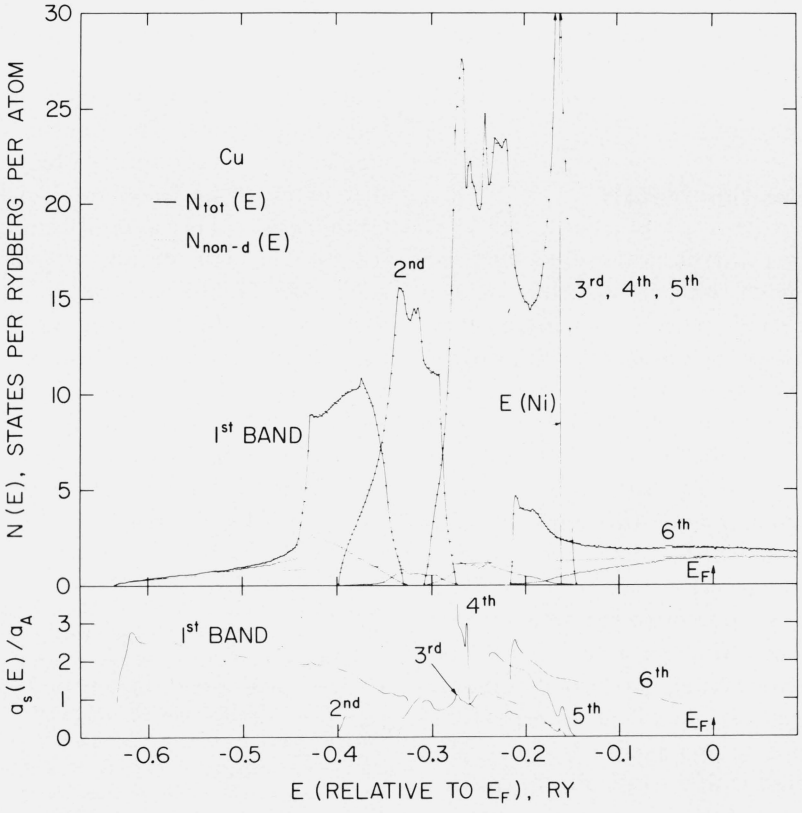

FIGURE 11. *(a) Total density of states and non-*d *density of states for the 1st, 2nd and 6th bands of Cu separately, and for the 3rd, 4th and 5th summed. The smooth, flat band is the free electron parabola containing 1.21 "conduction" electrons, as discussed in the text. This is shown for comparison with the $N_{non-d}(E)$ results. (b) Ratio of band to atomic hyperfine constants as defined by eqs (24a) and (24b).*

electron character is associated with the one electron in the sixth band.

The 3*d*-electron character can be expected to interact with the nucleus via a core polarization term of ~ -125 kOe per μ_B throughout the bands. The non-*d* character is expected to interact predominantly via the direct contact term. Its behavior is shown at the bottom of figure 11 in the form of the ratio

$$\frac{a_s(E)}{a_A} \equiv \frac{\langle a(E) N_{\mathrm{TOT}}(E) \rangle}{a_A N_{\text{non-}d}(E)} \tag{24a}$$

with respect to the non-*d* electron density of states at E, *i.e.*, the contact interaction normalized with respect to the non-*d* electron density at E, and to an atomic 4*s* hyperfine constant.[7] Omitting all core polarization contributions to $\mathscr{K}$, this ratio is then related to ξ by

$$\frac{a_s(E)}{a_A} = \xi(E) \frac{N_{\mathrm{TOT}}(E)}{N_{\text{non-}d}(E)}. \tag{24b}$$

A ratio of 2 to 2.5 occurs at the bottom of the bands reflecting the volume normalization enhancement of ξ discussed previously in connection with figure 4. Values closer to one are appropriate to the non-*d* character hybridized into the second, third, fourth and top of the first bands. This suggests that an $a_s(E)$ set equal to a_A can be used as a first approximation when estimating the effect of hybridization on reducing a *d*-band a_d from a pure *d*-core polarization value. The ratio is higher in the fifth band but here hybridization is almost zero. The ratio tends to fall with increasing E, as is seen in the lower part of the first and in the sixth bands. This is associated with the decrease in *s*-character in OPW's of increasing $\mathbf{k}$. The ratio has dropped to a value of 0.78 at the Cu Fermi level. Here $\xi(E_F)$, defined in the manner of eq (24b), has the value of 0.57. If one adds the negative core-polarization contribution which can be attributed to the twenty-eight percent *d*-character in the bands at E_F, $\xi(E_F)$ becomes 0.55.

The above $\xi(E_F)$ values agree with the upper end of the range estimated as the experimental ξ for Cu in table 5. Davis [118] has obtained[8] $\xi(E_F) = 0.67$ employing the method of Korringa-Kohn-Rostoker. Comparison with the experimental data may not be meaningful because core polarization terms, arising from "conduction band" spin character, have been omitted in the $\xi(E_F)$ estimates while being present in the quantities of tables 2 and 5. It is thus proper to make the comparison only if core polarization affects the numerator and denominator so as to leave the ratio constant. This seems unlikely since *s and p* character terms will contribute to the conduction electron core polarization.

These two band calculations yield $N(E_F)$ values which are in good numerical agreement with the electronic specific heat for Cu. Both calculations suggest that *d*-hybridization is a significant factor in reducing ξ. This is one reason for the tendency noted earlier for Ag to have a larger ξ than Cu or Au. The *d* bands are twice as far below E_F in Ag, and weaker *d* hybridization ($\sim 10\%$) occurs at the Fermi level of Ag.

Noting that the atomic *s*-contact interaction is typically ten times larger than, and opposite in sign to, *d*-core polarization, figure 11 suggests that hybridization is important throughout the transition metals. Consider the case of Ni. The Fermi level intersects the high peak of the fifth band. This band has almost no hybridization, as is shown in figure 11, which was obtained with Cu bands. The sixth band has an $N(E_F)$ value which is better than an order of magnitude smaller than the fifth band at E(Ni). However the sixth band has twenty percent *s*-admixture at E(Ni) causing a large, positive a_d, which compensates for this. Neglecting exchange enhancement of the susceptibility, the sixth band contribution can then cancel approximately one third of the Knight shift term, a_d, associated with the fifth band alone. Exchange enhancement is important and an estimate of the exact role of the sixth band requires opinions of interband exchange effects. Scanning the lower energy parts of the plot, it appears that hybridization may affect the a_d values for the lighter transition metals more severely. This hybridization trend should hold although changes occur in the crystal structures.

Despite the complexities just discussed, the two band model of the Knight shift has frequently proven fruitful, with hybridization absorbed in the a_d term. The various Knight shift contributions are normally disentangled in two ways. First, comparisons can be made between the relaxation time, T_1, and Knight shift results which weight the various terms differently. The Korringa relation [27] provides a test for the *s*-contact contribution. Secondly, one can employ the graphical technique of figure 10. This scheme, applied to Pt [20]

[7] An a_A of 1600 kOe/μ_B, omitting core polarization contributions, was used, since core polarization effects were omitted in the evaluation of $\langle a(E) N_{TOT}(E) \rangle$. With core polarization, correlation and relativistic effects present, the (experimental) a_A is ~ 2600 kOe/μ_B. For discussion of this see [7].

[8] Actually Davis [118] chose to quote a ξ-ratio by dividing his computed hyperfine term *without* core polarization by an atomic a_A *with* core polarization. This yields a smaller numerical value than we quote here.

appears in figure 12. The experimental data are plotted for $\mathcal{K}$ versus χ_{tot} with temperature the implicit parameter and, following eq (23), it is assumed that

$$\chi_{tot} = \chi_{dia} + \chi_{orb} + \chi_p^s + \chi_p^d \tag{25a}$$

and

$$\mathcal{K} = \langle b \rangle \chi_{orb} + \langle a_s \rangle \chi_p^s + \langle a_d \rangle \chi_p^d(T). \tag{25b}$$

The slope of the experimental data yields an empirical value for $\langle a_d \rangle$. The diamagnetic susceptibility is estimated and subtracted out, shifting the origin of the plot to point A. An estimate is then made of χ_p^s (usually with the free electron approximation) and of a_s and the s-band contributions are subtracted out shifting the origin, with respect to orbital and d-band Pauli terms, to point B. Finally, $\langle b \rangle$ is estimated, defining the slope of $\mathcal{K}_{orb}$ versus the χ_{orb} line, which is drawn until it intercepts the experimental $\mathcal{K}$ versus χ_{tot} curve (at point C). The intercept defines the relative roles of orbital and d-band Pauli terms. In this case, the d-band Pauli term dominates.

A value for the *unenhanced* χ_p^0, estimated from specific heat data is shown in figure 12. The larger value, deduced from the Knight shift, provides a measure of the effect of exchange enhancement. While

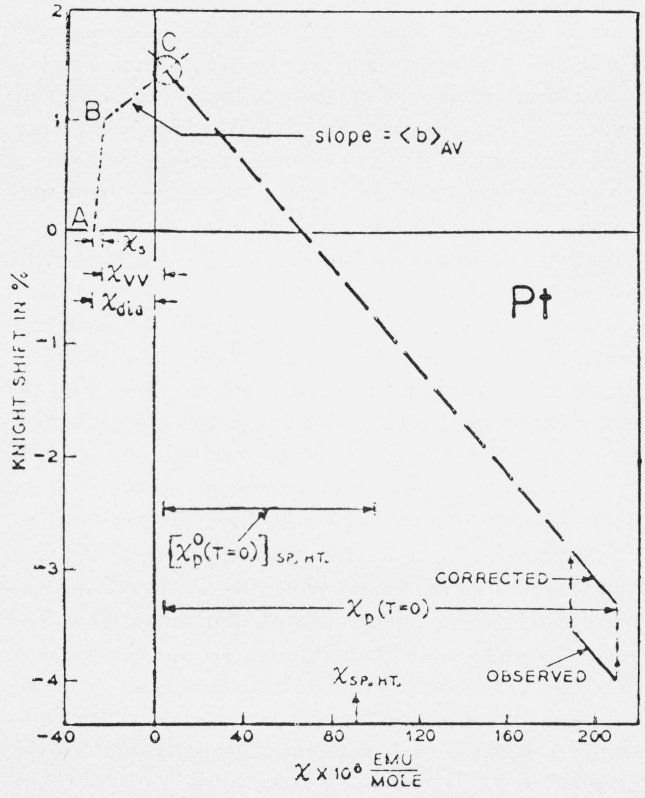

FIGURE 12. $\mathcal{K}$(T) *versus* χ(T) *for Pt, as taken from Clogston, Jaccarino and Yafet* [20].

quantitative results depend on the detailed choice of χ_{dia}, χ_p^s, $\langle a_s \rangle$ and $\langle b \rangle$, the qualitative conclusion does not. Changing the hyperfine constants by reasonable amounts or omitting the s band term altogether does not change the basic result. Analyses which compare T_1 and $\mathcal{K}$ data also rely on estimates of hyperfine constants. Results indicate that the d-band term also dominates in Pd (see fig. 10) and Rh [119]. Note that figures 10 and 12 indicate a greater exchange enhancement in Pd (5 to 6) than in Pt (~ 2). The enhancement in Pt is as expected, whereas the factor of 5 to 6 for Pd is somewhat smaller than is currently fashionable to believe. The orbital term dominates in V [19,20,22], Cr-rich Cr-V alloys [24], W [21] and Nb [22]. This is not surprising since these metals have roughly half-filled d-bands, encouraging orbital effects, whereas Pt, Pd, and Rh have almost filled d-bands. Equation (16) predicts the difference in magnitude of ortibal effects for these two groups of metals to within the uncertainty in the appropriate band occupation (n) factors appearing in that equation.

The slopes of the $\mathcal{K}$ versus χ plots for Pd, Rh and Pt yield a_d values of -345, -162 and -1180 kOe/μ_B respectively. The Pd result is in good agreement with the $4d$-core polarization value quoted in table 3 while that for Rh is half that value. It is believed [10] that core polarization is almost constant across the $4d$-row, implying that the variation in a_d arises from other sources. Two suggest themselves. First, different amounts of s character may be hybridized into the d bands at the Fermi surface: increased s-d hybridization in Rh would produce a less negative a_d. Figure 11 suggests that there is a distinct probability that this occurs. Secondly, there may be different *intersite* contributions to a_d. The Pauli term spin density induced on neighboring sites will, after all, make some contribution to the hyperfine coupling constants. These two contributions are expected to be present in Pt as well, and may contribute to the fact that the experimental a_d is not in numerical agreement with table 3. (Some uncertainty must be attached to the theoretical estimate quoted there.)

Intersite effects, s-hybridization and d-core polarization cannot be separated by inspection of a_d for a pure metal alone, but some insight can be gained by studying alloys. NMR results have been obtained for Cu in the Cu-Pd system [120] and Ag in AgPd [121]. The data for dilute Cu or Ag in Pd suggest that these atoms go in the lattice with filled d shells and with relatively little perturbation on the surrounding Pd matrix. Negative solute Knight shifts are obtained, in contrast with the positive ones appropriate to pure Cu and Ag. Using Ag

site T_1 data to estimate an $a_s\chi_p{}^s$ term, Narath obtained [121] an intersite hyperfine field of -140 kOe/μ_B for dilute Ag in Pd. (The susceptibility is essentially that of the host, measured in μ_B units.) He noted that this term is approximately twice the value obtained for dilute Cu in Pd, *i.e.*, that

$$\mathcal{H}^{\text{solute}}_{\text{intersite}} \propto \chi_p^{\text{host}} a_{\text{solute}} \tag{26}$$

where a_{solute} is the atomic valence *s*-electron hyperfine coupling constant appropriate to the solute (see table 4). Now the intersite term sampled by Pd in Pd can be quite different from that sampled by either Ag or Cu which are charge impurities but the above results suggest that approximately one third of the a_d value in Pd arises from intersite effects and that the numerical agreement with the 4*d* core polarization value was fortuitous. The presence of an intersite contribution of between -100 and -150 kOe/μ_B then implies an equal but positive contribution from *s* hybridization, or from polarization of the paired *s* character in the occupied conduction bands (*e.g.*, see sec. 2). A two or three percent admixture of *s* character in the *d* bands at E_F would produce such an effect (see table 4). The variation in a_d between Pd and Rh is within the realm of reasonable change in hybridization, though intersite effects can be expected to vary.

Negative shifts of the Cu resonance are also observed [122] for dilute Cu in Pt. Inspection of the results is again troubled by the question of perturbations on the host lattice (which are thought to be slight) and second order quadrupole shifts (which are estimated). The result is [122] an intersite term of somewhat less than -100 kOe/μ_B in agreement with Cu-Pd. There also exist results for the Pt Knight shift in Cu-Pt[122] and Au-Pt[123] alloys. A similar tendency, of negative shifts in pure Pt and positive shifts in the noble metal-rich alloys, arises. This is in qualitative agreement with the above observations concerning a negative intersite term in Pt. Questions concerning the perturbation on the solvent's local susceptibility, due to the presence of an atom such as Pt (or Pd) in a noble metal, makes quantitative estimates of an intersite hyperfine constant from the dilute Pt data less plausible.

Experience with solute hyperfine fields [124,125] for impurities in Fe, Co and Ni, and the above observations for noble metal alloys, suggest that substantial intersite effects arise in the heavy 3*d*, 4*d* and 5*d* metals. These are expected to be of the order of -100 kOe/μ_B (the moment being that characteristic of the solvent susceptibility). There is some suggestion of weaker intersite effects in the lighter elements of the various transition metal rows. The changes in crystal structure from fcc to bcc, and the associated decrease in the number of nearest neighbors to any one site may be a factor contributing to this.

8. Alloys and Local Effects

The introduction of a foreign atom in a pure metal has several effects. First, if the atom has a different number of valence electrons than the host, its insertion will change the number of conduction electrons per atom (the e/a ratio) in the metal. Neglecting other effects of the insertion, this acts to shift the Fermi level in the bands. The bands will, of course, be perturbed by the addition of impurities. If the perturbation is gradual, and relatively weak, it is often useful to scan alloy data as if the Fermi level shifts (as a function of e/a) over a set of "rigid" bands. This is a rigid band picture which may (or may not) bear some resemblance to the host metal conduction bands off their Fermi energy [126], but this picture properly describes the alloy system at E_F. Such a rigid band scheme has little or no relevance to some alloy systems (*e.g.*, Cu-Pd) while displaying striking trends between alloys of common e/a (*e.g.*, $Cr_{1-x}V_x$ versus $TiFe_yCo_{1-y}$) elsewhere. Some examples will be considered in the next section.

Any impurity in a metal will produce a charge disturbance. Atomic size and electronegativity effects cause this to be true, to a limited extent, even in the case when the valence of the host and that of the impurity is identical. The conduction electrons act to screen the charge difference associated with the impurity as is indicated schematically in figure 13. There will be a build up (as in fig. 13) or dilation in the total conduction electron charge in the vicinity of the impurity, depending on the sign of the difference[9]. There is a highly local "main peak" with the familiar Friedel oscillations to the outside. These arise from the presence of a conduction electron Fermi surface and have a period which is inversely proportional to $2k_F$, *i.e.*, the extremal caliper of the Fermi surface in the direction in question [127].

[9] The conduction electron distribution is distorted by the Coulomb perturbation in a very similar manner to the core polarization effects discussed earlier, the latter case being an exchange polarization and the spin difference resulting from it, the present case involving the sum of charge terms. Both may be viewed as involving the admixture of excited orbital character into the originally unperturbed occupied one-electron states.

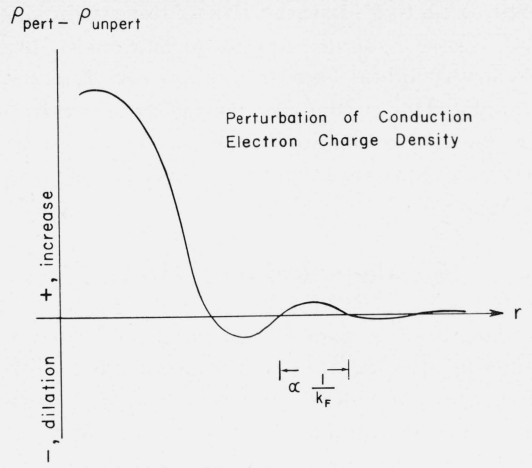

FIGURE 13. *Schematic illustration of conduction electron charge screening induced in a metal host by a single impurity at* R=0. *The half-period of the Friedel oscillations, which is proportional to* $1/k_F$, *is indicated.*

Solvent atoms can make various differently weighted samplings of this charge distribution, for example, by quadrupole interactions [128-133] and by isomer shifts.

The presence of an impurity also affects the solvent Knight shift. Only the perturbation of the Fermi surface electrons is important here, as it is these electrons which are involved in the Pauli term. The Fermi surface electrons undergo a redistribution [127,134] which is similar to the total charge screening in character and which can be sampled as a distribution through their $\langle a \rangle$ values appropriate to the different solvent sites in the lattice. This, and the bulk charge disturbance, are usually described in terms of free electron or simple OPW bands employing pseudopotential or phase shift scattering analyses of the perturbation. Due to the complex nature of the problem, neither scheme usually supplied quantitatively satisfying *a priori* predictions of experiment and, in the few cases where they have, there arise questions of the uniqueness of the result. In terms of the phase shift analysis, the change in Knight shift at a nucleus some distance R from the impurity is given [134] by

$$\frac{1}{\mathcal{K}}\frac{\Delta\mathcal{K}(R)}{\Delta c} = \sum_{\ell} \{\alpha_{\ell}(R) \sin^2 \eta_{\ell} + \beta_{\ell}(R) \sin 2\eta_{\ell}\}, \quad (27)$$

where

$$\alpha_{\ell}(R) \equiv (2\ell + 1) \sum_{R} \{n_{\ell}^2(k_F R) - j_{\ell}^2(k_F R)\}, \quad (28)$$

and

$$\beta_{\ell}(R) \equiv -(2\ell + 1) \sum_{R} j_{\ell}(k_F R) n_{\ell}(k_F R). \quad (29)$$

The ℓ^{th} term in the sum is associated with the ℓ^{th} partial wave, η_{ℓ} is the phase shift of the ℓ^{th} component, and j_{ℓ} and n_{ℓ} are spherical Bessel and Neumann functions respectively. To obtain the effect on a solvent metal Knight shift, the α_{ℓ} and β_{ℓ} must be suitably averaged over R. For "simple" solvent metals and "simple" solutes the effect is presumed to be dominated by s- and p-wave scattering. Changes in the relative roles of s- and p-wave scattering are important in rationalizing the variation in $\Delta\mathcal{K}/\mathcal{K}$ with varying valence of the solvent, or varying valence of a solute, relative to the solvent.

There is traditionally some question of how large an effect can be associated with pure s-screening. From a strictly atomic viewpoint, one might expect it to be limited to two electrons worth of charge. The recent investigations of Slichter *et al.* [135,136] conclude that higher ℓ scattering is very important to the screening when solute-solvent valence differences exceed two.

A local spin moment will produce a spin disturbance similar to that seen in figure 13. Such a spin disturbance is obviously important to magnetically ordered metals[10] but it also produces the dominant Knight shift term at some sites in certain paramagnetic alloys (see sec. 12). Consider the Knight shift of a nonmagnetic site in a paramagnetic rare-earth alloy. The principal term in the Pauli susceptibility, *i.e.*, in the spin induced by the magnetic field, is that of the open 4*f*-shells, and this spin will contribute to the nonmagnetic site $\langle a \rangle$ behavior via conduction electron polarization. The susceptibility associated with the moment would obey a Curie-Weiss law. Examples of this are the above mentioned rare earths with their open 4*f*-shells, and 3*d* alloys, such as Fe in Cu. Sometimes the moment may arise from band-paramagnetism involving localized *d* levels which are too weakly coupled by *intra-atomic* exchange to produce a true local paramagnetic moment. Curie-Weiss behavior is then not followed. The 3*d* elements as impurities in Ag, or dilute Ni in Cu are examples of such band paramagnetism.

Given an induced local spin monent of either of the above types, there will inevitably be a spin disturbance in the solvent conduction bands producing, in turn, a Knight shift term. There will be a variety of contributions to this. First, and most obviously, the exchange field due to the local moment will produce a spin dependent scattering of conduction electrons. As described

[10] We should note that in a magnetically aligned metal, cross terms will cause a magnetic imputiry to contribute a charge disturbance, and a charge impurity to contribute a magnetic disturbance (the charge impurity Knight shift contribution can be considered a special example of this).

by Ruderman, Kittel, Kasuya and Yosida (RKKY) [137-141], the Pauli response of the conduction electrons to the diagonal exchange term, $\mathcal{J}(k_F,k_F)$, contributes a net spin density which is then piled up in a screening distribution of the sort plotted in figure 13. Formally the theory is almost identical to the charge screening case. Exchange, rather than electrostatic Coulomb, terms are responsible for the disturbance, and details of the shape of the main peak and of the behavior of the phase and amplitude (relative to the main peak) of the Friedel oscillations should differ from the charge scattering distribution. The $\ell = 0$ and 1 partial waves will again tend to predominate. Details [141] of the intra-atomic term in the electrostatic exchange, $\mathcal{J}_{el}$, are such that if the local moment is of odd (or even) ℓ character, partial wave scattering of odd (or even) ℓ' is enhanced (*i.e.*, *s*-wave scattering is of increased importance with *d*-moments present while *p*-wave effects are amplified in 4*f*-moment scattering). Only *s*-wave spin density is nonzero at the solute's nucleus. In the scattering picture, it describes the intra-atomic conduction electron exchange polarization term discussed in section 2.

If the value of electrostatic exchange were somehow zero, the presence of a local spin moment would still cause a spin disturbance in the conduction bands [142-144]. Resonant scattering of spin-up and spin-down conduction electrons will occur at different energies as the result of the splitting of the local virtual (or real) bound state to form the local magnetic moment. One reason the scattering differs is the different occupation of spin up and spin down orbitals on the local moment site. Consider some partial wave component, with quantum members ℓ and m_ℓ of a scattered conduction electron at the local moment site. If the local moment had an occupied component of the same ℓ, m_ℓ and spin, the conduction electron component would be unaffected (except for any nonorthogonality effects which might arise); if there were a hole in that local moment orbital component, the orbital could be admixed into the conduction electron function to the extent it is energetically favorable. The existence of a net spin residing in the local moment implies a difference in hybridization (and orthogonalization) effects in conduction electron states of the same **k** and differing spin. This results in a spin density distribution similar to the core polarization effects discussed earlier. There is no net spin in the disturbance; instead there are regions of spin parallel and antiparallel to the local moment. In their original inspection of such hybridization effects, Anderson and Clogston concluded [142] that this disturbance would fall off as $1/r^4$; subsequent numerical estimates of their model [145] are consistent with this observation. It would seem that the effect is largely concentrated at the local moment site. An *effective* exchange interaction arises when the next order in hybridization effects is taken [142,143]. Consider the energy shift of a Fermi surface electron. The mixing of local moment *hole* components into the wave function will lower the state's energy whereas orthogonality with occupied components can only raise its energy. Hybridization thus stabilizes the energy of Bloch states with spin moment antiparallel to the local moment whereas those with spin moment parallel are less favored since they undergo orthogonalization and *decreased* hybridization. This produces [142-144] a *negative* interband exchange constant $\mathcal{J}_{ib}(k_F,k_F)$ in contrast with $\mathcal{J}_{el}(k_F,k_F)$ which is always positive.[11] A negative value implies a conduction electron Pauli spin density term of spin moment antiparallel to the local moment. Such situations occur experimentally, implying that "interband" hybridization (and higher order effects) do, on occasion, predominate over electrostatic exchange, which can only produce a net spin moment parallel to the local moments. (These effects are obviously intimately related to the Kondo effect.) The earliest evidence for negative exchange constants was obtained by nuclear magnetic resonance and electron paramagnetic resonance measurements for rare earths in several host metals [146-149] such as Pd. This has subsequently been borne out by magnetization and neutron diffraction studies.

Interband hybridization exchange also differs from electrostatic exchange in that hybridization will only be strong between band and local moment components of common ℓ. The summing over individual Bloch state contributions to the spin disturbance yields partial wave scattering only from those same ℓ components directly involved in the mixing. Thus, unlike electrostatic exchange, hybridization effects with their predominant *d*- or *f*-scattering, will not contribute an $\ell = 0$ contact spin density term to the hyperfine field at the scattering site, unless higher order (*i.e.*, double, triple, *etc.*) scattering processes are significant.

A disturbance of the type plotted in figure 13 produces a distribution in solvent site $\langle a \rangle$'s causing a broadening of the solvent Knight shift line. The distribution in $\langle a \rangle$ will not necessarily provide a detailed, accurate mapping of the bulk conduction electron disturbance. This is due to interference effects arising from orthogonalization of the conduction electron wave functions with the solvent site ion cores which are

[11] Schrieffer and Wolff [143] have explored the circumstances for which $\mathcal{J}_{ib}$ can be properly defined.

383-876 O - 70 - 9

penetrated. This interference is important in that it affects the apparent shape of the disturbance at sites near the impurity, while providing little more than scaling to the result for sites at asymptotically large R.

The sampling of the disturbance will inevitably cause the average solvent site $\langle a \rangle$ to increase or decrease with respect to the pure solvent value, thus causing a shift $\delta\mathcal{K}$, of the resonance line. Some sites will have values of $\langle a \rangle$ so different from the average that they will not contribute to the main resonance line, but satellites outside instead. This will cause a decrease in line intensity, *i.e.*, wipe-out, upon alloying. Blandin and Daniel's estimate [134] of one such distribution in $\langle a \rangle$ is seen in figure 14. The theoretical estimate is drawn to the same scale as an experimental [150] NMR derivative in Ag containing a small quantity of Sn. The

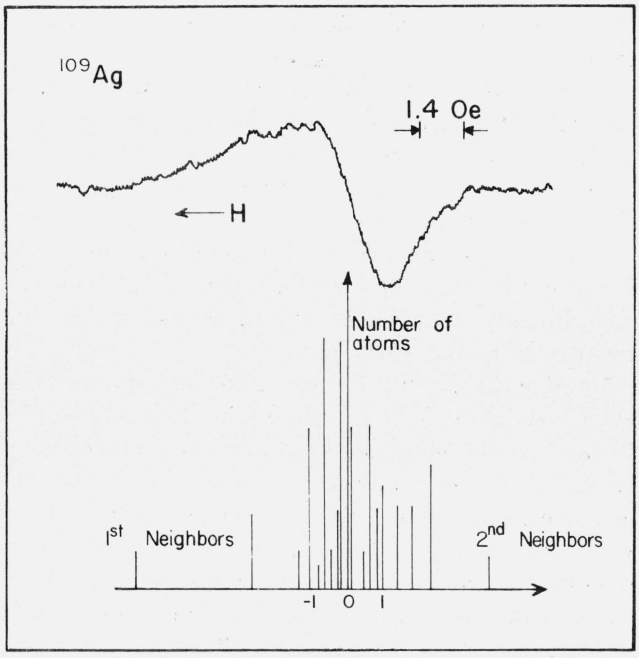

FIGURE 14. *(Above). Rowland's experimental [150] NMR absorption derivative curve in an alloy with 1 percent Sn in Ag. (Below). Blandin and Daniel's calculated [134] positions and relative contributions to silver Knight shifts at silver sites in near neighbor, next near neighbor, etc. . . positions with repsect to an Sn impurity in Ag. This is plotted on the same horizontal scale as the experimental curve.*

near and next near neighbor $\langle a \rangle$'s in Ag(Sn) may well be responsible for the partially resolved satellites. Another experimental example [151] of satellite structure is shown in figure 15 for Pt containing small quantities of Mo. Here three satellites are clearly resolved.

Details of the effect of alloying will depend on such

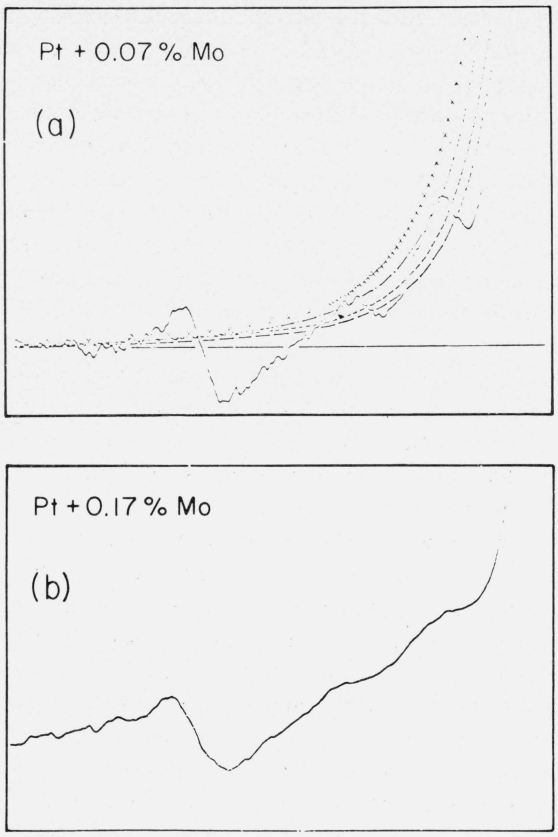

FIGURE 15. *Experimental NMR absorption derivative curve in Pt-Mo alloys as taken from Weisman and Knight [151]. The resonance in (a) shows several distinct satellites and that in (b) shows satellites in the same positions but those near the central resonance begin to merge with the central line, thus causing resonance broadening for increased alloy concentrations.*

factors as whether or not the main peak of the disturbance extends out and encompasses any neighboring nuclear sites. Little is known experimentally, and less from accurate calculation, concerning main peak behavior. (Most theoretical work makes the doubtful, but computationally necessary, use of asymptotic estimates for the entire disturbance.) It is generally thought that the main peak of the Coulomb screening is largely localized at the impurity site while the spin density peak is of longer range. For Fe in Pd the latter is known to cover many lattice sites. This is due to a large $1/2k_F$ value (which affects the main peak as well as the Friedel oscillations) and to the substantial conduction-electron conduction-electron enhancement of χ_p [152-154].

It has been seen that solvent data are largely limited to shifts of the main resonance line and this does not provide a unique test for any given detailed model of

alloy effects. Although such experiments are difficult, further observations of solvent satellite resonances in very dilute alloys would be invaluable for this purpose. Satellite lines would arise from near neighbor region $\langle a \rangle$'s and, providing they can be disentangled, would provide a severe test for any theory.

The interpretation of the alloy Knight shift data depends somewhat on the nature of the material in question. The change of $\mathcal{K}$, $\Delta\mathcal{K}$, upon introducing a second component into a metal, will cause a change in $\langle a \rangle \chi_p$. Whether one interprets $\Delta\mathcal{K}$ as a change in χ_p or in $\langle a \rangle$ [recall the latter is an average involving the product of a's and χ's, over all points of the Fermi surface; see eq (17)] depends upon one's preference for the particular case at hand.

In a simple form one may write, in analogy with eq (1),

$$\mathcal{K}_{\text{alloy}} = \langle a \rangle_{\text{alloy}} \chi_p^{\text{alloy}}. \tag{30}$$

Permitting both $\langle a \rangle$ and χ_p to vary, as in eq (30), is not as practical a viewpoint for scanning alloy data, as is holding one of the two quantities constant and attributing the trend in $\Delta\mathcal{K}$ to a variation in the other. For instance, in the case of the transition metal alloys such as the Ti-V-Cr series, the vanadium Knight shift change may be most conveniently discussed in terms of a change in density of states (*i.e.*, χ_p). We will discuss this case in more detail later and see that for this case such a description is a useful one. On the other hand, in dilute alloys, where the Friedel oscillation description may be used, the change in $\mathcal{K}$ is better described by considering the different $\langle a \rangle$ values as appropriate to the different environmental conditions of the host atoms, keeping χ_p constant.

A general version of eq (30), sampling the Knight shift behavior of the two types of atoms *(A,B)* in a binary alloy is

$$\chi_p = (1-c)\frac{\langle a\chi \rangle^A_{\text{alloy}}}{\langle a \rangle_{A \text{ in alloy}}} + \frac{c\langle a\chi \rangle^B_{\text{alloy}}}{\langle a \rangle_{B \text{ in alloy}}} \tag{31}$$

$$= (1-c)\frac{\mathcal{K}^A_{\text{alloy}}}{\langle a \rangle_{A \text{ in alloy}}} + \frac{c\mathcal{K}^B_{\text{alloy}}}{\langle a \rangle_{B \text{ in alloy}}}, \tag{32}$$

where $\mathcal{K}^A$ and $\langle a \rangle_A$, are the shift and averaged hyperfine constant of atom A in the alloy. χ_p is defined as the susceptibility per atom and c the concentration of B type atoms. Making the nontrivial assumptions that $\langle a \rangle_{\text{alloy}}$ is equal to its value in the pure metal *(A* or *B)*, and that there is no significant exchange enhancement of χ, this equation may be rewritten (using eq 17) in the form given by Drain [74],

$$N(E_F)_{\text{alloy}} = (1-c)N_A(E_F)\frac{\mathcal{K}^A_{\text{alloy}}}{\mathcal{K}^A_{\text{metal}}} + cN_B(E_F)\frac{\mathcal{K}^B_{\text{alloy}}}{\mathcal{K}^B_{\text{metal}}}. \tag{33}$$

Thus

$$N(E_F)_{\text{alloy}} \equiv (1-c)N_A(E_F)^{\text{alloy}} + cN_B(E_F)^{\text{alloy}}, \tag{34}$$

which defines *local* densities of states $N_A(E_F)^{\text{alloy}}$ and $N_B(E_F)^{\text{alloy}}$. The assumption of setting $\langle a \rangle$ in the alloy equal to $\langle a \rangle$ in the metal forces the whole effect of alloying to be described in terms of these local densities of states. At times this proves useful. Drain [74] has used eq (33) and the data of figure 8 to scan the AgCd alloy system. The results are in agreement with general trends seen within and between phases obtained in a "rigid band" scan of electronic specific heat data. However, using eq (33), such a scan should not *rigorously* reflect the variation in the density of states of Ag at and above E_F for a number of reasons. These include charge screening (for discussion see ref. 8) and the fact that the hyperfine constants are held fixed.

Local effects in covalent compounds, such as chalcogenides and SiC can also be examined using eq (31). Consideration of these materials is aided by the fact that the energy bands are often more well-known in these than in intermetallic compounds. An example is n-doped silicon carbide [78,155]. The ^{29}Si Knight shift is near zero whereas a substantial Knight shift is measured for ^{13}C. This information, together with T_1 data for both sites, permitted Alexander and Holcomb [78,155] to infer important wave function symmetries. It was concluded that a zero Knight shift implied a zero wave function density at Si but that symmetry allowed a substantial shift at the carbon site.

Lead telluride is another case where local effects are important and where a significant amount of experimental and theoretical information is available on the energy band structure. Although the results are affected by sample preparation, for the better samples the ^{207}Pb Knight shift in n-type PbTe was found [156] to be temperature independent, and relatively small and positive with respect to undoped PbTe. On the other hand in p-type, PbTe $\mathcal{K}$(Pb) was found to be large, negative and temperature dependent. This was interpreted [156] in terms of a band structure model in which the valence band possesses substantial s-

character with respect to the Pb atoms, whereas the conduction band lacks *s*-character at Pb. The small positive shifts in *n*-type material were assumed to be of orbital origin. The negative contact interaction is ascribed to a negative *g*-value for the *L*-point valence band states. The same band model was used to explain the ^{125}Te Knight shift results in these materials.

9. Correlations of $\mathcal{K}$, χ and γ with Electron Concentration in Transition Metal Alloys

There are many cases in the literature where the Knight shift has been observed to vary smoothly with composition in alloy systems. Where γ values are available from specific heat data, or other $N(E_F)$ information is known, a direct correlation between these quantities and $\mathcal{K}$ can sometimes be found. Usually the complex nature of $\mathcal{K}$ (eq 19) causes the correlation to be somewhat obscured, and the fact that $\mathcal{K}$ does not follow the $N(E_F)$ curve is not necessarily an indication of nonrigid band behavior. Examples are shown in figure 16a. Looking first at the 3*d*-alloys, there is a gradual increase in $\mathcal{K}$ with e/a, with a peak at about 5.6 electrons per atom. Between $e/a = 5.6$ to 6, there is a gradual decrease in $\mathcal{K}$. This decrease is steepest for V-Fe alloys. The vanadium hydride results follow those of V-Cr extremely closely, as if the electron of the hydrogen is absorbed in the common conduction band, filling the band in the same manner that Cr does. Recent data by Rohy and Cotts [169,170] on V-Cr hydrides (not shown) fall on the same line. The other data, including those for the 4*d* alloys, all are similar to the V-Cr curve in that they show a peak in $\mathcal{K}$ at about $e/a = 5.6$. The Nb-Tc alloy data shown in figure 16a deviate from the general trend. The reason for discrepancy in the case of $\mathcal{K}$ measurements may be a result of a difference in $N(E_F)$, but again may be due to local effects so that no direct conclusion can be drawn from the $\mathcal{K}$ versus e/a results alone.

To give a further picture of the shape of the density of states curves for these alloys we show the total susceptibility data in figure 16b. Both for the 3*d* and 4*d* series, there is a possible cusp at $e/a = 5$. Both χ curves have quite similar behavior. The V-Tc(3*d*-4*d*) alloy system also follows this trend. From this picture we get a different impression of the density of states curve than from the curves obtained from γ data as shown in figure 16c. Here there is no cusp at $e/a = 5$ and a major peak occurs between $e/a = 4$ and 5. Thus there is a discrepancy between the γ curves on one hand, and the χ curves on the other. Depending on which curves are used, the Knight shift data may be interpreted in a

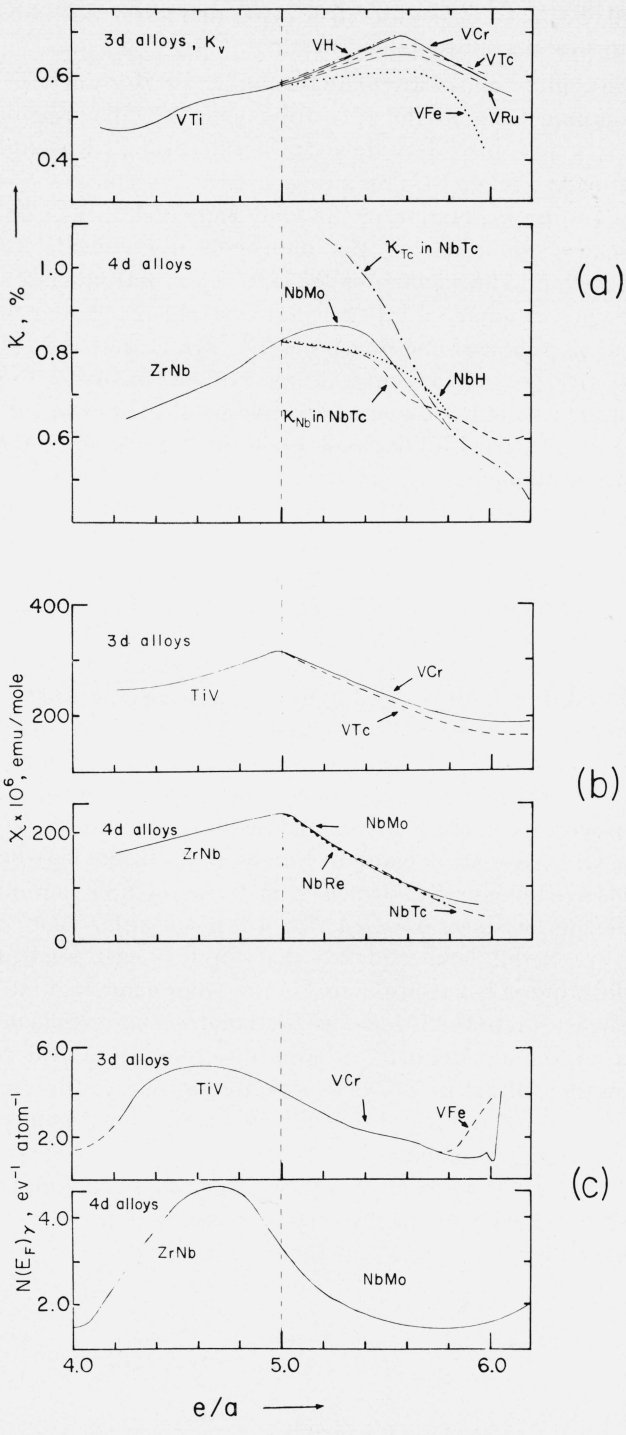

FIGURE 16. *Variation of (a) Knight shift, (b) susceptibility and (c) density of states as measured by electronic specific heat, with e/a ratio for the b.c.c. transition metals of the 3d, and 4d rows. While for $\mathcal{K}$ and χ there are substantial ranges where χ and $\mathcal{K}$ track one another, the $N(E_F)\gamma$ curves show less similarity. The data were taken from the following sources: (a) Ti-V [157], V-Cr [157,158], V-Tc [157], V-Fe [159], V-Ru [160], V-H [161], Nb-H [162], Nb-Tc [163], Zr-Nb and Nb-Mo [164]. (b) Ti-V [165], V-Cr [157,165], V-Tc [157], Zr-Nb [164], Nb-Mo [163,164], Nb-Re and Nb-Tc [163]. (c) Ti-V and V-Cr [164,166,167], V-Fe [164], Zr-Nb and Nb-Mo [168].*

quite different manner. In either case there is no direct correlation between $\mathscr{K}$ and the other data, and there must be an interplay of several terms as a function of e/a. A number of attempts have been made using γ, χ, $\mathscr{K}$, as well as T_1 data and the Korringa relation [27], to derive the various contributions to $\mathscr{K}$. For example, the results of figure 16 have been rationalized [24,163,164] by using a two-band model for the Pauli term, as in eq (23), and estimates of the Van Vleck orbital effects. Although these do explain the results, the description is not unique. An alternative explanation in terms of varying *s-d* admixture in a single band has been offered [171, 172] to explain the maximum in $\mathscr{K}$ at $e/a \approx 5.6$. In the region above 5.6 both γ and χ are decreasing. Within this model, the decrease in $\mathscr{K}$ arises from a Pauli contribution which becomes less negative, and, in fact, positive with increasing e/a. Only 10 to 15 percent *s*-character in the *d*-band is required to balance or overtake the negative *d*-core polarization term. Changes in *s*-character of only a few percent can produce the observed variations in $\mathscr{K}$. As noted earlier for Cu (see fig. 10), admixture and variations of admixture of this magnitude are not unreasonable. This model is more obviously appropriate to the $TiFe_{1-x}Co_x$ alloys, with e/a from 6 to 6.5 [172], where the slope of the $\mathscr{K}(^{59}Co)$ versus χ plot reverses sign across the alloy sequence. If the hybridization model is proven valid, the Knight shift can provide a useful probe of the variation of the density of *s*-states in "*d*"-bands.

An example of a different type of application of a rigid band model is the proposed band structure in the lanthanum-hydrogen system by Bos and Gutowsky [173]. Lanthanum is a metal and upon adding hydrogen up to 67 percent (LaH_2) the material remains metallic. At LaH_3, however, the material becomes an insulator. This, together with $\mathscr{K}$ and χ information, was then used [173] to propose the density of states shown in figure 17. These measurements lead to the conclusion that adding hydrogen means *lowering* the e/a ratio, which can be considered equivalent to the hydrogen absorbing an electron. This is in contrast to the other model in which hydrogen in the alloy gives up an electron to the conduction band and remains in the lattice as a proton. This latter model has been used, for example, to describe the V-H and Nb-H results shown in figure 16a, and for the compounds ScH_2 and YH_2 [174]. An interstitial proton is expected to be a larger perturbation in the La matrix and it may bind two 1*s* electron states to it (as in fig. 17) whereas such electrons might not be bound in the other systems where the perturbation is weaker. Such behavior can be anticipated from *s*-wave impurity scattering theory.

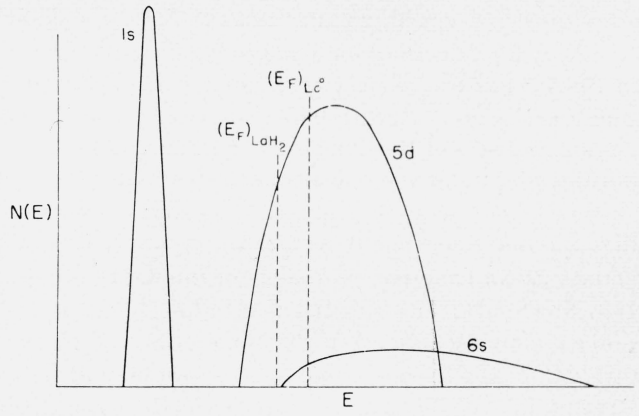

FIGURE 17. *Proposed band structure for lanthanum dihydride [173]. For each hydrogen atom entering the metallic lattice, two electrons are assumed to be transferred to localized hydrogen 1s orbitals. Formation of LaH_3 would correspond to complete emptying of the conduction band.*

10. Solvent Knight Shifts

Confidence that the Friedel oscillations (fig. 13) can be observed was given by Rowland's quadrupole wipeout data in Cu alloys [129], and reinforced by his solvent Knight shift results [150]. Rowland measured the change of the Knight shift upon alloying, $\Delta\mathscr{K}$, for a large number of *B*-subgroup solutes in Ag. From these, he obtained values for Γ ($\Gamma \equiv \mathscr{K}^{-1}\Delta\mathscr{K}/\Delta c$, where c is the fractional impurity concentration). These Γ data are plotted in figure 18. While there is a general tendency

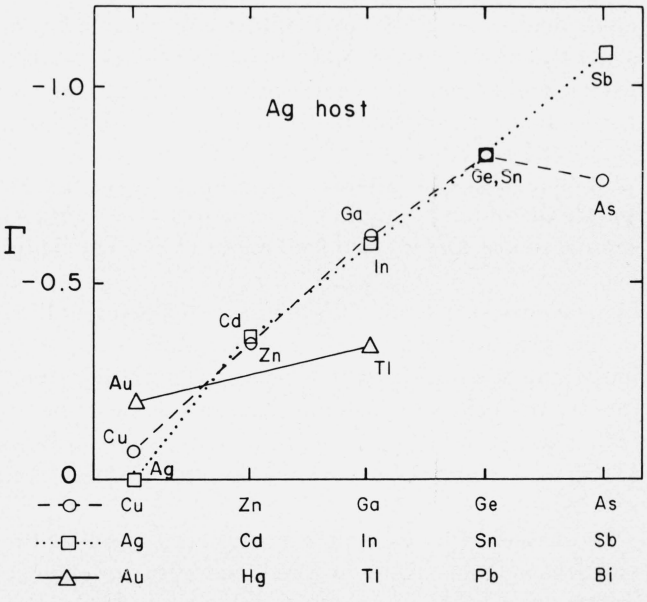

FIGURE 18. $\Gamma = 1/\mathscr{K} \cdot \Delta\mathscr{K}/\Delta c$ *values for impurities in a Ag host versus position of the impurity in the periodic table. The dashed, dotted and solid lines connect points for impurities occurring in the Cu, Ag and Au rows, respectively. These data are taken from Rowland [150], from his table 1. As pointed out by Rowland, the* Γ *values are dependent on the range of data employed.*

for Γ to increase with solute valence, there is a slight turn back (*i.e.*, decrease in magnitude) of Γ from Ag-Ge to Ag-As. For the silver row (namely Cd, In, Sn, and Sb), there is no such turn back. In figure 19a we have chosen two sets of Rowland's $\Delta\mathcal{K}$ data, for pairs of impurities of common valence, which clearly display the valence effect seen in figure 18. Rowland [150] noted that curved lines could be drawn to fit the datum points, as we have done for some of the data in figure 19b. Rowland points out that due to lineshape effects (for example, see fig. 14), the uncertainty of the individual points is such that his representation by a straight line is all that is quantitatively reasonable. Granted this uncertainty, the possibility of nonlinearity in these plots of $\mathcal{K}$ versus c may be real, as was noted by Rowland. Using Rowland's raw data, a Γ defined for low concentrations is smaller than that defined by fitting out to larger concentrations. This fact was used by Alfred and Van Ostenburg [175] in *their* version of the Γ plot which differs from figure 18, for the Sb in Ag point. By using low concentration data, this Γ point was reduced from the value given by Rowland, bringing it into line with their [175] predicted turn back. If the same treatment over the same concentration range is used for *all* of Rowland's datum points, then all the Γ points in figure 18 will tend to be somewhat lower but the general picture will remain as shown in our figure 18. Alfred and Van Ostenburg neither used Rowland's choice for Γ, nor treated the data for all the alloys equivalently. If all of the Γ values are obtained consistently, their phase shift analysis yields neither better, nor worse, agreement with experiment than the earlier phase shift estimates of Kohn and Vosko [176], and of Blatt [177].

Similar valence effects have been seen for *B*-subgroup solutes in liquid copper alloys [178] and, as seen in figure 20a, in solid lead alloys [179]. The liquid copper results of Odle and Flynn [178] also display the high valence turn back. This result is more evident than in the solid Ag case, the $\mathcal{K}$ versus c plots being more linear and the turn back in Γ being larger, although errors for the points of most interest are somewhat large. Odle and Flynn [178], utilized the phase shifts of Blatt [176] and Kohn and Vosko [177] to discuss their results.

In the solid Pb case, the Γ values are largest for the smallest valence (Hg), but a reduced effect of valence difference (*i.e.*, the beginning of a turn back) is also evident. The raw data in figure 20a also reveal curvature in $\mathcal{K}$(Pb) versus concentration for solid PbTl [179], similar to the Ag data in figure 19b. This curvature is not evident for the other Pb alloys. In liquid lead alloys, as seen in figure 20b, taken from Heighway and

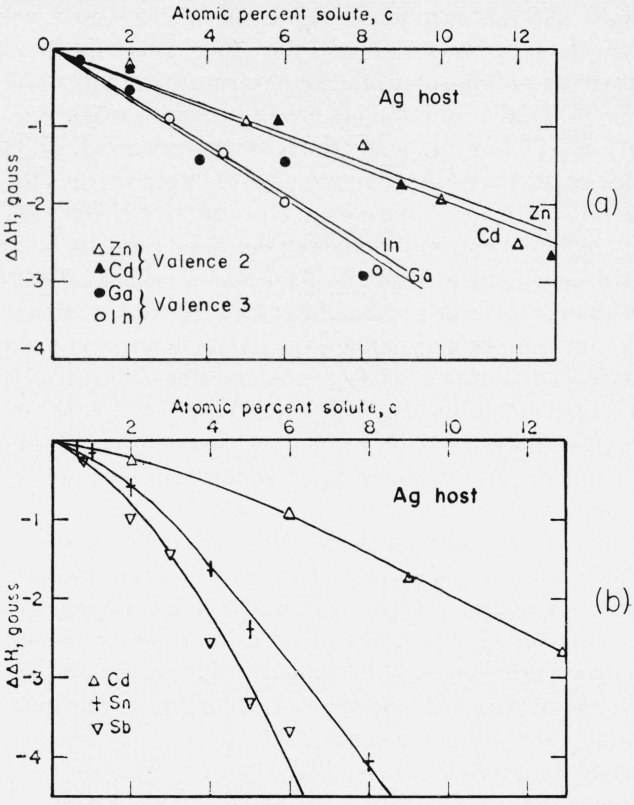

FIGURE 19. *(a) Silver solvent Knight shift datum points with straight lines, as chosen by Rowland [150]. (b) Silver solvent Knight shift datum points [150], indicating smooth curves through these points, without the assumption of linearity.*

Seymour [180], there are some cases of linearity and others of nonlinearity. A very interesting fact here is that, in the solid, Γ has the opposite sign to Γ in the liquid for many of these alloys. This result was verified [180] by following the resonance in Pb-Bi from the liquid to the solid state.

In figure 21a and c, $\mathcal{K}$ versus c plots for solid InPb and InSn alloys [123] are shown. These are examples where there is a tremendous dip in $\mathcal{K}$ versus c, before a more linear behavior is achieved. This dip falls within a 1% impurity concentration in one case, and 2% in the other. The magnitude of these dips is up to 10% of the total Knight shift. For comparison, data for these alloys in the liquid state [181] are shown in figure 21b and d on the same vertical scale as the solid data [182]. Dips may also exist in the liquid state, but, if so, were missed due to the coarse grain scans over the dilute range of alloying. On the other hand the dip may be peculiar to these alloys in the solid state only.

The linearity of $\mathcal{K}$, bearing in mind the coarse composition mesh studied, is striking for the liquid alloys displayed in figure 21 b and d. This linearity is characteristic of many, though by no means all alloy systems.

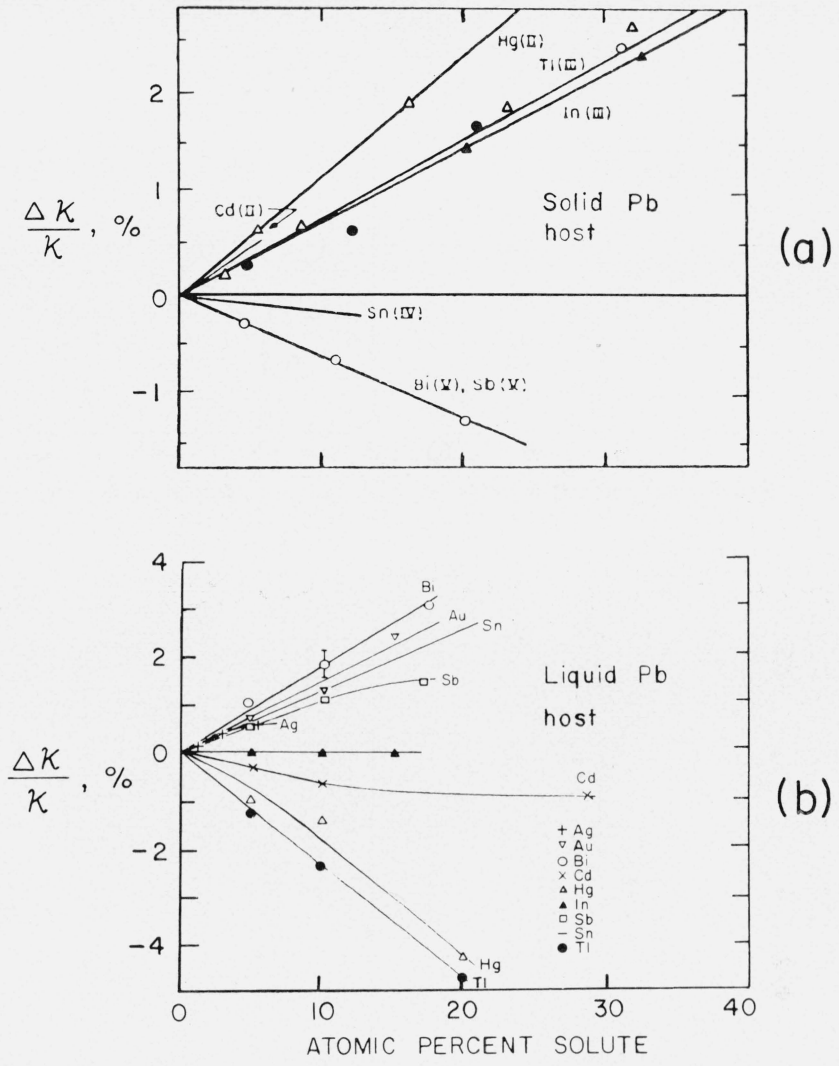

FIGURE 20. *(a) Pb solvent Knight shifts upon alloying in solid alloys, as taken from Snodgrass and Bennett [179]. (b) Pb solvent Knight shifts upon alloying in liquid alloys, as taken from Heighway and Seymour [180].*

Several other examples of linear behavior have been observed [183-188]. In these papers some cases of nonlinear behavior are also encountered. The linearity, even at higher concentrations, may be relevant to some suitable phase shift description. However, it should be recalled that in its formulation the traditional phase shift analysis was developed for infinite dilution only.

A dip in $\mathscr{K}$ versus c is also suggested by the solid Cd-In data [189] shown in figure 22. In this case we have drawn a straight line through the higher concentration data points merely to show a very general trend for the alloys. Although the scatter is large, it is again clear that the data are not best represented by a single straight line from the origin.

The complexity of the various terms contributing to $\mathscr{K}$, and the local nature of $\mathscr{K}$, is such that the observation of nonlinearities should not be surprising. These nonlinearities are not amenable to simple phase shift analyses, although the turn back in Γ is.

For the liquid alkali alloys a form of the single scattering model was employed by van Hemmen *et al.* [190]. Agreement with experiment was obtained by including volume renormalization, without considering the details of the charge oscillations. The phase shift description used by Odle and Flynn [178] for liquid Cu alloys, and similar attempts by Rigney and Flynn [191] using newly derived phase shifts, as well as pseudopotential methods as employed by Moulson and Seymour [192] have been partially successful in describing $\mathscr{K}$ versus c behavior in liquid alloys.

The observed behavior of $\mathscr{K}$ upon alloying should be described by a "nondilute" scattering model coupled

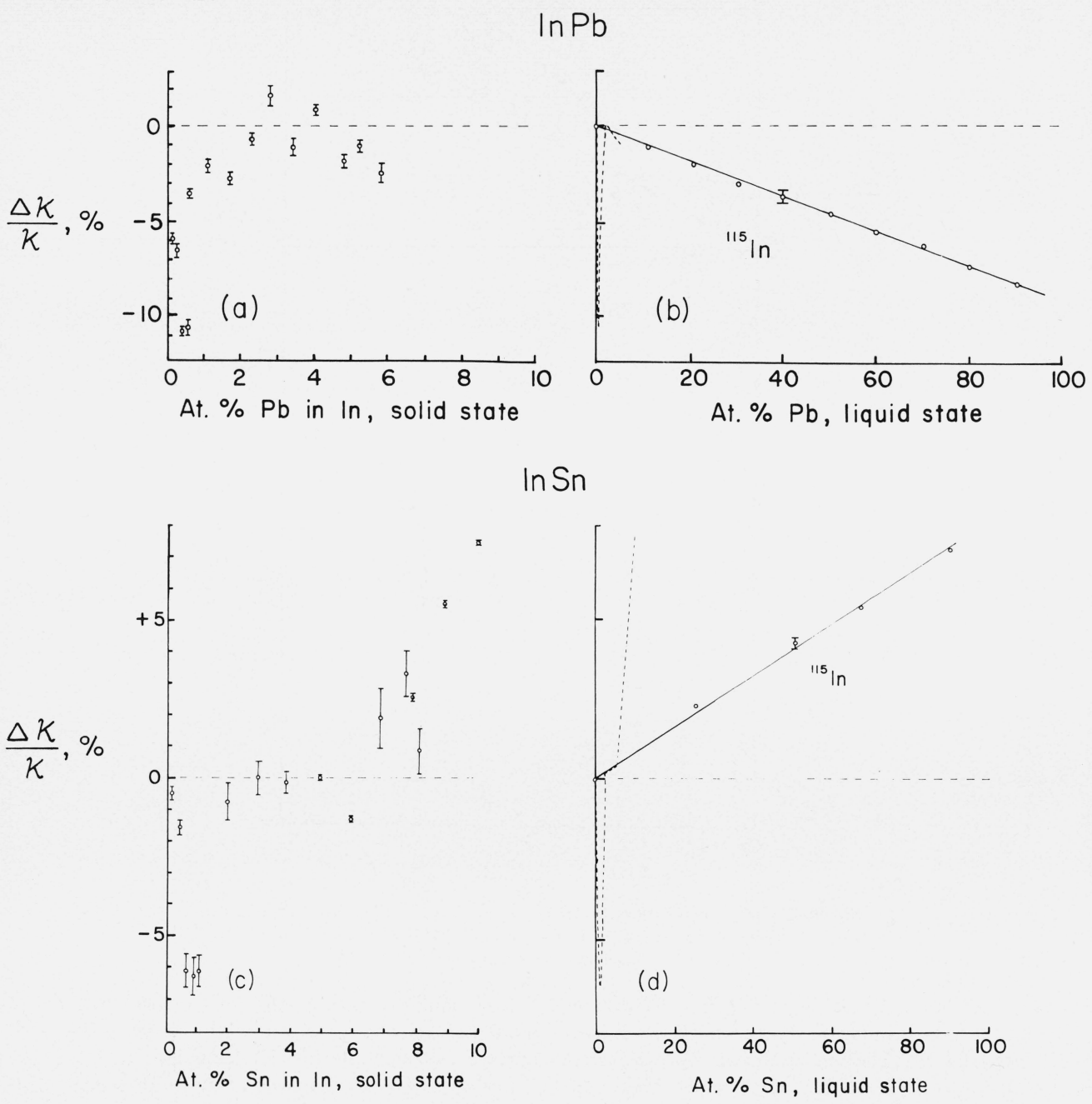

FIGURE 21. *Solvent Knight shifts for two alloy systems in the solid and the liquid state. The indium shift is shown for InPb alloys in (a) and (b), and for InSn alloys, in (c) and (d). In the left hand picture, (a) and (c), data are shown for solid alloys of up to ten percent impurity taken from Anderson, Thatcher and Hewitt [182]. On the right, (b) and (d), data for these same alloys in the liquid state by Seymour and Styles [181] are shown on the same vertical scale over the full range of alloy composition. All the reported alloy datum points are shown. (Note that there is* no *overlap of the data in the dilute region. We have merely transferred the solid data as dashed lines, onto the liquid curves for ease of comparison.) Lacking data there may or may not be strong structure in these liquid alloys in the dilute region.*

with some accounting of "rigid band" effects [8], in addition to other possible mechanics. Such a combined theory is not yet available.

{**Note added in proof:** An interesting proposal to explain the low composition dip was given by R. A. Craig. (We thank the author for sending us a preprint of his manuscript, to be published in the Journal of Physics and Chemistry of Solids.) Anisotropic many-body effects were found to give a contribution to $\mathcal{K}$ in a pure metal. According to Craig, the contribution

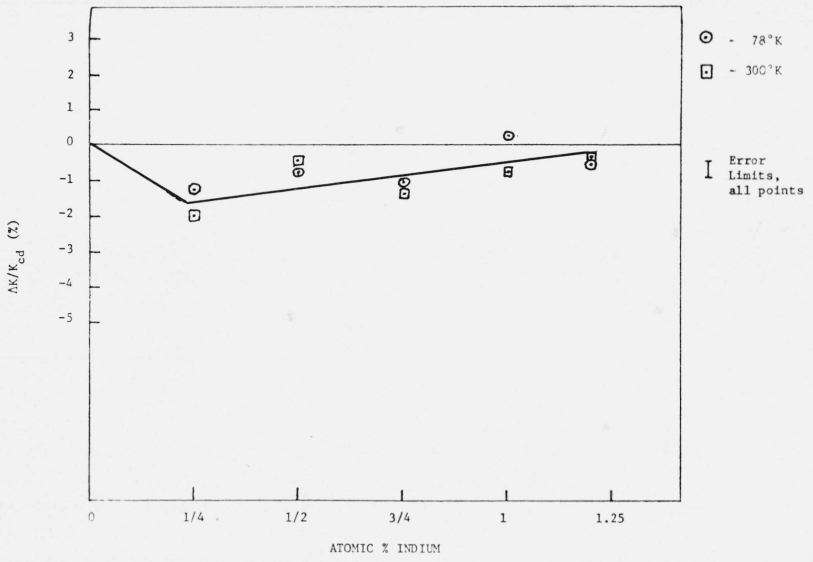

FIGURE 22. *Change of the cadmium Knight shift in CdIn alloys, as taken from Slocum [189]. The indicated straight line through these points has been drawn to demonstrate that these points are clearly nonlinear with respect to the origin.*

is expected to become unimportant upon introducing impurities and at high temperatures (e.g. absent in the liquid), because impurity scattering of the quasiparticles will cause a loss of memory of the angular correlations between the quasiparticle-quasiparticle collisions.}

11. Solute Knight Shifts

When a foreign atom is substituted in a lattice, it causes a certain amount of screening about it, and long range charge oscillations, as discussed in previous paragraphs. Let us now look at what this impurity atom sees as situated in a foreign host. The Knight shift will respond to such a situation in the same way noted above, namely by an $\langle a \rangle$ of the impurity (be it altered somewhat by its environment) and a χ_p of the host, which may also be changed by the introduced impurity. Again it is a matter of how Knight's ξ factor is used as to whether we use χ_p to mean the measured average derived from χ_{expt}, or whether to ascribe a local χ nature to the immediate environment as the impurity sees it. To make this situation more clear we rewrite eq (11) for the Knight shift of an impurity, B, in a given host, A, as

$$\mathcal{K}_{B \text{ in } A} = \frac{1}{\mu_B} \chi_p^A \xi H_{\text{eff}}^B. \tag{35}$$

This definition then uses ξ to absorb solute site changes in both $\langle a \rangle$ and χ_p from the free atom and pure solvent behavior, respectively.

It is useful to explore eq (35) for a sequence of alloys, varying either impurity or host. One might follow the quantity $\mathcal{K}_{B \text{ in } A}$, or $\mathcal{K}_{B \text{ in } A}/\chi_p^A$, for a specific impurity through a series of host metals. For example, we have done this for charge impurities in the sequence Cu, Ag, Au. A similar type of scan is often done for Mössbauer hyperfine data across rows in the periodic table.

Alternatively, one can dissolve a series of impurities in a particular host. The observed trends are less difficult to interpret as we have the advantage of remaining within one crystal structure. Such solute studies have been done for example for Cu and Ag [6], for lead [193], and for Au [7,194] based alloys. Taking these data, we have plotted the quantity $\mathcal{K}_{B \text{ in } A}/H_{\text{eff}}^B$ in figures 23 and 24. We have connected points of impurities belonging in the same row of the periodic table, and dissolved in the same host metal. We see a general downward trend as we go to higher valence for three of the four host materials, but for gold there is a definite reversal of trend. If we now assume an experimental χ_p^A of the pure host material, A, then this behavior reflects directly the nature of ξ, or $\langle a \rangle$, in Au versus that in Cu, Ag and Pb. In other words, the gold host causes the details of the wave function at the impurity site to change quite differently from the other three hosts. This could, of course, involve local density of states effects as well. We believe [7] that strong *s-d* hybridization, arising from the proximity of the *d* band to the Fermi level, is important to the Au behavior. Unfortunately, auxiliary specific heat, susceptibility, and other experimental data which might help resolve this

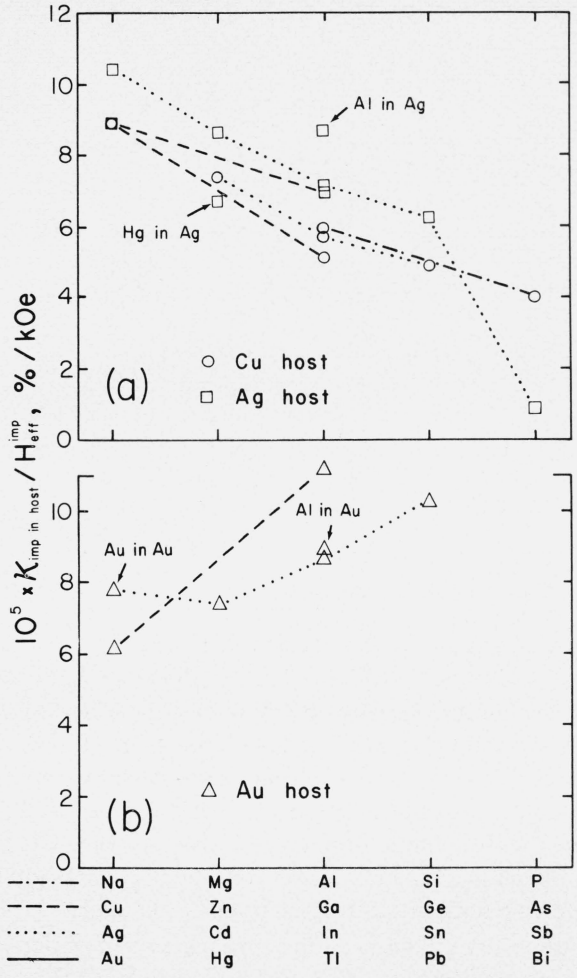

FIGURE 23. *Impurity Knight shifts in Cu, Ag and Au hosts. Atomic effects due to the hyperfine coupling constants are divided out, using our* H_{eff} *values for the impurities, listed in table 2. The resulting trends are opposite for a gold host than for copper and silver hosts. (Data for boron in gold [195] of* 15×10^{-5}% *per kOe agrees with the upward trend for the gold host. The uncertainty in this value is greater than that of the points given in the plot.) Points for impurities occurring in the same row of the periodic table are connected with the line symbols indicated in the lower left hand corner (e.g., the dotted line connecting the square datum points is for Ag, Cd, In, Sn, and Sb in a silver host). The Cu and Ag data were taken primarily from Rowland and Borsa [6]; the Au data from Bennett* et al. *[7]. This latter paper gives in its table 1 further references to the literature for several of the shown points. The Sb in Ag point was taken from Matzkanin* et al. *[194].*

matter is not readily available for the Au alloys. More data of this type would be worth obtaining.

12. Magnetic Disturbances

The effects of a charge impurity in a metal have been described above (sections 8, 10, 11). When a *magnetic* impurity is introduced into the metal, a similar

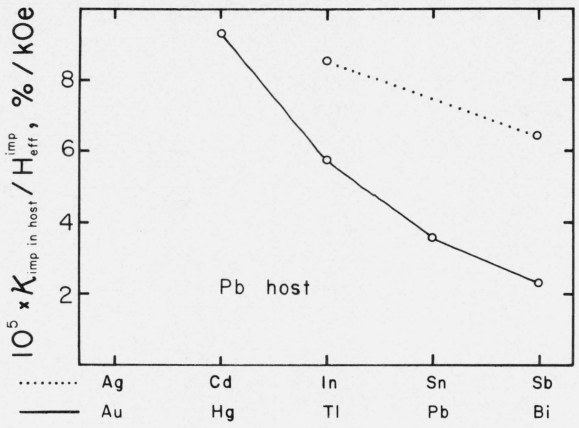

FIGURE 24. *Impurity (B) Knight shifts in a lead host divided by the impurity hyperfine fields,* H_{eff}^{B}. *Data taken from Bennett* et al. *[193]. The dotted line connects points for impurity atoms belonging to the Ag row of the periodic table and the solid line connects those for impurity atoms belonging to the Au row. The trend is similar to that for Cu and Ag hosts and opposite that for an Au host.*

response occurs: spin density oscillations (rather than, or in addition to, charge oscillations) are set up around the impurity, as discussed in section 8. The behavior is similar to the oscillations shown in figure 13. The unbalanced spin at a neighboring site interacts with that nucleus via a spin-dependent interaction. Generally this interaction is rather strong compared to charge effects causing correspondingly larger variations in the Knight shift and thus larger values of Γ.

Gardner and Flynn [196] have reported susceptibility and solvent Knight shift results for transition element (3*d*) impurities in liquid Cu. The dominant Knight shift term in these cases is associated with the 3*d*-magnetic moment aligned at impurity sites by the magnetic field. The susceptibilities of alloys with Cr, Mn, Fe, and Co as impurities obey the Curie-Weiss law implying the existence of local paramagnetic *d*-moments at impurity sites. The moment values, μ, inferred from the susceptibilities are plotted in figure 25. Sc, Ti and Ni alloys do not follow a Curie-Weiss law, suggesting that local virtual *d*-level *band* paramagnetism dominates.[12] The Mn, Fe, and Co moments plotted in figure 25 are of some interest if one assumes that they are entirely associated with impurity site *d*-character, *i.e.*, little or no moment either residing on the host lattice, or in conduction band character at an impurity site. The moments then equal the number of holes in the *d*-bands and the quantity (10-μ) provides an estimate of the number of *d*-electrons at a local site.

[12] The detailed susceptibility behavior of the Cr, Mn, Fe and Co alloys suggests the presence of a small term, of perhaps this sort, in addition to local moment paramagnetism.

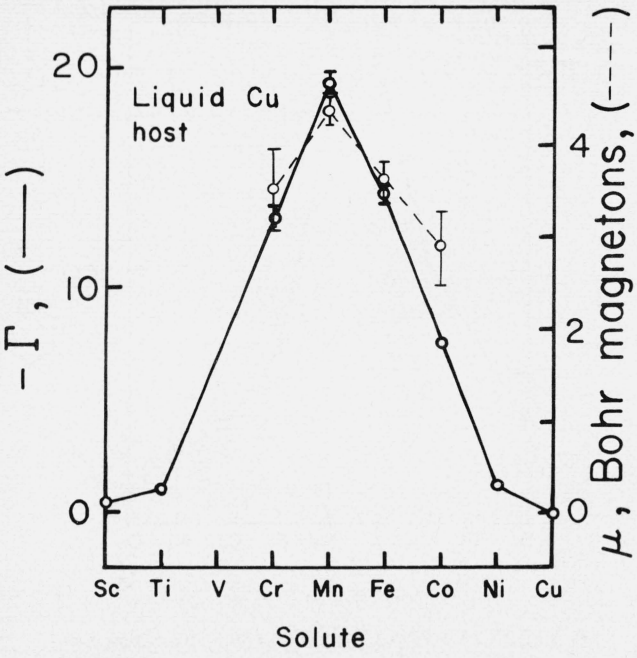

FIGURE 25. $\Gamma = 1/\mathcal{K} \cdot \Delta\mathcal{K}/\Delta c$ *values for* 3d *transition metal impurities in liquid copper (solid line) and effective magnetic moment,* μ, *(dashed line) plotted versus position in the periodic table. Both sets of data are taken from Gardner and Flynn* [196]. *The vertical scale of the* μ *plot was arbitrarily chosen so that the height of the* Γ *and* μ *peaks are nearly equal.*

Gardner and Flynn [196] obtained values of 7.1, 6.4, and 5 for the number of Co, Fe and Mn respectively. These numbers are 0.5 to 1.0 electrons smaller than the *d*-electron counts believed appropriate to the pure solute transition metals and, if real, this trend offers valuable evidence as to the electronic character of these impurities. The estimate, of course, relies strongly on the assumption that the moments are entirely of impurity site *d*-character with no hybridization with the conduction bands. Electron count estimates for lighter 3*d*-element impurities, such as Cr, are further hampered by the question of whether or not there is any occupied *d*-character of spin antiparallel to the net spin of the moment. The density of states with and without such behavior is shown schematically in figure 26. It is probably reasonable to assume that a strong paramagnetic moment such as Cr in Cu has little or no *d*-spin moment component antiparallel to the net local moment.

The Γ values appropriate to the various 3*d*-Cu alloys are also plotted in figure 25. These roughly follow the moment behavior, are negative, and are large when compared with the charge perturbation Γ's of, for example, figure 17. They are large because a local 3*d*-susceptibility, and its associated spin density disturbance, contributes a larger Knight shift effect

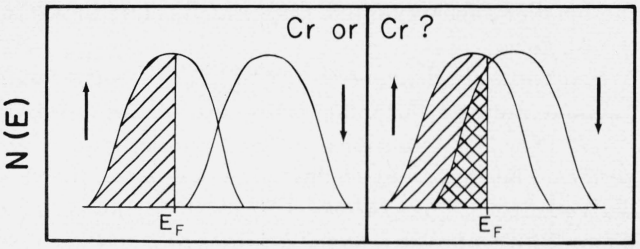

FIGURE 26. *Schematic density of states as a function of energy for Cr metal. In the first case the spin up (* $\uparrow$ *) band and spin down (* $\downarrow$ *) band do not overlap at the Fermi surface; in the second case both spin up, and spin down bands are partially filled.*

than the weak perturbation of charge impurities. Charge effects are undoubtedly also present in the vicinity of 3*d*-impurity sites, but these appear to be insignificant if a local paramagnetic moment is formed. The strength of the magnetic term, relative to other effects, is a prime reason for the observed linearity in $\mathcal{K}$ versus impurity concentration. (This assumes that the magnetic term above tends to be linear.) The negative sign of the Γ's might imply that the main peak of the conduction electron spin disturbance (see fig. 13) has its moment antiparallel to the local moment. This negative sign is reminiscent of charge impurity effects and might instead indicate, as in the charge case, that the main peak either fails to overlap solvent nuclear sites or, if it does overlap, contributes satellite lines which are shifted out of the main resonance (*e.g.*, see fig. 14). While the latter would be consistent with charge impurity experience, most workers believe that the main peak is sampled by the main resonance line, and that a negative Γ indicates spin moment antiparallel to the local moment. This in turn implies that hybridization and higher order effects predominate over electrostatic exchange scattering. Combined hybridization and electrostatic exchange terms will provide an *effective* exchange coupling which is *not* constant as one traverses the 3*d*-elements. One thus expects a crude but *by no means linear* relation between Γ and μ. This is seen to be the case in figure 25. Gardner and Flynn showed that a partial wave description involving *d*-wave scattering crudely reproduces the trend and magnitude of the Γ's.

Flynn and coworkers have also obtained [197] results for 3*d*-impurities in liquid Al and these are summarized in figure 27. Since band, rather than local moment, paramagnetism prevails for all impurities, the added susceptibilities per mole of solute have been plotted (rather than local moment μ values). The Γ values, except for Sc and Ti, are smaller than those obtained in the Cu alloys. This is largely accounted for by

the smaller susceptibilities (per added solute atom) in the Al alloys.

The Cu and Al hyperfine fields, per effective spin moment induced on solute sites, are of the order of -100 kOe for impurities in the middle of the $3d$-series. The hyperfine fields obtained (and the ξ's derived from them) for the Cu alloys are plotted in figure 28. (A similar plot for $3d$-impurities in liquid Al alloys results in much larger uncertainties.) One might expect a somewhat smaller value of H_{eff} for Al relative to that of Cu, since the free atom s-contact interaction of Al is approximately half that of Cu. The fact that it has a similar value suggests that the magnetic response in the Al matrix, due to a given moment on the impurities, is slightly larger[13] than in Cu.

If one attributes H_{eff} on an average solvent site to an s-moment, with its associated atomic $\langle a \rangle$, the results correspond to antiparallel spin moments of 0.05 to 0.08 μ_B for Al and up to 0.05 μ_B for Cu for every Bohr magneton of moment aligned at solute sites and in the solvent matrix. The moment at any given solvent site is small but the total moment residing in the solvent lattice can become a significant fraction of that residing on the solutes thus affecting the arithmetic average of d-electron population estimates from susceptibility data.

A comparison of the Γ behavior and the susceptibilities for the Al alloys (fig. 27) shows Γ tracking χ more poorly than was the case in the Cu alloys (fig. 25). When making such a comparison it should be noted that the Γ for Sc, Co, Ni and Cu are of the order of charge impurity Γ's. Thus, charge as well as magnetic effects, may be contributing to Γ. As we have discussed, the negative sign of the Γ's in figures 25 and 27 would seem to indicate that hybridization exchange scattering predominates over direct exchange effects (see sec. 8). There is no reason why such hybridization effects should be constant across the $3d$ row and the deviation in Γ from the χ curve in figure 27 is of a magnitude appropriate to such a variation in hybridization effects. Flynn and coworkers explain the trend with a particular version of such higher order effects, in which the exchange enhancement of the virtual d-level susceptibility (see eq. 20) plays an important role. The fact that Γ lies higher for the lighter $3d$ impurities could be due to charge effects but it would seem to imply that hybridization effects are stronger (and/or coulomb exchange weaker) for the lighter elements in Al. The peaking of Γ at Cr or Mn seen in figures 25 and 27 is characteristic of the $3d$ elements. Quite different behavior is seen for the rare earths (*e.g.*, see fig. 29).

As already noted, the variation in Knight shift with impurity concentration is strikingly linear in both the Al and Cu alloys over the ranges of concentration studied.

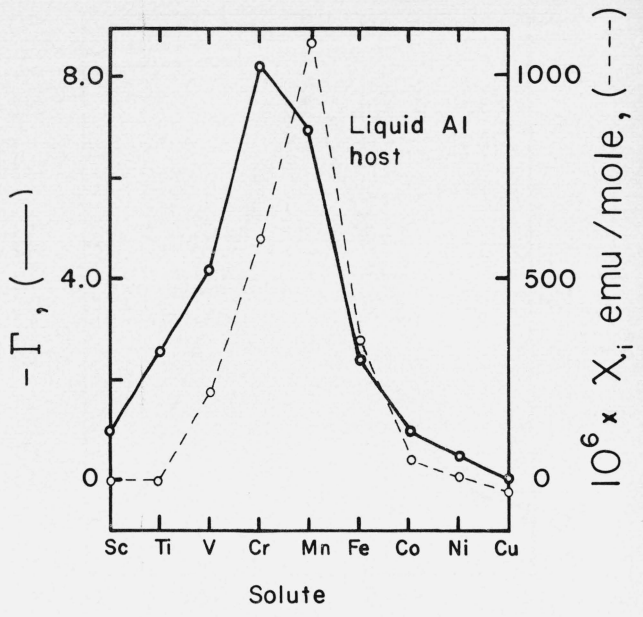

FIGURE 27. $\Gamma = 1/\mathcal{K}\,\Delta\mathcal{K}/\Delta c$ *values for* 3d *transition metal impurities in liquid aluminum (solid line) and* χ_i, *the susceptibilities per mole of solute plotted versus position in the periodic table. Both sets of data are taken from Flynn* et al. [*197*].

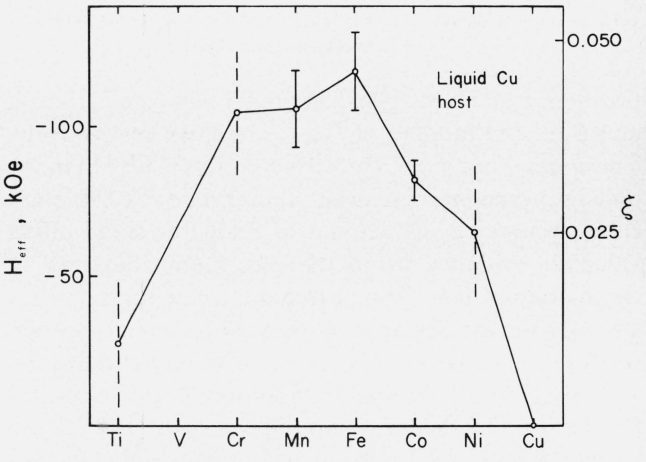

FIGURE 28. *Hyperfine fields and effective* ξ *values for liquid copper sampling the effects produced by liquid transition metal impurities. Unlike the normal definition of such quantities these are defined with respect to the impurity susceptibility. This is accomplished by using composition, rather than temperature, as the implicit parameter in a* $\mathcal{K}$ *versus* χ *plot.*

[13] One might be tempted to attribute this to band effects associated with the band paramagetism of the impurities in Al versus the local moment paramagnetism of Cr, Mn, Fe and Co in Cu, but note the small effective fields for the band paramagnetic impurities of V and Ni in Cu.

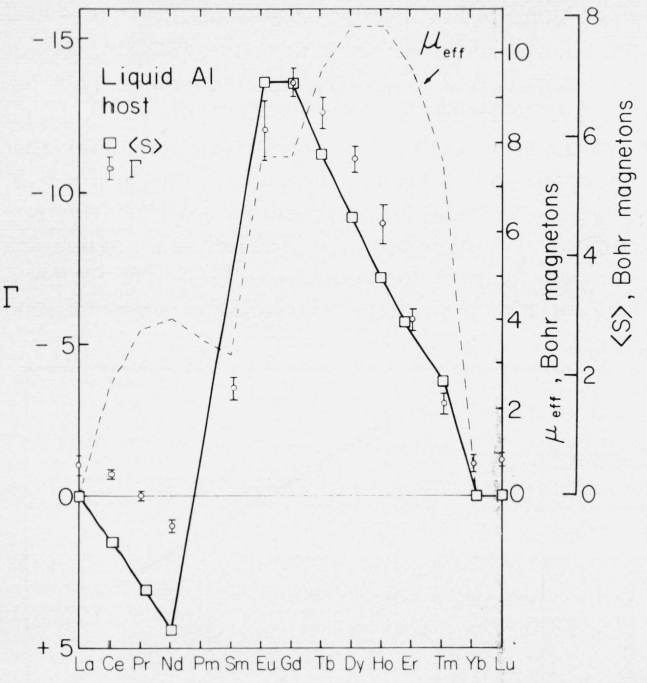

FIGURE 29. $\Gamma = 1/\mathscr{K} \cdot \Delta\mathscr{K}/\Delta c$ *for rare earth metal impurities in liquid aluminum (circles with error bars) and* μ_{eff}, *the effective total magnetic moment (dashed line) plotted versus position in the periodic table. Both sets of data are taken from Stupian and Flynn* [200]. *Also plotted is the effective spin moment* ⟨S⟩, *as discussed in the text (solid lines with squares).*

In some cases these extended up to five and six percent. These are concentrations at which one magnetic impurity would have another magnetic impurity as a near neighbor roughly half the time. At such concentrations it is doubtful that a Friedel or RKKY type of theory should be expected to work, for they assume noninteracting impurities which are dilute enough that there are no saturation effects in the solvent. Any effective local-moment local-moment exchange coupling is reduced due to the fact that the experiments were done at high temperature (above 1000 K). This may serve to reduce apparent nonadditive effects. It may be that averaged multimoment effects are contributing to the Γ's. Extremely dilute alloys were not examined; with one exception the lower ranges of alloy concentrations were one-half to one percent.

Knight shift data in alloys have also been obtained by γ-γ, perturbed angular correlation experiments [198]. In such an experiment, a nucleus is observed which has emitted a gamma ray in some particular direction. Thus defining the nuclear orientation, one then observes that nucleus as it emits a second gamma ray in some characteristic multipole distribution. Application of an applied magnetic field produces a Larmor precession of the nucleus between the emission of the first and second gamma ray. The precession rate, with its associated Knight shift term, can be deduced from its effect on the second gamma ray distribution. Rao *et al.* [198] have recently used the technique to obtain the Knight shift of very dilute Rh in Pd over a temperature range of 4.2 to 1053 K. They then used existing susceptibility data, extrapolated to infinite Rh dilution, to obtain a $\mathscr{K}$ versus impurity site χ plot, which was not linear. The $\mathscr{K}$ versus χ slope appropriate to particular temperature regimes are uncertain due to questions concerning scatter in the Knight shift data and the purity of the samples used in two different sets of susceptibility measurements. (These are strongly paramagnetic alloys and any magnetic impurities will strongly perturb the magnetic response.) The results yield a large negative $\mathscr{K}$ versus χ slope at high temperatures, which is of the order of 4*d*-core polarization effects, but a much smaller slope at low temperatures. This is consistent with a picture where the impurity contribution to the susceptibility at high temperatures is almost entirely associated with Rh sites, but, due to exchange enhancement effects involves the entire Rh-Pd matrix at low temperatures. The low temperature $\mathscr{K}$ versus χ slope is consistent with an effective magnetic moment of $\sim 10\mu_B$ residing largely on the solvent matrix. Such a moment was *independently* deduced [199] from Curie-Weiss fits for these alloys at low temperatures.

Stupian and Flynn [200] studied the effect of adding rare earth impurities to liquid Al. The susceptibilities were consistent with local moments as predicted by Van Vleck [201]. With the exception of Sm($4f$)^5 where there is strong multiplet mixing, the moments are approximately

$$\mu_{\text{eff}} = [J(J+1)]^{1/2} g\mu_B \equiv \frac{\mathbf{L}\cdot\mathbf{J} + 2\mathbf{S}\cdot\mathbf{J}}{[J(J+1)]^{1/2}}\,\mu_B, \qquad (36)$$

where the Landé g-factor has been written out. Very substantial orbital terms contribute to μ and therefore the Γ's should not, and do not, track μ. The Γ's are compared with $\langle S\rangle$ in figure 29 where $\langle S\rangle$ is the spin component along **J**, *i.e.*

$$\langle S\rangle \equiv \frac{2\mathbf{S}\cdot\mathbf{J}}{[J(J+1)]^{1/2}} = \mu_{\text{eff}}\left(\frac{2\mathbf{S}\cdot\mathbf{J}}{\mathbf{L}\cdot\mathbf{J} + 2\mathbf{S}\cdot\mathbf{J}}\right) = 2\mu_{\text{eff}}\left(\frac{g_j - 1}{g_J}\right) \qquad (37)$$

is a measure of the spin component (in μ_B) parallel to the aligned **J**. This provides a crude first order measure of effective exchange perturbations. **S** is antiparallel to **J** in the first half of the rare earth row and parallel in the second, hence the sign reversal in $\langle S\rangle$. The Γ's dis-

play a weaker reversal which is, in part, associated with uncertainties such as the *natural* zero line for magnetic contributions to Γ. [Note that La, Yb and Lu impurities have zero-valued magnetic moments yet their Γ's lie above the zero line.] The differences between Γ and $\langle S \rangle$ are on a similar scale to the effects seen in figure 27. Otherwise there are fundamental differences in Γ behavior as one transverses the rare earths in contrast to the 3*d*'s. Negative Γ's prevail suggesting a tendency for the conduction electron spin disturbance to be antiparallel to the spin of the rare earth moment. This is consistent with almost all experience with rare earth elements in alloys or intermetallics. This sign was also observed for rare earths as impurities in Pd [202-204], at Al sites in $REAl_2$ intermetallic compounds [205], and for ^{31}P, ^{75}As and ^{121}Sb in PrP, PrAs, TmP, TmAs and TmSb[14] [206]. There is general agreement that hybridization effects are responsible for these results.[15]

The situation with magnetic alloys is seen to be similar to the charge impurity case. Both can be described with models of the perturbations which reproduce the experimental behavior, usually crudely, although occasionally in detail. The magnetic alloy problem is complicated by the presence of several scattering mechanisms and by the fact that a magnetic impurity is also a charge impurity. Solvent Knight shift experiments provide unique data for testing alloy models in both magnetic and charge difference systems, but as yet they have provided little *unique* insight into alloy behavior. Further studies of very dilute systems and of satellite lines outside the main resonance peak should prove invaluable for this purpose.

13. Intermetallic Compounds

Relating the Knight shift to the electronic density of states in ordered alloys or intermetallic compounds presents some problems which we have tacitly ignored when considering disordered systems. Let us review the analysis of the Knight shift results [22,208,209] for the technologically important V_3X compounds [X = As, Au, Ga, Ge, Pt, Sb, Si or Sn]. It was in their now classic investigation of these intermetallic compounds that Jaccarino and Clogston developed the graphic $\mathcal{K}$ versus χ analysis described earlier [13]. $\mathcal{K}$ versus χ plots (with temperature an implicit parameter) are shown in figure 30 for V and Ga in V_3Ga. The temperature variation in χ is huge. The variation in χ *per* V atom

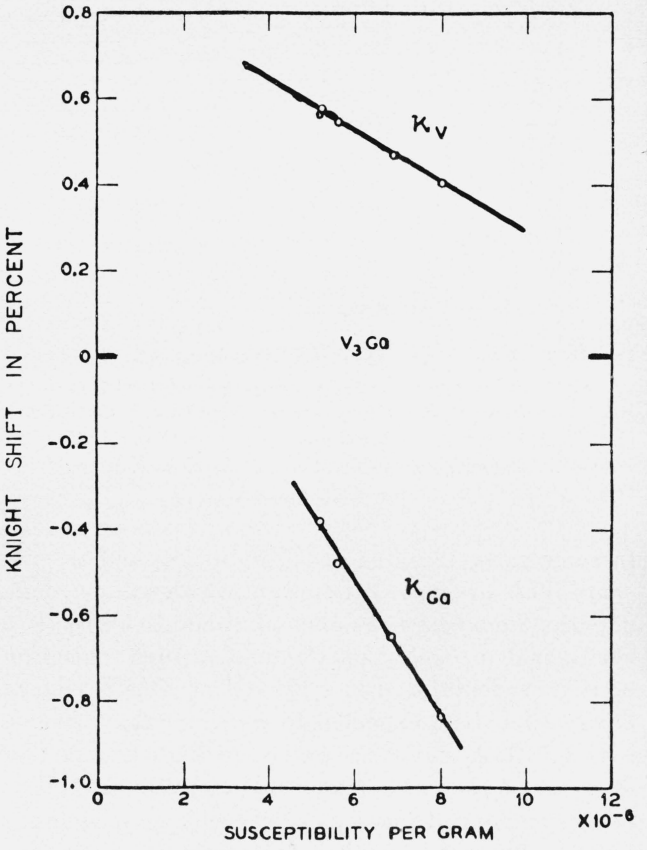

FIGURE 30. *Knight shift versus susceptibility for V and Ga in V_3Ga, as taken from Clogston and Jaccarino [13].*

as a function of temperature in V_3Ga is somewhat larger than that per Pd atom in Pd metal. This strong variation requires significant structure in the density of states (*e.g.*, see [110]) within kT of the Fermi energy. To investigate possible sources of density of states structure, Weger [210] considered the role of the linear chains of V atoms which occur on the cube faces in the V_3X structure. These chains impose anisotropic electronic properties which, in turn, could produce strong structure in $N(E)$ near E_F. Gossard [211] has studied Knight shift and quadrupole effect changes in V_3Si across the low temperature cubic-to-tetragonal phase

[14] Jones [207] also succeeded in observing the ^{141}Pr and ^{169}Tm Knight shifts in these paramagnetic compounds. Shifts as large as 8,900 percent were observed. Jones showed that this is consistent with theory and is due to large orbital hyperfine effects associated with the 4*f*-moments. He also noted that the temperature dependence of the rare earth and of the nonmagnetic site Knight shifts tracked each other quite faithfully.

[15] But other effects may also play a role. For example, direct electrostatic exchange scattering was not added to hybridization effects in Stupian and Flynn's consideration of the rare earth-Al alloys. Reasonable estimates of the appropriate exchange integrals suggest contributions to Γ of the order of (and opposite sign to) the observed Γ behavior. Inclusion of the effect would have overburdened the model with too many disposable parameters.

transition. He interpreted the transformation in terms of such a linear chain model. Labbé and Friedel [212] presented an alternative linear chain model which also is in accord with the experimental situation.

Strong negative $\mathcal{K}$ versus χ slopes are seen in figure 30. The slope for Ga is twice as steep as that for V. The $\chi=0$ intercepts of $\mathcal{K}$ are positive and were attributed to a temperature independent Pauli term arising from a broad conduction band with *s*-like wave function character at both Ga and V sites. (There is probably also a significant orbital Knight shift term contributing to the V site intercept.) The temperature dependent Knight shift was attributed to a narrow V 3*d*-band into which Ga 4*p*-character is hybridized, contributing shifts of the form

$$\mathcal{K}_V(T) = w_V \langle a \rangle_V \chi_p$$
$$\mathcal{K}_{Ga}(T) = w_{Ga} \langle a \rangle_{Ga} \chi_p \qquad (38)$$

where χ_p is the *d*-band Pauli susceptibility per formula unit. The w_i are weights *per atom* of V and Ga character in a formula unit in the band. They *also* account for any deviation in the hyperfine constants from the chosen values. With correct $\langle a \rangle$'s chosen, then the w_i are simply weights and subject to the normalization requirement[16]

$$3\,w_V + w_{Ga} = 1. \qquad (39)$$

The $\langle a \rangle$'s were assumed to arise from V 3*d* and Ga 4*p* core polarization. The free atom values of -117 and -44 kOe/μ_B (consistent with table 3) were used, respectively. Given these $\langle a \rangle$'s, the slopes of the $\mathcal{K}$ versus χ plots yield $w_V = 0.13$, and $w_{Ga} = 0.92$. The greater w_{Ga} value is in large part due to the steeper slope of the Ga plot. Testing the normalization condition yields

$$3\,w_V + w_{Ga} = 1.31, \qquad (40)$$

a sum remarkably close to one. This might suggest that the *w*'s are essentially measures of wave function weight. Clogston and Jaccarino observed trends in Knight shift behavior of various V_3X compounds which further suggest this. If the *w*'s are real weights, their values are surprising, for they would indicate that Ga *p*-character, rather than transition metal *d*-character, dominates at the Fermi surface. Subsequent band calculations by Mattheiss [213], yield $2 \leq w_V/w_{Ga} \leq 3$ unlike a value of 1/7 obtained from $\mathcal{K}$ versus χ plots. The V_3X compounds have large $N(E_F)$'s and their susceptibilities are strongly temperature dependent. Such behavior is characteristic of a *d*-band metal. This would suggest that the ratio obtained by Mattheiss is reasonable, and thus, that the w_i's obtained from the Knight shifts are largely a measure of hyperfine field behavior. Assuming a value for the weight ratio, the Knight shift slopes can be used to estimate experimental $\langle a \rangle$ values for this compound. A ratio of 2 yields values of -53 and -283 kOe/μ_B for V and Ga respectively. The reduced $\langle a \rangle_V$ could be caused by interatomic effects, by intrasite *s*-band polarization, or by *s-d* hybridization. Three percent *s*-character admixture into the *d*-band at E_F will account for the reduction. Large negative intra-atomic effects, over and above the core polarization term, are unknown. The value for the core polarization term, shown in table 3, includes the polarization of the closed valence *s*-shell. Wave function changes on going from a neutral atom to the metal might effect this core polarization term by a factor of two or three but not likely by an order of magnitude. Thus the enhanced $\langle a \rangle_{Ga}$ is most likely due to interatomic effects [$\langle a \rangle_{Ga}$ goes to -400 kOe/μ_B if w_V/w_{Ga} is taken equal to 3]. A similar situation occurs in V_3Si. The $\langle a \rangle_{Si}$ is observed to be negative yet the core polarization hyperfine field appropriate to atomic P, and thus presumably Si, is positive. The P atomic behavior might be irrelevant to Si but the result again suggests the presence of substantial negative interatomic terms at X sites in the V_3X compounds. An X-site in these compounds has twelve nearest V neighbors. This implies the presence of a nearest neighbor spin moment which is 20 to 40 times that induced at the X site itself by the magnetic field. Conduction electron polarization effects of the order of those encountered for transition metals in either liquid Cu or Al can, given such a large neighboring moment, account for the value of $\langle a \rangle_{Ga}$ as well as the apparent sign reversal in $\langle a \rangle_{Si}$. With such a large *near neighbor* moment, it is also possible that there is a substantial contribution to $\langle a \rangle$ via direct exchange polarization of the X-site ion core. Knight shift data [214,215] suggest that similar effects occur at Sn sites in the isostructural system Nb_3Sn.

Subsequent investigations of rare earth and transition metal intermetallic compounds have often relied on $\mathcal{K}$ versus χ plots to disentangle terms. Most of the data are associated with nonmagnetic atomic sites and band hybridization. Interatomic effects are featured heavily when rationalizing the behavior of the hyperfine constants. Interatomic effects are normally interpreted

[16] Noting that the molar susceptibility appears in eq (38) and an atomic χ_p in eqs (31) and (32), eqs (38) and (39) are equivalent to, and can be used to derive, eqs (31) and (32).

in terms of an RKKY type of spin distribution induced by the aligned spin moments on the magnetic ion sites. A variant of the two-band description of the nonmagnetic site Pauli shift has frequently proved useful, namely

$$\mathcal{K}(T)=\mathcal{K}_0+\mathcal{K}_{loc}(T), \tag{41}$$

where $\mathcal{K}_0$ is the Knight shift associated with the conduction band Pauli term and $\mathcal{K}_{loc}$ is the shift arising from the interatomic response to the aligned spin moment on the magnetic atom site. $\mathcal{K}_{loc}$, which is presumably responsible for the temperature dependence of $\mathcal{K}$, has the form

$$\mathcal{K}_{loc}(T)=\frac{2(g_J-1)}{g_J}H'_{eff}\chi_{loc}(T)/N\mu_B. \tag{42}$$

Here χ_{loc} is the Pauli susceptibility of either the local moment or band type associated with the moment induced on the local moment site. The $2(g_J-1)/g_J$ factor is included in anticipation of the rare earths, so that H'_{eff} is the hyperfine field at the nonmagnetic site per local *spin* moment (per molecule) at the magnetic site. The details of the conduction electron distribution arise in the sampling

$$H'_{eff}\sim\sum_R\rho(R), \tag{43}$$

where we have assumed that H'_{eff} arises from the contact interaction and the sum spans all interatomic radii, R, connecting all magnetic sites with a nonmagnetic atom. Efforts [216,217] have been made to relate such a sum to $\mathcal{K}$ values. These have been hampered by inadequate knowledge of $\rho(R)$. Asymptotic RKKY distributions were of necessity used, although it is the near R (nonasymptotic) region which is most important to H'_{eff}. More often the alternate approach of assuming that H'_{eff} effectively samples the *average* ρ, *i.e.*, the Pauli or Zener response to the local moment exchange field is used. Then

$$H'_{eff}=\mathcal{K}_\alpha\mathcal{J}/2\mu_B, \tag{44}$$

where $\mathcal{J}/2\mu_B$ is the exchange coupling per unit local moment between the local moment and the Fermi surface conduction electrons. $\mathcal{K}_\alpha$ is the Pauli response of the conduction electrons to this exchange field. If one assumes that the *average* hyperfine coupling in the RKKY disturbance equals that associated with Fermi surface states alone, then $\mathcal{K}_\alpha=\mathcal{K}_0$ and

$$\mathcal{K}(T)=\mathcal{K}_0[1+(g_J-1)\mathcal{J}\chi_{loc}(T)/g_JN\mu_B{}^2]. \tag{45}$$

Knowing $\mathcal{K}_0$ from an isostructural nonmagnetic compound, $\mathcal{J}$ can be estimated. Physically reasonable numbers for the exchange constants normally result. Even assuming that the average spin moment sample is equal to the Pauli term in the RKKY response, it is not inevitable that $\mathcal{K}_\alpha$ should equal $\mathcal{K}_0$. The spin response involves states off E_F and the hyperfine coupling for these states can vary radically from that at E_F, as is indicated for the case of Cu in figure 11. Another possible shortcoming of the scheme is that the entire resonant scattering disturbance is not necessarily describable in terms of an effective exchange scattering. Although $\mathcal{J}$ can be numerically affected by factors other than exchange coupling, tabulation of shift results in this form can prove useful when comparing results in a sequence of intermetallic compounds. For example, Jones [206] has tabulated the nonmagnetic site Knight shift results of rare earth intermetallic compounds in terms of $\mathcal{J}$. The same results [205,218-230] are plotted in a different form in figure 31, namely in terms of $\xi\equiv H'_{eff}/H^{At}_{eff}$. Atomic hyperfine behavior is thus normalized out, providing a crude estimate, in μ_B, of the spin moment residing at a nonmagnetic site due to the local moment disturbance. The resulting ξ's are an order of magnitude smaller than those appropriate to the transition metal alloys (compare with figure 28) implying much weaker magnetic perturbations in rare earth compounds.[17] The ξ's appear to be in three distinct groups; the Al compounds, the P, As and Sb compounds, and those involving elements in the 6*s*-6*p*-5*d* row of the periodic table. (Data also exist for two hexaborides yielding ξ's of ~ -0.005.) We presume the grouping is associated with band and wave function character specific to the various sets of compounds. More interesting than the grouping is the variation in ξ across the rare earth row; ξ is largest at the Ce end, falling and becoming relatively constant for the heavy rare earths. The trend is very different than that seen for 3*d*-moments in figure 28 and appears characteristic of rare earth 4*f*-moment effects. This trend was first observed in electron spin and nuclear resonance of the $REAl_2$ compounds [202,205] and subsequently in ESR of rare earth impurities in Pd [203]. The negative sign of ξ suggests that hybridization polarization effects dominate. One contributing factor to the large ξ at the Ce end is the well-known tendency for the occupied 4*f* levels to be close to E_F. The resulting small energy

[17] This comparison underestimates the drop in polarization because the ξ values natural to ordered intermetallic compounds are intrinsically larger than those in alloys by the nature of the differing definition of these two ξ factors. For example, the ξ appropriate to the intermetallic compounds $REAl_2$ and $REAl_3$ (see fig. 31) are larger than those for the RE-Al alloys.

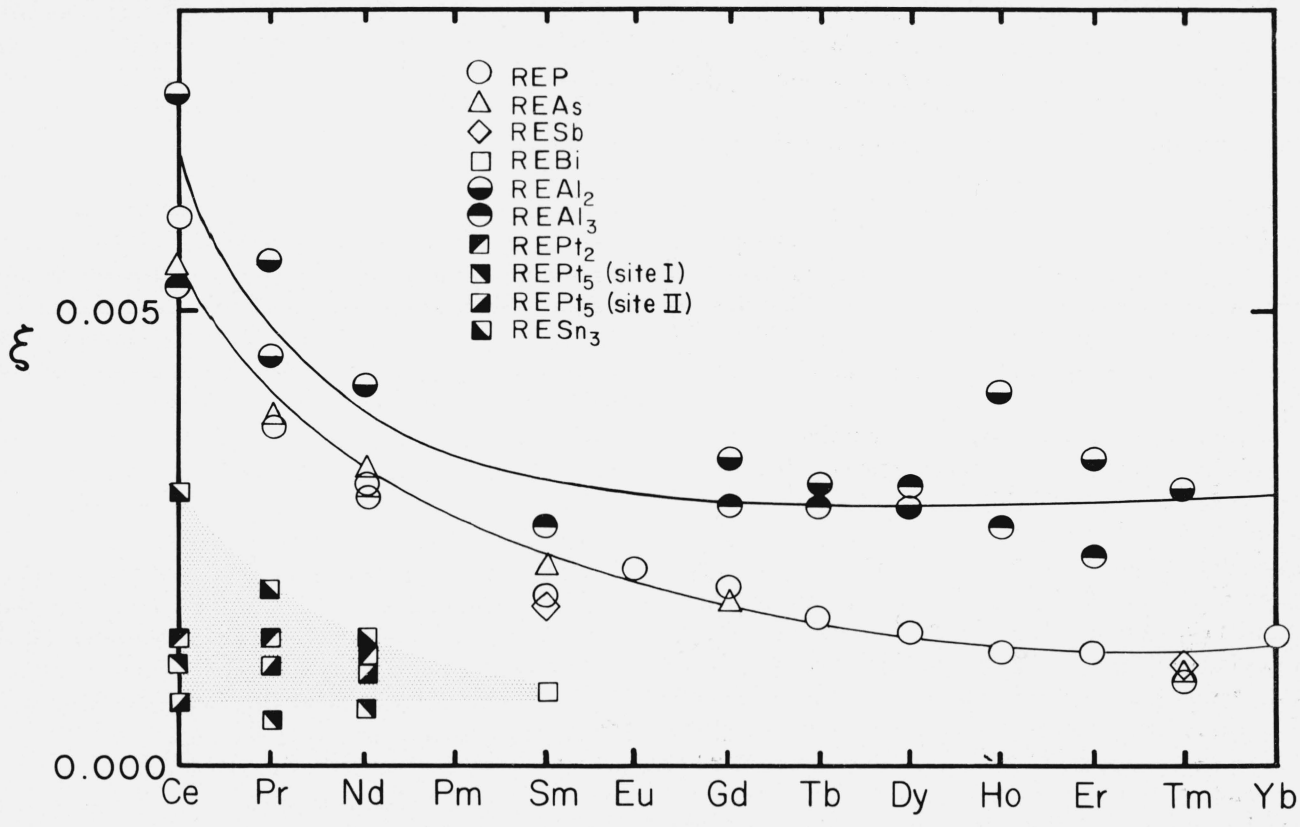

FIGURE 31. *Behavior of Knight's ξ factor as defined in the text, for the light metal site in rare earth intermetallic compounds. The data are from a number of sources [205, 218-230], as collected in tabular form by Jones [206].*

denominators tend to enhance hybridization, and hence ξ. An example of this 4*f* behavior is that a phase transition occurs in metallic Ce, one phase involving no 4*f* electrons, and the other, one.

Positive, strongly temperature dependent $\mathcal{K}$'s have been observed for nonmagnetic sites in UAl_2 [216] and USn_3 [231]. The susceptibility behavior suggests the presence of 5*f* band paramagnetism, rather than local moment paramagnetism. The resulting ξ's ($\sim$ 0.1 to 0.3) for the two compounds are opposite in sign and substantially larger than the values appropriate to the isostructural rare earth compounds (fig. 31). The authors [216,231] pointed out that the results could arise from several percent Al (or Sn) valence *s*-orbital hybridization into the 5*f* bands at E_F and/or from RKKY polarization with quite reasonable $\mathcal{J}$ values. The positive sign of the ξ's implies that electrostatic exchange then dominates. The $\mathcal{K}$ versus χ plots for the two compounds also indicated the presence of a strong χ_{orb} term associated with 5*f* character at the U sites, which makes no contribution to the Al (or Sn) site $\mathcal{K}$.

Abundant data exist for a variety of transition metal compounds. In some of the more magnetic systems the results are strongly dependent on metallurgical details of the samples. For example, NiAl, CoAl and FeAl have been studied by West [232,233] and by Seitchik and Walmsley [217,234] at and off stoichiometry. West found that the Co susceptibility results in CoAl are very sensitive to the thermal history. These results suggested nonequilibrium magnetic clustering. The effects of thermal history on the Knight shift are less important, because the number of atoms near clusters is small and do not contribute sensibly to the observed resonance. Despite these difficulties there are several distinct features of the results which give insight into the character of these compounds. First, the Al shift in FeAl is negative and temperature dependent, suggesting the existence of intersite effects of the sort encountered in the Al alloys and the V_3X compounds. Second, while the Co shift can be strongly temperature dependent (depending on Co concentration), the Al shift in CoAl is small and is effectively independent of temperature (not depending on Co concentration). From this it was concluded that there is little Al *s*-character in the Fermi surface states of CoAl. The slope of a $\mathcal{K}$(Co) versus χ plot, using composition as the intrinsic parameter, is negative at room temperature and positive at low temperature. Thus there are at least two par-

383-876 O - 70 - 10

tially cancelling temperature dependent mechanisms operative at the Co site in this system. West attributed the positive slope to a temperature dependent orbital term. Finally in NiAl, the Al shift, the Al relaxation time, and the susceptibility are characteristic of an *s*-band metal, suggesting that Al electrons "fill" the Ni 3*d* band. This does not imply that there are ten 3*d*-electrons at a Ni site in NiAl, just as there aren't at a Cu site in pure Cu (see discussion of fig. 11). Instead, charge effects have so affected the bands that there is no substantial *d*-band character at or within kT of E_F. A similar situation appears to occur in dilute alloys of Ni in Cu [235].

Knight shift results have been obtained for both transition metal sites and nonmagnetic sites in itinerant ferromagnets [236,237,14] such as $ZrZn_2$. These systems are characterized by having ferromagnetic saturation moments, q_s, which are small compared with *effective* moments, q_c, associated with the paramagnetic susceptibility. This implies a band rather than local Heisenberg type of ferromagnetism. A plot of the q_c/q_s ratio for a variety of compounds is shown in figure 32. These were obtained with the Rhodes-Wohlfarth "intermediate model" [238]. There has been some uncertainty as to whether magnetic impurities drive some of the "itinerant" systems ferromagnetic. In cases,

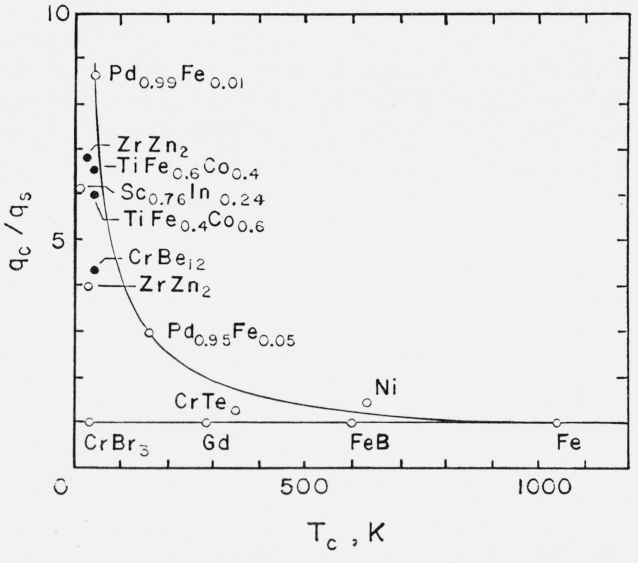

FIGURE 32. *The ratio q_c/q_s of the number of magnetic carriers deduced from the paramagnetic Curie-Weiss constant to the number deduced from the saturation magnetization. Datum points are identified by Rhodes and Wohlfarth [238] and Swartz* et al. *[15].*

such as $CrBe_{12}$ [237], the NMR lines are sharp and the hyperfine fields track the magnetization, indicating that the ferromagnetism is a bulk effect, whether or not triggered by impurities. The slopes of the $\mathcal{K}$ versus χ plots for hyperfine fields associated with magnetic atom sites, such as Zr in $ZrZn_2$, or Fe or Co in $TiFe_xCo_{1-x}$, are generally small, ranging between 0 and ± 100 kOe/μ_B. Similar small fields occur for Ti in paramagnetic $TiBe_2$, and V in the V_3X compounds, suggesting the presence of band effects such as *s-d* hybridization. Weaker hyperfine constants occur at nontransition metal sites in the itinerant ferromagnets, implying that only weak intersite effects are present in this class of compounds. This contrasts with the X site behavior of the localized paramagnetic V_3X systems which we believe is due, in large part, to substantial intersite effects.

There are a number of examples where $\mathcal{K}$ versus χ plots, with $\langle a \rangle$ assumed constant, have proven to be very useful. This is not always the case. For example, the Ga resonance in $AuGa_2$ is temperature dependent [12] and while $\mathcal{K}$ follows χ quite faithfully, T_1 data indicate a substantial variation with temperature in the contact *s* contribution to $\langle a \rangle$. This has led to a model of thermal population of an *s* band [239], which, however, does not explain the susceptibility behavior. As of yet, this system is not completely understood.

14. Summary

In this paper, we have dealt with the Knight shift and its interpretation in terms of various models of the electronic behavior in metals, emphasizing recent developments. It is apparent that the relation of the Knight shift to the density of states is complicated, but there are compensations in that a large amount of closely related and more intricate information may be deduced from Knight shift studies in metals, compounds and alloy systems. Information may be obtained concerning the wave functions of the electrons at the Fermi surface as probed at the resonating nuclei. Contributions to $\mathcal{K}$ can be separated into terms arising from *s*-electron and *d*-electron character, and in some instances there are indications of contributions due to *p*-character. In addition, orbital and diamagnetic contributions can be deduced at times. We have discussed most of the methods with which one obtains wavefunction insight from Knight shifts. This wavefunction information is related directly to $N(E)$ and is needed in the evaluation of $\langle a \rangle$. The relations between $\mathcal{K}$, $\langle a \rangle$, and the density of states are shown quantitatively in several equations throughout the text.

These same equations display the unique relation of $\mathcal{K}$ with a *local* density of states due to the weighted averaging associated with $\langle a \rangle$. This becomes useful particularly in the case of intermetallic compounds and

less so for alloys where atoms occupy positions with a random arrangement. Often it is preferable to absorb this randomness into $\langle a \rangle$. In intermetallic compounds, the Knight shift behavior definitely suggests a description in terms of wavefunctions *and* densities of states that are different for inequivalent sites. In such a situation the magnetic response of one site to another is of concern. In other words now there are *inter-* as well as *intra-*atomic effects. In the case of pure metals this complication also arises but is hidden in $\langle a \rangle$.

In this Symposium, a number of advanced theoretical and experimental techniques for studying the electron density of states have been discussed. It is to be hoped that fruitful correlations between these methods and Knight shifts will be obtained in the future.

15. Acknowledgments

Valuable assistance with the bibliographical aspects and preparation of the Knight shift tables, by D. J. Kahan of the Alloy Data Center (part of the National Standard Reference Data System) is gratefully acknowledged. Useful suggestions and comments by T. J. Rowland, M. N. Alexander, A. T. Fromhold and I. D. Weisman have aided in preparation of this manuscript. We wish to thank J. A. Hofmann for making a draft of his work [156] available to us prior to publication.

16. References

[1] Knight, W. D., Phys. Rev. **76,** 1259 (1949).
[2] Townes, C. H., Herring, C., and Knight, W. D., Phys. Rev. **77,** 852 (1950).
[3] Knight, W. D., Solid State Phys. **2,** 93 (1956).
[4] Rowland, T. J., Prog. Materials Sci. **9,** 1 (1961).
[5] Drain, L. E., Metallurgical Rev. **119,** 195 (1967).
[6] Rowland, T. J., and Borsa, R., Phys. Rev. **134,** A743 (1964).
[7] Bennett, L. H., Mebs, R. W., and Watson, R. E., Phys. Rev. **171,** 611 (1968).
[8] Watson, R. E., Bennett, L. H., and Freeman, A. J., Phys. Rev. Letters **20,** 653 (1968); ibid. **20,** 1221 (1968); Phys. Rev. **179,** 590 (1969).
[9] Bennett, L. H., Phys. Rev. **150,** 418 (1966).
[10] Watson, R. E., and Freeman, A. J., in Hyperfine Interactions, A. J. Freeman and R. B. Frankel, Editors (Academic Press, N.Y. 1967) p. 53.
[11] Bagus, P. S., Liu, B., and Schaefer, H. F., III, Phys. Rev. **A** (to be published Sept. 1970).
[12] Jaccarino, V., Weger, M., Wernick, J. H., and Menth, A., Phys. Rev. Letters **21,** 1811 (1968).
[13] Clogston, A. M., and Jaccarino, V., Phys. Rev. **121,** 1357 (1961).
[14] Bennett, L. H., Swartzendruber, L. J., and Watson, R. E., Phys. Rev. **165,** 500 (1968).
[15] Swartz, J. C., Bennett, L. H., Swartzendruber, L. J., and Watson, R. E., Phys. Rev. **B1,** 146 (1970).
[16] Winkler, R., Phys. Letters **23,** 301 (1966).
[17] Pleiter, F., (private communication).
[18] Kubo, R., and Obata, Y., J. Phys. Soc. Japan **11,** 547 (1956).
[19] Orgel, L. E., J. Phys. Chem. Solids **21,** 123 (1961).
[20] Clogston, A. M., Jaccarino, V., and Yafet, Y., Phys. Rev. **134,** A650 (1964); Clogston, A. M., Gossard, A. C., Jaccarino, V., and Yafet, Y., Phys. Rev. Letters **9,** 262 (1962); Jaccarino, V., Proc. Col. Ampère **13,** 22 (1964).
[21] Narath, A., and Fromhold, A. T., Jr., Phys. Rev. **139,** A794 (1965).
[22] Clogston, A. M., Gossard, A. C., Jaccarino, V., and Yafet, Y., Rev. Mod. Phys. **36,** 170 (1964).
[23] Barnes, R. G., and Graham, T. P., Phys. Rev. Letters **8,** 248 (1962); Denbigh, J. S., and Lomer, W. M., Proc. Phys. Soc. (London) **82,** 156 (1963).
[24] Butterworth, J., Proc. Phys. Soc. (London) **83,** 71 (1964); Erratum, *ibid.* **83,** 893 (1964).
[25] Seitchik, J., Jaccarino, V., and Wernick, J. H., Bull. Am. Phys. Soc. **10,** 317 (1965).
[26] Andersson, L. O., Phys. Letters **26A,** 279 (1968).
[27] Korringa, J., Physica **16,** 601 (1950).
[28] Herring, C., in Magnetism, G. T. Rado and H. Suhl, Editors (Academic Press, N.Y. 1966) **Vol. IV,** Section III.
[29] Silverstein, S. D., Phys. Rev. **128,** 631 (1962); and Silverstein, S. D., Phys. Rev. **130,** 912 (1963).
[30] Wolff, P. A., Phys. Rev. **120,** 814 (1960).
[31] Wolff, P. A., Phys. Rev. **129,** 84 (1963).
[32] Herring, C., in Magnetism, G. T. Rado and H. Suhl, Editors (Academic Press, N.Y. 1966) **Vol. IV,** Sections X and XII.
[33] Hurd, C. M., and Coodin, P., J. Phys. Chem. Solids 28, 523 (1967).
[34] Schumacher, R. T., and Slichter, C. P., Phys. Rev. **101,** 58 (1956).
[35] Schumacher, R. T., and Vehse, W. E., J. Phys. Chem. Solids **24,** 297 (1963).
[36] Schumacher, R. T., and Vander Ven, N. S., Phys. Rev. **144,** 357 (1966).
[37] Hultgren, R. R., Orr, R. L., Anderson, P. D., and Kelley, K. K., Selected Values of Thermodynamic Properties of Metals and Alloys (John Wiley & Sons, Inc., N.Y. 1963) and Addenda (unpublished).
[38] O'Sullivan, W. J., Switendick, A. C., and Schirber, J. E., this Symposium.
[39] Ziman, J. M., Advances in Phys. **16,** 421 (1967).
[40] Kohn, W., Phys. Rev. **96,** 590 (1954).
[41] Kjeldaas, T., Jr., and Kohn, W., Phys. Rev. **101,** 66 (1956).
[42] Cohen, M. H., Goodings, D. A., and Heine, V., Proc. Phys. Soc. (London) **73,** 811 (1959).
[43] Jones, H., and Schiff, B., Proc. Phys. Soc. (London) **67A,** 217 (1954).
[44] Holland, B. W., Phys. Stat. Solidi **28,** 121 (1968).
[45] Micah, E. T., Stocks, G. M., and Young, W. H., J. Phys. C (Solid St. Phys.) **2,** 1653 (1969); Meyer, A., Stocks, G. M., and Young, W. H., this Symposium.
[46] Kmetko, E. A., this Symposium.
[47] Pauling, L., Proc. Roy. Soc. **196A,** 343 (1949).
[48] Micah, E. T., Stocks, G. M., and Young, W. H., J. Phys. C (Solid St. Phys.) **2,** 1661 (1969).
[49] Shyu, Wei-Mei, Das, T. P., and Gaspari, G. D., Phys. Rev. **152,** 270 (1966).
[50] Pomerantz, M. and Das, T. P., Phys. Rev. **119,** 70 (1960).
[51] Shyu, Wei-Mei, Gaspari, G. D., and Das, T. P., Phys. Rev. **141,** 603 (1966).
[52] Jena, P., Mahanti, S. D., and Das, T. P., Phys. Rev. Letters **20,** 544 (1968); ibid. **20,** 977 (1968).

[53] Gerstner, J., and Cutler, P. H., Phys. Letters **30A,** 368 (1969), and this Symposium.
[54] Gaspari, G. D., and Das, T. P., Phys. Rev. **167,** 660 (1968).
[55] Jena, P., Das, T. P., Mahanti, S. D., and Gaspari, G. D., this Symposium.
[56] Moore, R. A., and Vosko, S. H., Canadian J. Phys. **46,** 1425 (1968).
[57] Moore, R. A., and Vosko, S. H., Canadian J. Phys. **47,** 1331 (1969).
[58] Hartree, D. R., Hartree, W., and Swirles, B., Phil. Trans. Royal Soc. (London) **A238,** 229 (1939).
[59] Kabartas, Z. V., Kavetskis, V. I., and Yutsis, A. P., JETP **2,** 481 (1956).
[60] Linderberg, J., and Shull, H., J. Mol. Spectros. **5,** 1 (1960).
[61] Watson, R. E., Ann. Phys. **13,** 250 (1961).
[62] Knight, W. D., Berger, A. G., and Heine, V., Ann. Phys. (N.Y.) **8,** 173 (1959).
[63] Feldman, D., Ph. D. Thesis, University of California, Berkeley, (1959).
[64] Seymour, E. F. W., and Styles, G. A., Phys. Letters **10,** 269 (1964).
[65] Borsa, F., and Barnes, R. G., J. Phys. Chem. Solids **27,** 567 (1966).
[66] Sharma, S. N., and Williams, D. L., Colloque Ampère **XIV,** 480 (1967).
[67] Dickson, E. M., Phys. Rev. **184,** 294 (1969).
[68] Kasowski, R. V., and Falicov, L. M., Phys. Rev. Letters **22,** 1001 (1969).
[69] Schone, H. E., Phys. Rev. Letters **13,** 12 (1964).
[70] Shaw, R. W., and Smith, N. V., Phys. Rev. **178,** 985 (1969).
[71] Matzkanin, G. A., and Scott, T. A., Phys. Rev. **151,** 360 (1966).
[72] Kushida, T., and Rimai, L., Phys. Rev. **143,** 157 (1966).
[73] Allen, P. S., and Seymour, E. F. W., Proc. Phys. Soc. (London) **85,** 509 (1965); Warren, W. W., Jr., and Clark, W. G., Phys. Rev. **177,** 600 (1969).
[74] Drain, L. E., Phil. Mag. **4,** 484 (1959).
[75] Umeda, J., Kusumoto, H., Narita, K., and Yamada, E., J. Chem. Phys. **42,** 1458 (1965).
[76] Adler, D., Solid State Physics **21,** 1 (1968).
[77] Sundfors, R. K., and Holcomb, D. F., Phys. Rev. **136,** A810 (1964).
[78] Alexander, M. N., and Holcomb, D. F., Revs. Mod. Phys. **40,** 815 (1968).
[79] Alexander, M. N., and Holcomb, D. F., Solid State Communications **6,** 355 (1968).
[80] O'Reilly, D. E., J. Chem. Phys. **41,** 3729 (1964).
[81] Acrivos, J. V., and Pitzer, K. S., J. Phys. Chem. **66,** 1693 (1962).
[82] McConnell, H. M., and Holm, C. H., J. Chem. Phys. **26,** 1517 (1957).
[83] Hughes, T. R., Jr., J. Chem. Phys. **38,** 202 (1963).
[84] Bardeen, J., Cooper, L. J., and Schrieffer, J. R., Phys. Rev. **106,** 162 (1951); **108,** 1175 (1957).
[85] Yosida, K., Phys. Rev. **110,** 769 (1958).
[86] Ferrell, R. A., Phys. Rev. Letters **3,** 262 (1959).
[87] Anderson, P. W., Phys. Rev. Letters **3,** 325 (1959).
[88] Wright, F., Jr., Phys. Rev. **163,** 420 (1967).
[89] Appel, J., Phys. Rev. **139,** A1536 (1965).
[90] Das, T. P., and Sondheimer, E. H., Phil. Mag. **5,** 529 (1960).
[91] Yafet, Y., J. Phys. Chem. Solids **21,** 99 (1961).
[92] Williams, B. F., and Hewitt, R. R., Phys. Rev. **146,** 286 (1966).
[93] Christensen, R. L., Hamilton, D. R., Bennewitz, H. G., Reynolds, J. B., and Stroke, H. H., Phys. Rev. **122,** 1302 (1961).
[94] Bloembergen, N., and Rowland, T. J., Acta. Met. **1,** 731 (1953).
[95] Schone, H. E., and Knight, W. D., Acta. Met. **11,** 179 (1963).
[96] Bennett, L. H., Acta Met. **14,** 997 (1966).
[97] Setty, D. L. Radhakrishna, and Mungurwadi, B. D., Phys. Rev. **183,** 387 (1969).
[98] Watson, R. E., Bennett, L. H., Weisman, I. D., and Carter, G. C. (to be published).
[99] Reynolds, J. M., Goodrich, R. G., and Khan, S. A., Phys. Rev. Letters **16,** 609 (1966).
[100] Khan, S. A., Reynolds, J. M., and Goodrich, R. G., Phys. Rev. **163,** 579 (1967).
[101] Kaplan, J. I., J. Phys. Chem. Solids **23,** 826 (1962).
[102] Stephen, M., Phys. Rev. **123,** 126 (1961).
[103] Dolgopolov, D. G., and Bystrik, P. S., Sov. Phys. JETP **19,** 404 (1964).
[104] Dolgopolov, D. G., Phys. Metal Metaloved **22(3),** 6 (1967).
[105] Hebborn, J. E., Proc. Phys. Soc. (London) **80,** 1237 (1962).
[106] Hebborn, J. E., and Stephen, M. J., Proc. Phys. Soc. (London) **80,** 991 (1962).
[107] Glasser, M. L., Phys. Rev. **150,** 234 (1966).
[108] Goodrich, R. G., Khan, S. A., and Reynolds, J. M., Phys. Rev. Letters **23,** 767 (1969).
[109] Seitchik, J. A., Gossard, A. C., and Jaccarino, V., Phys. Rev. **136,** A1119 (1964).
[110] Mott, N. F., and Jones, H., The Theory of the Properties of Metals and Alloys, (Clarendon Press, N.Y. 1936).
[111] Misetich, A., Hodges, L., and Watson, R. E. (unpublished).
[112] Hodges, L., Ehrenreich, H., and Lang, N. D., Phys. Rev. **152,** 505 (1966).
[113] Ehrenreich, H., and Hodges, L., Methods in Comp. Physics **8,** 149 (1968).
[114] Watson, R. E., Ehrenreich, H., and Hodges, L., Phys. Rev. Letters **24,** 829 (1970).
[115] Mueller, F. M., this Symposium.
[116] Goodings, D. A., and Harris, R., Phys. Rev. **178,** 1189 (1969), and J. Phys. C. **2,** 1808 (1969).
[117] Dobbyn, R. C., Williams, M. W., Cuthill, J. R., and McAlister, A. J., Phys. Rev. **2B** (to be published).
[118] Davis, H., Phys. Letters **28A,** 85 (1968).
[119] Seitchik, J., Jaccarino, V., and Wernick, J. H., Phys. Rev. **138,** A148 (1965).
[120] Kobayashi, S., Asayama, K., and Itoh, J., J. Phys. Soc. (Japan) **18,** 1735 (1963).
[121] Narath, A., J. Appl. Phys. **39,** 553 (1968).
[122] Itoh, J., Asayama, K., and Kobayashi, S., Proc. Col. Ampère **13,** 162 (1964).
[123] Froidevaux, C., Gautier, F., and Weisman, I., Proc. Col. Ampère **13,** 114 (1964).
[124] Balabanov, A., and Delyagin, N., Soviet Phys. JETP 27, 752 (1968).
[125] Shirley, D. A., and Westenbarger, G. A., Phys. Rev. **138,** A170 (1965).
[126] Stern, E. A., Phys. Rev. **157,** 544 (1967) and in Energy Bands in Metals and Alloys, L. H. Bennett and J. T. Waber, Editors (Gordon and Breach, 1968) p. 151.
[127] Watson, R. E., in Hyperfine Interactions, A. J. Freeman and R. B. Frankel, Editors (Academic Press, N.Y., 1967) p. 413.
[128] Kohn, W., and Vosko, S. H., Phys. Rev. **119,** 912 (1960).
[129] Rowland, T. J., Phys. Rev. **119,** 900 (1960).
[130] Drain, L. E., J. Phys. C. **1,** 1690 (1968).

[131] Redfield, A. G., Phys. Rev. **130,** 589 (1963).
[132] Fernelius, N. C., Thesis, University of Illinois (1966); Proc. Colloque Ampère **14,** 497 (1967); ibid. **15,** 347 (1968).
[133] Minier, M., Phys. Letters **26A,** 548 (1968); Minier, M., and Berthier, Cl., Proc. Colloque Ampère **15,** 368 (1968); Minier, M., Phys. Rev. **182,** 437 (1969).
[134] Blandin, A., and Daniel, E., J. Phys. Chem. Solids **10,** 126 (1959).
[135] Asik, J. R., Ball, M. A., and Slichter, C. P., Phys. Rev. **181,** 645 (1969).
[136] Ball, M. A., Asik, J. R., and Slichter, C. P., Phys. Rev. **181,** 662 (1969).
[137] Vonsovski, S., JETP **16,** 981 (1946); ibid. **24,** 419 (1953).
[138] Ruderman, M. A., and Kittel, C., Phys. Rev. **96,** 99 (1954); Mitchell, A. H., Phys. Rev. **105,** 1439 (1957).
[139] Kasuya, T., Prog. Theoret. Phys. **16,** 45 (1956).
[140] Yosida, K., Phys. Rev. **106,** 893 (1957).
[141] Condon, E. U., and Shortley, G. H., The Theory of Atomic Spectra (University Press, Cambridge, 1964).
[142] Anderson, P. W., and Clogston, A. M., Bull. Am. Phys. Soc. **6,** 124 (1961).
[143] Schrieffer, J. R., and Wolff, P. A., Phys. Rev. **149,** 491 (1966).
[144] Watson, R. E., Koide, S., Peter, M., and Freeman, A. J., Phys. Rev. **139,** A167 (1965).
[145] Watson, R. E., and Freeman, A. J., J. Appl. Phys. **37,** 1444 (1966).
[146] Jaccarino, V., Matthias, B. T., Peter, M., Suhl, H., and Wernick, J. H., Phys. Rev. Letters **5,** 251 (1960).
[147] Peter, M., J. Appl. Phys. **32,** 338S (1961).
[148] Peter, M. Shaltiel, D., Wernick, J. H., Williams, H. J., Mock, J. B., and Sherwood, R. C., Phys. Rev. **126,** 1395 (1962).
[149] Shaltiel, D., Wernick, J. H., Williams, H. J., and Peter, M., Phys. Rev. **135,** A1346 (1964).
[150] Rowland, T. J., Phys. Rev. **125,** 459 (1962).
[151] Weisman, I. D., and Knight, W. D., Phys. Rev. **169,** 373 (1968).
[152] Wolff, P. A., Phys. Rev. **120,** 814 (1960).
[153] Wolff, P. A., Phys. Rev. **129,** 84 (1963).
[154] Giovannini, B., Peter, M., Schrieffer, J. R., Phys. Rev. Letters **12,** 736 (1964).
[155] Alexander, M. N., Phys. Rev. **172,** 331 (1968).
[156] Senturia, S. D., Smith, A. C., Hewes, C. R., Hofmann, J. A., and Sagalyn, P. L., Phys. Rev. B, **Vol. 1,** 40–45 (1970).
[157] Van Ostenburg, D. O., Lam, D. J., Trapp, H. D., and MacLeod, D. E., Phys. Rev. **128,** 1550 (1962).
[158] Drain, L. E., J. Phys. Radium **23,** 745 (1962).
[159] Lam, D. J., Van Ostenburg, D. O., Nevitt, M. W., Trapp, H. D., and Pracht, D. W., Phys. Rev. **131,** 1428 (1963); ibid. **133I,** 1 (1964).
[160] Bernasson, M., Descouts, P., Donzé, P., and Treyvaud, A., J. Phys. Chem. Solids **30,** 2453 (1969).
[161] Betsuyaku, H., Takagi, Y., and Betsuyaku, Y., J. Phys. Soc. Japan **19,** 1089 (1964).
[162] Zamir, D., Phys. Rev. **140,** A271 (1965).
[163] Van Ostenburg, D. O., Lam, D. J., Shimizu, M., and Katsuki, A., J. Phys. Soc. Japan **18,** 1744 (1963).
[164] Masuda, Y., Nishioka, M., and Watanabe, J. Phys. Soc. Japan **22,** 238 (1967).
[165] Taniguchi, S., Tebble, R. S., and Williams, D. E. G., Proc. Roy. Soc. **265A,** 502 (1962).
[166] Cheng, C. H., Gupta, K. P., Van Reuth, E. C., and Beck, P. A., Phys. Rev. **126,** 2030 (1962).
[167] Gupta, K. P., Cheng, C. H., and Beck, P. A., Metallic Solid Solutions, J. Friedel and A. Guinier, Editors, (W. A. Benjamin, Inc., N.Y., 1963) chapter 25.
[168] Morin, F. J., and Maita, J. P., Phys. Rev. **129,** 1115 (1963).
[169] Rohy, D., and Cotts, R. M., Phys. Rev. **1B,** 2070 (1970).
[170] Rohy, D., and Cotts, R. M., Phys. Rev. **1B,** 2484 (1970).
[171] Swartz, J. C., Swartzendruber, L. J., Bennett, L. H., and Watson, R. E., Phys. Rev. **B1,** 146 (1970).
[172] Bennett, L. H., Swartzendruber, L. J., and Watson, R. E., Phys. Rev. **165,** 500 (1968).
[173] Bos, W. G., and Gutowsky, H. S., O.N.R. Tech. Rept. No. 93, (available as AD-640514) (1966).
[174] Schreiber, D. S., Phys. Rev. **137,** A860 (1965).
[175] Alfred, L. C. R., and Van Ostenburg, D. O., Phys. Rev. **161,** 569 (1967).
[176] Kohn, W., and Vosko, S. H., Phys. Rev. **119,** 912 (1960).
[177] Blatt, F. J., Phys. Rev. **108,** 285 (1957).
[178] Odle, R. L., and Flynn, C. P., Phil. Mag. **13,** 699 (1966).
[179] Snodgrass, R. J., and Bennett, L. H., Phys. Rev. **134,** A1294 (1964).
[180] Heighway, J., and Seymour, E. F. W., Phys. Letters **29A,** 282 (1969).
[181] Seymour, E. F. W., and Styles, G. A., Proc. Phys. Soc. (London) **87,** 473 (1966).
[182] Anderson, W. T., Jr., Thatcher, F. C., and Hewitt, R. R., Phys. Rev. **171,** 541 (1968).
[183] Kaeck, J. A., Ph. D. Thesis University of Cornell, N.Y. (1968).
[184] Van der Molen, S. B., Van der Lugt, W., Draisma, G. G., and Smit, W., Physica **38,** 275 (1968).
[185] Van der Molen, S. B., Van der Lugt, W., Draisma, G. G., and Smit, W., Physica **40,** 1 (1968).
[186] Van der Lugt, W., and Van der Molen, S. B., Phys. Stat. Solid **19,** 327 (1967).
[187] Seymour, E. F. W., Styles, G. A., and Taylor, B., Proc. Col. Ampère **11,** 612 (1962).
[188] Seymour, E. F. W., and Styles, G. A., Proc. Phys. Soc. (London) **87,** 473 (1966).
[189] Slocum, R. R., Ph. D. Thesis, College of William and Mary, Virginia (1969).
[190] Van Hemmen, J. L., Caspers, W. J., Van der Molen, S. B., Van der Lugt, W., and Van de Braak, H. P., Z Physik **222,** 253 (1969).
[191] Rigney, D. A., and Flynn, C. P., Phil. Mag. **15,** 1213 (1967).
[192] Moulson, D. J., and Seymour, E. F. W., Advan. Phys. **16,** 449 (1967).
[193] Bennett, L. H., Cotts, R. M., and Snodgrass, R. J., Proc. Colloque Ampère **13,** 171 (1965).
[194] Matzkanin, G. A., Spokas, J. J., Sowers, C. H., Van Ostenburg, D. O., and Hoeve, H. C., Phys. Rev. **181,** 559 (1969).
[195] Wells, J. C., Jr., Williams, R. L., Jr., Pfeiffer, L., and Madansky, L., Phys. Letters **27B,** 448 (1968).
[196] Gardner, J. A., and Flynn, C. P., Phil. Mag. **15,** 1233 (1967).
[197] Flynn, C. P., Rigney, D. A., and Gardner, J. A., Phil. Mag. **15,** 1255 (1967).
[198] Rao, G. N., Matthias, E., and Shirley, D. A., Phys. Rev. **184,** 325 (1969).
[199] Clogston, A. M., Matthias, B. T., Peter, M., Williams, H. J., Corenzwit, E., and Sherwood, R. C., Phys. Rev. **125,** 541 (1962).
[200] Stupian, G. W., and Flynn, C. P., Phil. Mag. **17,** 295 (1968).
[201] Van Vleck, J. H., Theory of Electric and Magnetic Susceptibilities, (Oxford University Press, 1932).

[202] Peter, M., Shaltiel, D., Wernick, J. H., Williams, H. J., Mock, J. B., and Sherwood, R. C., Phys. Rev. **126,** 1395 (1962).
[203] Shaltiel, D., Wernick, J. H., Williams, H. J., and Peter, M., Phys. Rev. **135,** A1346 (1964).
[204] Cragle, J., Phys. Rev. Letters **13,** 569 (1964).
[205] Jaccarino, V., Matthias, B. T., Peter, M., Suhl, H., and Wernick, J. H., Phys. Rev. Letters **5,** 251 (1960).
[206] Jones, E. D., Phys. Rev. **180,** 455 (1968).
[207] Jones, E. D., Phys. Rev. Letters **19,** 432 (1967).
[208] Shulman, R. G., Wyluda, B. J., and Matthias, B. T., Phys. Rev. Letters **1,** 278 (1958).
[209] Blumberg, W. E., Eisinger, J., Jaccarino, V., and Matthias, B. T., Phys. Rev. Letters **5,** 149 (1960).
[210] Weger, M., (to be published).
[211] Gossard, A. C., Phys. Rev. **149,** 246 (1966); Errata, ibid. **164,** 878 (1967) and **185,** 862 (1969).
[212] Labbé, J., and Friedel, J., J. Physique **27,** 153 (1966).
[213] Mattheiss, L. F., Phys. Rev. **138,** A112 (1965).
[214] Shulman, R. G., Wyluda, B. J., and Matthias, B. T., Phys. Rev. Letters **1,** 278 (1958).
[215] Lűtgemeier, H., Z. Naturforsch. **20A,** 246 (1965).
[216] Gossard, A. C., Jaccarino, V., and Wernick, J. H., Phys. Rev. **128,** 1038 (1962).
[217] Seitchik, J. A., and Walmsley, R. H., Phys. Rev. **137,** A143 (1965).
[218] Cooper, B. R., Phys. Letters **22,** 244 (1966).
[219] Jaccarino, V., J. Appl. Phys. **32S,** 102 (1961).
[220] Jones, E. D., and Busick, J. I., J. Appl. Phys. **37,** 1250 (1966).
[221] Barnes, R. G., and Jones, E. D., Solid State Comm. **5,** 285 (1967).
[222] de Wijn, H. W., van Diepen, A. M., and Buschow, K. H. J., Phys. Rev. **161,** 253 (1967).
[223] van Diepen, A. M., de Wijn, H. W., and Buschow, K. H. J., J. Chem. Phys. **46,** 3489 (1967).
[224] Buschow, K. H. J., van Diepen, A. M., and de Wijn, H. W., Phys. Letters **24A,** 536 (1967).
[225] van Diepen, A. M., de Wijn, H. W., and Buschow, K. H. J., Phys. Letters **26A,** 340 (1968).
[226] Gossard, A. C., and Jaccarino, V., Proc. Phys. Soc. (London) **80,** 877 (1962).
[227] Vijayaraghavan, R., Malik, S. K., and Rao, V. U. S., Phys. Rev. Letters **20,** 106 (1968).
[228] Barnes, R. G., Borsa, F., and Peterson, D., J. Appl. Phys. **36,** 940 (1965).
[229] Rao, V. U. S., and Vijayaraghavan, R., Phys. Letters **19,** 168 (1965).
[230] Borsa, F., Barnes, R. G., and Reese, R. A., Phys. Status Solidi **19,** 359 (1967).
[231] Rao, V. U. S., and Vijayaraghavan, R., J. Phys. Chem. Sol. **29,** 123 (1968).
[232] West, G., Phil. Mag. **9,** 979 (1964).
[233] West, G., Phil. Mag. **15,** 855 (1967).
[234] Seitchik, J., and Walmsley, R. H., Phys. Rev. **131,** 1473 (1963).
[235] Asayama, K., J. Phys. Soc. Japan **18,** 1727 (1963).
[236] Yamadaya, T., and Asanuma, M., Phys. Rev. Letters **15,** 695 (1965).
[237] Wolcott, N. M., Falge, R. L., Jr., Bennett, L. H., and Watson, R. E., Phys. Rev. Letters **21,** 546 (1968).
[238] Rhodes, P., and Wohlfarth, E. P., Proc. Roy. Soc. (London) **273A,** 247 (1963).
[239] Switendick, A. C., and Narath, A., Phys. Rev. Letters **22,** 1423 (1969).

(Paper 74A4—624)